Volume 2, Issue 2, 2024

Print ISSN: 2960-0138

Online ISSN: 2960-0146

WORLD JOURNAL OF MATERIALS SCIENCE

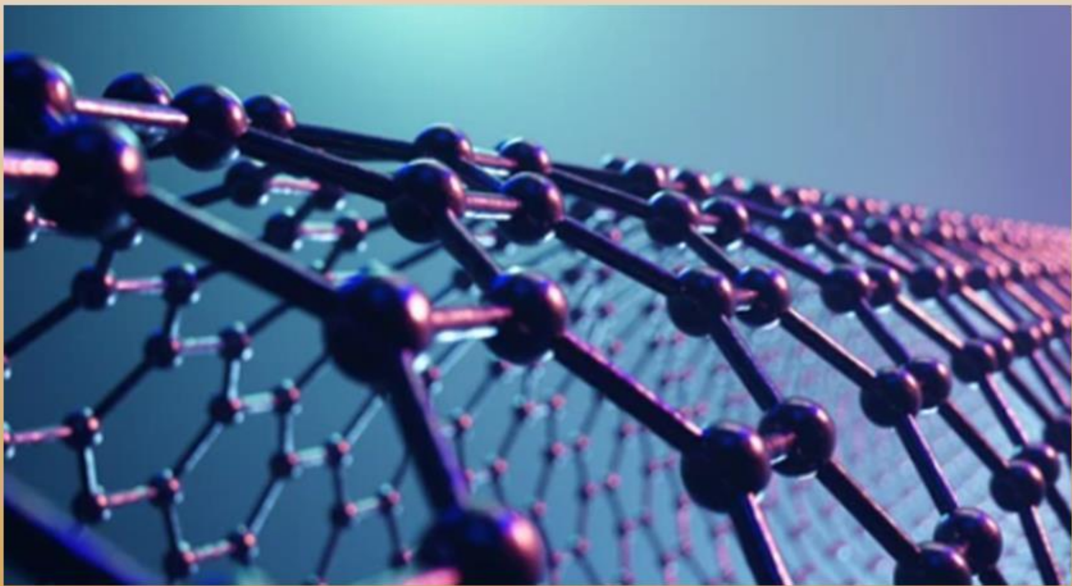

World Journal of Materials Science

Volume 2, Issue 2, 2024

Published by Upubscience Publisher

World Journal of Materials Science
Print ISSN: 2960-0138 Online ISSN: 2960-0146
Email: info@upubscience.com
Website: http://www.upubscience.com/

Table of Content

World Journal of Materials Science
ISSN: 2960-0146
DOI: 10.61784/wjmsv2n244

RESEARCH ADVANCEMENTS IN THE AREA OF GRAPHENE AND TECHNIQUES FOR DISPERSING GRAPHENE OXIDE

John Stains
Centre for Advanced Engineering Materials, School of Engineering, Robert Gordon University, United Kingdom.

Abstract: Graphene has excellent application value in many fields due to its unique lamellar structure. However, its easy agglomeration problem has always restricted the further application of graphene. Therefore, the dispersion problem of graphene has become a hot research issue in recent years. This article reviews graphene oxide and graphene dispersion methods (physical and chemical modification), conducts key analysis based on the dispersion principle, and provides an outlook for future graphene dispersion research.
Keywords: Graphene oxide; Graphene; Dispersion preparation; Physical and chemical modification

1 PHYSICAL METHODS OF GRAPHENE DISPERSION

Graphene is a two-dimensional carbon atom crystal with a unique structure and excellent properties. Its uniform and stable particle material dispersion is crucial to the composite synthesis industry, especially when preparing nanoscale materials. This requirement is even greater. protrude. The structural stability and excellent performance of graphene make it a hot topic in research and application today [1]. Due to the localized characteristics of graphene, the localization of sp2 carbon atoms and π electrons makes it chemically inert, and π-π stacking interactions easily form agglomerates. These factors hinder the development of graphene. development and application.

Graphene oxide (GO) has a large number of oxygen-containing functional groups (such as hydroxyl-OH, carboxyl-COOH and ether bond-COC) on its surface, which can be reduced to reduced graphene oxide (rGO) through a disproportionation reaction. Under the influence of oxygen functional groups, GO has good dispersion stability in water or other solvents. There are a large number of oxygen-containing functional groups on the edge of GO and it is extremely hydrophilic, while on the plane it is relatively hydrophobic, making it amphiphilic. However, in non-polar solutions similar to xylene, graphene oxide has extremely poor dispersion due to the strong π-π interaction and strong van der Waals forces between the sheets. The severe agglomeration between these lamellae greatly interferes with the good performance of graphene as a material. Therefore, in order to change these phenomena, surface repair work on graphene oxide is very necessary. At present, people have used various methods to deal with these phenomena in the laboratory, including chemically and physically destroying the interactions between the sheets, and bonding through special functional groups formed by graphene oxide on its surface. Various initiators, monomers and other reactive groups, etc., and on this basis, the edges and surfaces of graphene oxide are grafted with polymers in different ways.

Improving the stability and dispersion efficiency of GO dispersions through covalent or non-covalent methods has attracted more and more attention from researchers, and it also shows broad application prospects. This article starts from the current research status of graphene dispersion, reviews the research methods of chemical modification of graphene, and focuses on analyzing the reaction mechanism of covalent modification and non-covalent modification of graphene.

Among the methods for preparing dispersions, physical methods are relatively low-cost and fastest-acting methods. Through water bath ultrasonic treatment, high shear mixing method, jet cavitation or microfluidization, the graphene sheets are peeled off into single or oligo-layer graphene by physical means to achieve the purpose of dispersion.

(1) Preparation of graphene dispersion by water bath ultrasound. Among the current research methods, the water bath ultrasonic liquid phase exfoliation method is a relatively common method to prepare dispersions, which uses high energy to generate cavitation to stably disperse graphene sheets in the solvent. Chen Kui et al. [2] used ultrasonic liquid phase exfoliation to prepare graphene molybdenum disulfide (MoS_2). They used a mixture of 1, 4-butanediol (BDO) and water (alcohol-water mixture instead of alcohol). Molybdenum disulfide was added, the sample was sealed, and then centrifuged in a water bath for 40 hours at a power of 600 W for 30 minutes at a speed of 10, 000 r/min to prepare a dispersion. Although water bath ultrasonic treatment is low-cost and has low technical requirements, due to uneven energy during the peeling process, defects will be produced in the local groups of graphene due to high temperature and high pressure due to the cavitation effect, further affecting the graphite. Dispersion stability of ene. (2) Preparation of graphene dispersion liquid by high shear mixing method. The high-shear mixing method uses the joint influence of shear force, collision effect and jet cavitation to separate graphene sheets in its space through a high-shear mixer. In 2014, Paton et al. [3] demonstrated the use of high-speed shearing technology to process graphene dispersed in solvent. In 2019, Wang Chen et al. [4] used high-pressure homogeneous liquid phase exfoliation (HPH-LPE) to prepare an aqueous dispersion of graphene with a maximum lamella of 3.0 μm under the condition of PHAH=120MPa. In 2020, Miao Weijun et al. [5] used in-situ research on the effect of high shear rate on the epitaxial crystallization behavior of polyvinyl lactone (PCL)/reduced graphene oxide (RGO) and concluded that when the high shear rate is 75 s^{-1}, the viscosity of the material is decreasing and dispersed in the base material at temperatures of 65°C, 70°C and 75°C respectively. At the same time, the functional relationship can be

constructed through the graphene concentration C, rotor speed N, shearing time t, rotor diameter D and solvent volume V, and the graphene sheets were sheared and peeled under different solvent volumes. On the basis of this method, high-speed shearing suppresses van der Waals forces and stacking effects, and oliglayer or single-layer graphene stably exists in various solutions.

2 CHEMICAL PREPARATION METHOD OF GRAPHENE DISPERSION

Due to the large specific surface area and hydrophobic properties of graphene's surface functional groups, it is not easily dispersed in different solvents, thus hindering the application prospects of graphene materials. In order to solve the problem of difficulty in dispersion, chemical modification is one of the more common methods. Chemical modifications are mainly divided into two categories: covalent modification and non-covalent modification.

2.1 Covalent Modification to Prepare Graphene Dispersion

The main way to modify the dispersion by covalent method is to use covalent bonding to graft to the boundary or defect site between graphene and graphene oxide, and then pass through the active points existing therein, and through this activity At this point, the required substances can be directly grafted to GO to achieve the experimental purpose. Modified polymer materials are usually differentiated by the size of their molecular weight.

2.1.1 Modification of small organic molecules

In the coupling agent, organic small molecules such as organic amines and isocyanates are grafted to the surface of graphene oxide, which can regulate the interface structure with the base material and the compatibility of the material, thus changing the properties of graphene oxide. KH550 is a common amino-containing silane coupling agent. The primary amino group in KH550 is used to undergo a nucleophilic substitution reaction with the epoxy functional group in the GO sheet, and KH55O is grafted to the surface of the GO sheet. At the same time, the primary amino group in KH550 and the carboxyl group (-COOH) on the edge of graphene oxide can proceed. Amidation reaction[6]. Su Tian et al. [7] prepared GO (KH550-GO)/PSS dispersion in the ratio of GO:PSS:KH550=1:1:1.7. Wang Xinhui et al. [8] modified graphene oxide with organosilane in a one-step method, and the resulting graphene sheets had clear color and stretched structure, thus proving that after one-step organosilane modification, the obtained graphene oxide layer had a van der Waals forces are reduced and the risk of chemical stacking is reduced. In addition, -OH and -COOH on the surface of graphene oxide can also react with -NCO groups in isocyanate. Stankovivh et al. [9] first reported the use of isocyanates to graft-modify GO. They used different isocyanates to graft a series of different side chains on the surface of GO. The results show that compared with the original GO, the water solvent of GO connected with -NCO group is reduced, but after a short period of time in DMF, dimethyl sulfoxide (DMSO), N-methylpyrrolidone (NMP), etc. After ultrasonic treatment, a uniform dispersion system can be formed, and the system has good suspension stability. In covalent modification, some researchers use aminosilane coupling agents to modify GO and apply it to polymers. The results showed that the mechanical properties of the modified polymer materials were improved. Polyethylene glycol (PEG) can also be used for covalent modification of GO, which is an amphoteric GO with both hydrophilic and lipophilic properties.

In the modification of organic small molecules, functionalized graphene and GO not only improve the dispersion in solvents, but also improve their amphiphilicity and mechanical properties. At the same time, the modified GO prepared can be used in the biological field, broadening the application scope of graphene.

2.1.2 Modification of organic macromolecules

When organic polymers such as polyaniline, polyvinylpyrrolidone and polyethylene are used to modify GO, the steric hindrance caused by expanding the distance between graphene sheets can prevent agglomeration and improve dispersion. sex. Esterification reaction is a commonly used chemical reaction for the modification of macromolecules. Cheng HK[10] used polyvinyl alcohol (PVA) to graft onto the surface of GO sheets, and proposed a method to create advanced polymer nanocomposites from polyvinyl alcohol (PVA) by incorporating PVA-grafted graphene oxide. new method. It was found that by adding PVA-g-GO, the mechanical properties of PVA greatly improved adhesion. The strong interfacial adhesion between PVA-g-GO and PVA matrix is attributed to the good compatibility between PVA-g-GO and matrix PVA as well as the hydrogen bonding interaction between them. At the same time, NAndi AK et al. [11] produced related modified silicone products by grafting polyvinylpyrrolidine acid (PVP) from GO, and modified PVP onto the GO layer to obtain The dispersion rate of GO sheets in different solutions, among which Hansen solubility values range from 6.3 to 5.8. Modified products of PVP and related silicones will not only improve the dispersion of GO in different solvents but also broaden the application space of GO and graphene.

The modified graphene/GO not only improves the dispersion in different solvents, but also improves the solubility during the blending process. However, in the modification of organic macromolecules, the continuity of the original structure of GO is destroyed during the reaction between the molecules and the groups on the surface of GO, thus inhibiting the development of its conductivity and optical properties.

2.2 Preparation of Graphene Dispersion by Non-Covalent Modification

The non-covalent bonding method is used to functionalize the graphene surface, and the interaction force between specific functional macromolecules and GO sheets is used to hybridize to obtain GO hybrid particles with corresponding functions.

The non-covalent method is another effective technology for using polymers to modify the surface of graphene oxide. Compared with the covalent bonding method, it has a particularly good feature, that is, the conjugated metal system on the surface of graphene oxide is not damaged during the polymer chain modification, and it can also improve the thermal dispersion performance of graphene oxide. Kim BJ's research group [12] used a similar method to prepare pH-responsive polymer-stabilized fluorescent quantum dot functionalized GO with pyrene end groups, and obtained quantum dot-GO hybrid nanomaterials with better performance within a certain range. Dispersion. Yang Yongfang et al. [13] used the ATRP (atom transfer radical) method to prepare pyrene-terminated poly-2-dimethylaminoethyl methacrylate (PDMAEMA), and grafted it to pyrene-terminated poly(PDMAEMA) based on π-π stacking. Electrostatic interactions coat the surface of graphene oxide on the surface of polystyrene microspheres to form a hydrophilic polymer brush-like structure. Then polystyrene microspheres were dissolved in THF to obtain amphiphilic polymer brush-modified Jannus structure GO nanosheets. Based on the amphiphilic principle of polymer brushes, the obtained Janues structure nanomaterial sheets also have an excellent effect on stabilizing emulsions. The use of π-π stacking can achieve a stable effect by overcoming the van der Waals forces between the sheets through electrostatic interaction. Compared with this method, it is simpler, but the corresponding cost also increases.

In addition, the in-situ polymerization of polystyrene microspheres can solve the dispersion problem of graphene oxide solution in oily solution. The use of dispersions to prepare liquid crystals has extremely high requirements on the stability of high-concentration colloids composed of anisotropic colloidal particles. Because of its negative charge (highly oxidized graphene fragments), GO solution can achieve very good colloidal stability in water. As one of the most important non-covalent binding substances, the π-π effect widely appears in nature. It has a great impact on the work of supramolecular preparation and material identification. In the experiment of Professor Yan Haichen [14], it was proved that GO composite microspheres were successfully prepared through in-situ polymerization reaction, and it was proved that an ethanol-water mixture with an alcohol-to-water mass ratio of 4:1 was used as the dispersion medium. , after prepolymerization for 2 hours and then adding the GO diffusion solution, GO composite microspheres with ultra-high composite solution rate can be obtained. The particle size of composite microspheres is 0.78~1.15μm, and the standard deviation is less than 0.1μm. It is also proven that there is a strong π-π stacking effect between GO and PS, and this stacking effect is used to load the nanoparticles on the surface of GO and graphene sheets so that they can be stably dispersed in non-polar solvents for a long time.

GO has good physical and chemical properties and its unique two-dimensional layered planar structure with large specific surface area, which provides good conditions for the loading of inorganic nanoparticles. By loading GO on inorganic nanocomposites, inorganic hybrid functionalization of GO can be achieved. Through inorganic hybrid functionalization, many properties that GO does not have can be realized. At the same time, loading inorganic nanoparticles on the surface of GO can also effectively prevent its own damage. Reunion.

3 CONCLUSION

This review summarizes the preparation of polymer-functionalized graphene/graphene oxide surfaces by covalent and non-covalent methods of physical modification as well as chemical modification. Graphene oxide is currently relatively cheap to produce, and its dispersibility in a variety of solvents, including water, coupled with its tunable surface chemistry, make graphene oxide a versatile material. At present, there are still some challenges in graphene oxide and graphene dispersion technology, such as dispersion performance under high concentration, high temperature, high pressure and other conditions, impact on graphene properties, large-scale production and other issues. Therefore, further research on the mechanism and optimization methods of graphene dispersion is needed in the future to improve the stability and controllability of graphene dispersion and lay a more solid foundation for its widespread application.

COMPETING INTERESTS

The authors have no relevant financial or non-financial interests to disclose.

REFERENCES

[1] Huang BR, Chan HW, Jou S.Surface Structure-Dependent Molecular Oxygen Activation of BiOCl Single-Crystal- line NanosheetsApplied Surface.Science, 2016, 362, 250.

[2] Chen Kui, Liu Guangqiao, Zhang Tianyun. Preparation of graphene-like molybdenum disulfide by ultrasonic liquid phase exfoliation method. Nonmetallic Minerals, 2022, 45(03): 15-17.

[3] Paton KR, Varrlae, Back ES.C. Scalable Produc- tion of Large Quantities of Defect-Free Few Layer Graphene by Shear Exfoliation in Liquids. Nature Materials, 2014, 13(6): 624-630.

[4] Wang Chen, Yan Shaojiu, Nan Wenzheng. Preparation and characterization of high-concentration graphene aqueous dispersion. Materials Engineering, 2019, 47(04): 56-63.

[5] Miao Weijun, Wu Feng, Wang Yong. In-situ study on the effect of high shear rate on the epitaxial crystallization behavior of PCL/RGO. Journal of Chemistry in Colleges and Universities, 2021, 42(03): 910-918.

[6] Y Matsuo, T Tabata, T Fukunaga, T Fukutsuka. Preparation and characterization of silylated graphite oxide. Chemistry Select, 2017, 2(33): 10786-10792.

[7] Su Tian, Xie Lili, Zheng Long, Xu Zongchao, Liu Li, Wen Shipeng. Research on the properties of graphene oxide/sodium polystyrene sulfonate modified by coupling agent KH550 and its composite material with styrene-butadiene rubber. Rubber Industry, 2019, 66(12):908-916.
[8] Wang Xinhui, Hao Jianjun, Li Hengjun. One-step preparation of silane-modified graphene oxide. Electroplating and Coating, 2022, 41(06): 431-436.
[9] Stankovich S, Richard DF, Sonbinh T N.Synthesis and exfoliation of isocyanate-treated graphene oxide nanoplatelets. Carbon, 2006, 44(15): 3342-3347.
[10] Cheng HK, Sahho NG, Tan Y P. Functionalized Porous Aromatic Framework for Efficient Uranium Adsorption from Aqueous Solutions. ACS Appl Mater Interfaces, 2012, 4(5): 2387-2394.
[11] Cheng HK, Sahho NG, Tan Y P. Functionalized Porous Aromatic Framework for Efficient Uranium Adsorption from Aqueous Solutions. ACS Appl Mater Interfaces, 2012, 4(5): 2387-2394.
[12] Pake K, Yang H, Lee J. Efficient Colorimetric pH Sensor Based on Responsive Polymer-Quantum Dot Integrated Graphene Oxide. ACS Nano, 2014, 8(3): 2848-2856.
[13] Yang YF, Zhang LT, Jix T. Molecular Geometry-Directed Self-Recognition in the Self-Assembly of Giant Amphibiles. Macromol Rapid Comm, 2016, 37(18): 1520-1526.
[14] Yan Haichen, Li Yanbao. In-situ preparation of polystyrene/graphene oxide composite microspheres by dispersion polymerization. Journal of Nanjing University of Technology: Natural Science Edition, 2019(2):135-140.

World Journal of Materials Science
ISSN: 2960-0146
DOI: 10.61784/wjmsv2n245

PERFORMANCE DETERIORATION AND MICROSTRUCTURE OF VITRIFIED MICROBEAD INSULATION CONCRETE AFTER HIGH TEMPERATURE

Leandro T. Azevedo
State University of the Northern Rio de Janeiro, Brazil.

Abstract: Prepare ordinary concrete (NC) and vitrified microbead insulation concrete (GHB/NC), and study the deterioration process of changes in apparent phenomena, quality, loss of compressive strength and other properties after heating from normal temperature to 1000°C, and discuss ultrasonic non-destructive testing at the same time The method is used to evaluate the universality of the performance of concrete after high temperatures, comparatively analyze the relationship between relative wave speed, damage degree, heating temperature, and compressive strength loss rate, and use SEM to observe the microstructural changes of specimens after different high temperatures.
The results show that the use of relative wave speed and damage degree to evaluate the performance of concrete after high temperature has good correlation, and the regression formula has a high fitting degree; as the temperature increases, the internal damage of NC and GHB/NC concrete gradually intensifies, and the cement gelation decomposes due to heat and moisture Dissipation, etc. produce gaps, cracks and interconnections on the surface and inside of the specimen, and the bonding force at the interface between vitrified microspheres, coarse aggregate and cement stone gradually weakens or even loses, causing the macroscopic mechanical properties to deteriorate and the compressive strength loss rate to increase. After heating to 800℃, the strength loss of NC is 72.3%, the strength loss of GHB/NC is 74.6%, and the load-bearing capacity is basically lost at 1000℃.
Keywords: Vitrified microbead insulation concrete; High temperature; Ultrasonic nondestructive testing; Performance degradation; Microscopic analysis; Interface transition zone

1 EXPERIMENTAL MATERIALS AND METHODS

At present, my country's building energy consumption accounts for a large proportion of national energy consumption and is on the rise. Therefore, building energy conservation is a topic of widespread concern at present. The key is to improve the heat insulation and heat preservation performance of the building envelope to reduce indoor heat loss and save energy [1]. Commonly used external wall insulation systems include insulation systems based on organic insulation materials such as polystyrene particles and polystyrene boards, and insulation systems based on inorganic insulation materials such as vitrified microbead insulation mortar and expanded vermiculite insulation mortar [2- 3]. A large number of engineering practices have proven that organic materials have poor durability and fire resistance, while inorganic materials have excellent properties such as heat insulation, fire retardancy, high temperature resistance, and green environmental protection, and have gradually received widespread attention and application [4].
Research on vitrified microbead inorganic exterior wall insulation materials focuses on the discussion of the performance of thermal insulation mortar. For example, Gong Jianqing et al. [5] studied the effect of different water-binder ratios on the performance of vitrified microbead thermal insulation mortar; Zhu Jiang et al. [6] discussed the The influence of propylene fiber content on the mechanical properties and softening coefficient of vitrified microsphere composite insulation materials; Wu Wenjie et al. [7] analyzed the influence of each component of thermal insulation mortar on material properties. However, using insulation mortar as exterior wall insulation material increases the construction process. Therefore, relevant scholars have proposed vitrified microsphere insulation concrete materials that can effectively bear load and have thermal insulation functions. MA et al. [8], ZHAO et al. [9], ZHANG [10] and Dai Xueling et al. [11] conducted a series of studies on this, including the macroscopic physical and mechanical properties, thermal insulation capabilities, microscopic characteristics, etc. of the material, as well as the exploration and application of structural self-insulating walls. practice. However, there are few studies on vitrified microbead self-insulating concrete after high-temperature fires. The use of ultrasonic non-destructive testing to evaluate the internal damage of building structures is a convenient, fast, and highly repeatable method [12]. Since vitrified microbeads The beads are mixed into cement mortar as fine aggregate so that the bonding with the cement stone is different from that of conventional concrete, and the ultrasonic wave propagation characteristics are also different. However, there are few public reports on the use of ultrasonic method to evaluate the performance of vitrified microbead concrete after high temperature. Relevant studies have shown that cement slurry becomes more loose and porous after high temperature, causing the occurrence and development of macro cracks [13-14]. However, the unique embedded interface structure of vitrified microspheres and cement stones is different from ordinary concrete [15]. Structural changes in the interface zone and internal degradation processes and mechanisms after high temperatures deserve attention.
To this end, this article tests the quality and strength loss of vitrified microsphere thermal insulation concrete (GHB/NC) after high temperature treatment. Non-destructive ultrasonic detection technology is used to use relative wave speed and

damage degree as evaluation indicators to analyze the interior of the material after different temperatures. Damage and strength loss rate, use scanning electron microscope to observe the microstructural changes of the specimen after high temperature. Exploring the high-temperature degradation mechanism of vitrified microbead insulation concrete from macro and micro perspectives.

1.1 Raw Materials

The cement uses Huainan Bagongshan brand P·C42.5 grade composite Portland cement. Its 3-day and 28-day compressive strengths are 29.99 MPa and 49.75 MPa respectively. Huainan Pingwei Power Plant produces grade I fly ash., its chemical composition content is shown in Table 1; the fine aggregate is medium sand, with a fineness modulus of 2.8; vitrified microbeads produced by Henan Xinyang Jinhualan Company are used as lightweight fine aggregate, and its main performance indicators are shown in Table 2 ; The coarse aggregate is calcareous gravel with a particle size of 5 to 15 mm and is continuously graded; the admixture is HPWR high-performance water-reducing agent produced by Shaanxi Qinfen Building Materials.
Vitrified microbeads (GHB) are a kind of non-metallic lightweight thermal insulation material. They are formed by crushing, screening and vitrification of turpentine ore after mining, instantaneous combustion at high temperature, and vitrification. They are porous inside and vitrified on the surface, and are in the form of spherical fine particles. diameter particles. The micromorphology of vitrified microbeads observed using scanning electron microscopy (SEM) is shown in Figure 1. It can be seen that the interior has a honeycomb porous structure. This special structure extends the heat transfer path inside the material and increases the internal pores, allowing heat to spread both in the material and in the air, and the air itself is a good thermal insulation material., the thermal conductivity is only 0. 023W/(m·K)[16], thereby increasing energy dissipation loss and improving thermal insulation capacity; while the outer surface is vitrified and closed in a spherical shape, but it is easily squeezed during the concrete mixing process. Broken due to pressure, vibration, etc., resulting in loss of strength.

1.2 Concrete Mix Proportion Design

According to JGJ55 - 2011 [17], the concrete mix ratio was designed. The vitrified microspheres were subjected to water absorption treatment for 1 hour before the experiment. After the experimental trial mix, the water-cement ratio was adjusted accordingly to ensure consistent water consumption. The specific data are shown in Table 3, where NC (Normal concrete) is C30 ordinary concrete, and GHB/NC (Glazed hollow bead insulation normal concrete) is vitrified microbead insulation concrete. The basic performance test results are shown in Table 4. It can be seen that after adding vitrified microsphere lightweight aggregate, the apparent density, compressive strength, and thermal conductivity of concrete are reduced to varying degrees. The compressive strength at 28 days decreased by about 29%, and the thermal conductivity decreased by about 26 %. Due to the good water retention of vitrified microspheres, the moisture content has increased. After pre-wet treatment, the workability and fluidity of the mixture are greatly improved, which is in line with the current multi-functional requirements of building materials such as lightweight, good workability, and thermal insulation development trend.

Table 1 Chemical composition of fly ash (wt%)

Composition	SiO2	Al2O3	Fe2O3	CaO	MgO	Na2O	Lgnitionloss
Content	53.26	34.72	4. 07	2.47	0.39	1.9	4. 07

Table 2 Performance indicators of vitrified microspheres

Particle size/mm	Bulkdensity/ (kg·m-3)	Apparent (kg·m-3)	density/Cylinder compressive strength/MPa	Thermalconductivity/ W·(m·K) - 1)	(R efractoriness/°C	Volumeloss rateat1 MPa/%
0. 5-1. 5	80-120	80-130	≥150	0. 032-0. 045	1 280-1 360	38-46

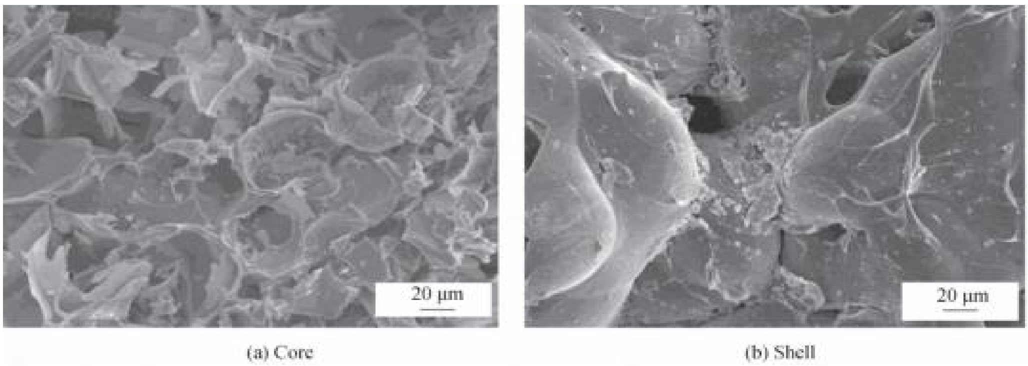

Figure 1 Microstructure morphology of vitrified microbeads (GHB)

Table 3 Concrete mix ratio (kg/m ^{3})

Concrete	Cementing material		Gravel	Fine aggregate		Water	Water reducer	Water cement ratio
	Cement	Flyash		Sand	Glazedhollowbead			
NC	421	47	856	856	—	177.84	4.68	1： 0.38
GHB/NC	421	47	856	571	100	168.48	4.68	1： 0.36

Notes: NC— Normalconcrete; GHB/NC— Glazedhollowbeadinsulationnormal concrete.

Table 4 Basic performance of mixed soil

Concrete	Workability		Compressive strength/MPa		28dapparent density/(kg·m-3)	28dmoisture content/%	Thermal conductivity/ (W·(m·K) - 1)
	Slump/mm	Slump flow/mm	3D	28d			
NC	175	350	15.61	36.80	2 272	1. 10	1. 65
GHB/NC	200	410	8.12	26.13	2 102	1. 73	1. twenty two

1.3 Experimental Methods

A cube test block with a size of 100 mm × 100 mm × 100 mm is used. The mold is removed after 1 day of molding and cured under standard curing conditions (relative humidity ≥ 95%, temperature (20 ± 1) ℃) for 28 days. Before the experiment, all test blocks were placed in an oven at (105±5) ℃ to dry for 24 hours to eliminate the influence of moisture in the test blocks on the experiment. A box-type resistance furnace is used to heat the test block. The design target temperature is 100~1000℃, the temperature interval is 100℃, and the heating rate is 10~15℃/min. After rising to the target temperature, the temperature is kept constant for 2 hours to ensure that the furnace temperature and the internal temperature of the test piece are maintained. Consistent, cool the furnace to about 100℃, take out the furnace and let it stand for more than 48 hours to measure various properties of the specimen.

The NM-4B non-metal ultrasonic detector produced by Beijing Kangkerui Company was used to measure the sound speed, main frequency and amplitude of the specimen at each temperature. Each specimen was arranged with 2 relative measuring points to calculate the average. The ultrasonic frequency was 50kHz and the emission was set. The voltage was 500 V and the sampling period was 0. 4 μs; after ultrasonic measurement, the CSS-YAN3000 press produced by Changchun Testing Machine Research Institute was used to conduct a pressure failure experiment. According to the difference between the compressive strength of each specimen after high temperature and drying treatment ratio, and calculate the strength loss rate; finally, samples were taken from the crushed test blocks, and a Hitachi S-3400N scanning electron microscope was used to select the connecting parts of cement stone, vitrified microspheres and cement stone for microscopic morphology observation of the interface area.

2 RESULTS AND DISCUSSION

2.1 Appearance Phenomenon of Concrete at High Temperature

It was observed that the appearance phenomena of NC and GHB/NC concrete specimens after high temperature are similar, as shown in Table 5. It can be seen that as the temperature increases, the appearance color gradually deepens from blue-gray and then lightens to off-white to white. When the temperature is lower than 300℃, there is no obvious change in the appearance of the specimen, the knocking sound is crisp and no cracks occur; when 300~500℃, the color of the specimen deepens and is slightly brown, the knocking sound becomes gentler, and fewer fine cracks appear. The reason is that the coarse aggregate itself does not change significantly in this temperature range, and the cracks and deformation are mainly concentrated in the coarse aggregate and cement. Fine cracks appear at the interface of the mortar matrix and inside the cement mortar matrix. In addition, the calcium ferrite hydrate in the concrete reacts with Ca (OH) 2 to generate brown Fe(OH) 3 precipitation, causing the specimen to appear slightly brown [18].

Table 5 Appearance phenomena of NC and GHB/NC concrete specimens at various temperatures

Temperature/℃	Apparent color of specimen	Knocking sound of specimen	Crack, scaling and loose
20	Cinerous	Clearand melodious	None
100	Cinerous	Clearand melodious	None
200	Cinerous	Slightly clearand melodious	None
300	Slightly brown	Slightly clearand melodious	None
400	Mediumbrown	Gentle	Minorcrack
500	Brown	Gentle	Minorcrack
600	Grey white	Slightly low	Obviouscrack
700	Grey white	Slightly low	Obviously crack, mildloose
800	White	Low	Obviously crack, a smallnumberoflong and wide cracks, increasing loose
900	White	Low	Coarsecrack, p eeling andscaling, obviously loose
1 000	White	Low	Coarseandthrough cracks, broken, missing cor- ners, looseness

When the temperature is higher than 600°C, obvious cracks will appear, the appearance will be off-white, and the knocking sound will be low; when the temperature is 800℃, the specimen will turn white, and long cracks will appear; when the temperature exceeds 900℃, a large amount of peeling and peeling will occur. Leave it for 48 hours. The phenomenon of broken and missing corners is serious, the overall structure is loose, and the strength is seriously reduced. The reasons are that the limestone gravel decomposes into CO2 after being decomposed into CO2 at a high temperature of 600°C, the volume expansion of cement mortar and other materials after high temperature, and the different thermal expansion coefficients of the gravel and cement mortar matrix. The cracks in the specimen increase and the strength is lost [19-20].

2.2 Quality Loss of Raw Materials and Concrete at High Temperatures

Figure 2 shows the mass loss of each main raw material and concrete specimen with temperature changes. The quality of gravel remains basically unchanged when the temperature is lower than 600°C. The mass loss is about 5% at 600~800°C. The quality drops significantly at 900°C. The mass loss reaches 40% at 1000°C. Sand experiences high temperatures. The final quality loss is small. Since the main component of gravel is $CaCO_3$, it decomposes into CaO and CO2 at a temperature of 600~820°C, resulting in significant quality reduction [21].

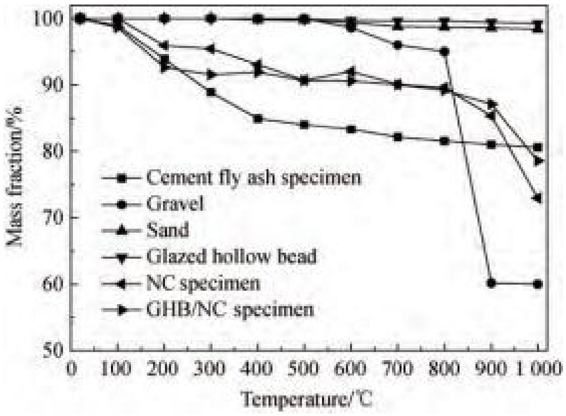

Figure 2 Quality loss of raw materials and concrete after high temperature

After experiencing a high temperature of 1,000°C, the mass loss rate of vitrified microspheres is less than 1%, and the strength and quality are almost unaffected. This is because the vitrified microspheres are processed by a special expansion and firing method. The temperature exceeds 1000°C. Comparing the appearance characteristics of gravel and vitrified microspheres after high temperature treatment at 1000°C (Figure 3), it can be seen that the gravel has changed from bluish white to snow white, with a large loss of strength, while the vitrified microspheres have changed from White particles have no obvious change when heated to 700°C. When the temperature continues to rise to 1000°C, they gradually turn into red particles with a small amount of agglomeration. Figure 4 shows the microstructure of vitrified microbeads after high temperature at 1000°C, and the micromorphology at normal temperature. (Figure 1) Comparison, there is almost no change between the two, indicating that the material is an excellent high temperature resistant material.

Figure 3 Appearance changes of gravel and vitrified microspheres after high temperature

The mass loss trend of the two groups of specimens after experiencing high temperatures is consistent. When the temperature is lower than 200°C, the mass loss is less than 5%. When the temperature is lower than 600°C, the mass loss is controlled at 10%. At this time, the mass loss is mainly caused by the mass loss of cement gel. As a result, the quality further decreases when the temperature exceeds 600°C, and the quality decreases significantly when the temperature reaches 800°C. The mass loss of NC specimens after high temperature treatment at 1000°C reaches 27.01%. After GHB/NC treatment at 1000°C, the quality loss It is 21. 44%, which is better than NC, reflecting the advantages of vitrified microsphere lightweight aggregate in high temperature resistance compared with sand and gravel.

2.3 High-Temperature Internal Damage to Concrete

Ultrasonic testing is used to evaluate the internal damage of the test block after high temperature treatment. The ultrasonic propagation characteristics are affected by the type, particle size, cement type and dosage of coarse and fine aggregates. Referring to the literature [12], the relative wave speed, damage degree, relative main frequency and The relative amplitude is calculated as the evaluation parameter as follows:

vR =vT /v0 (1)

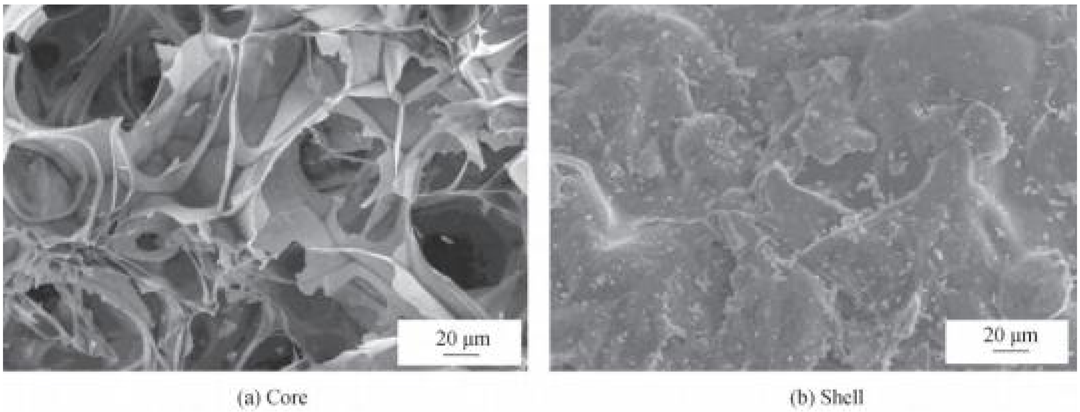

Figure 4 Microstructural morphology of vitrified microbeads after high temperature of 1000℃

Table 6 Processing of concrete ultrasonic test results

Group	Temperature/℃	Revative v	Damage Degree D	R elative dominant frequency fR	R elative amplitudeAR	Compressive strength loss rate/%
NC	100	0.976	0.047	0.997	1.599	-6.5
	200	0.886	0.215	0.997	1. 545	-11.2
	300	0. 773	0. 403	1. 029	1. 639	-20. 5
	400	0. 641	0. 589	1. 019	1. 537	-24. 5
	500	0. 539	0. 709	0. 951	1. 662	12. 7
	600	0. 375	0. 859	1. 006	1. 649	26. 2
	700	0. 295	0. 913	0. 987	1. 518	38. 6
	800	0. 277	0. 923	0. 985	1. 342	72. 3
	900	0. 209	0. 956	0. 377	0. 932	79. 0
	1 000	0. 176	0. 969	0. 219	0. 756	88. 5
GHB/NC	100	0. 970	0. 059	1. 009	0. 996	-2. 7
	200	0. 811	0. 343	1. 019	1. 103	-20. 6
	300	0. 599	0. 641	0. 975	1. 086	-14. 8
	400	0. 510	0. 740	0. 990	1. 084	-2. 1
	500	0. 367	0. 865	0. 997	1. 038	20. 5
	600	0. 324	0. 895	1. 004	1. 062	21. 7
	700	0. 302	0. 909	0. 968	0. 926	57. 7
	800	0. 234	0. 945	0. 519	0. 707	74. 6
	900	0. 185	0. 966	0. 087	0. 660	85. 8
	1 000	0. 127	0. 984	0. 104	0. 486	88. 2

Note: Negativevalueinthe compressive strengthloss rate indicatesanincreasein strength at the target temperature.

D =1-(vT /v0) 2 (2)

AR =AT /A0 (3)

fR =fT /f0 (4)

ΔFcu =1-FcuT /Fcu0 (5)

In the formula: vR is the relative wave speed; vT is the wave speed after high temperature of the specimen (m/s); v0 is the wave speed of the specimen before high temperature (m/s); D is the damage degree of the specimen; AR is the relative amplitude; AT is the first wave amplitude after high temperature (dB); A0 is the first wave amplitude before high temperature value (dB); fR is the relative dominant frequency; fT is the dominant frequency of the first wave after high temperature (kHz); f0 is the dominant frequency of the first wave before high temperature (kHz); ΔFcu is the compressive strength loss rate; FcuT is the resistance of the specimen after high temperature damage Compressive strength value (MPa); Fcu0 is the compressive strength value (MPa) of the specimen before high temperature treatment. The measured raw data were processed, and the results are shown in Table 6. It can be seen that the relative amplitude and relative main frequency do not change much when the heating temperature is lower than 800°C. After experiencing high temperatures above 800°C, the amplitude and main frequency decrease significantly, indicating that these two parameters are very important for evaluating the specimen. The reflection of internal property differences of heated materials is insensitive and is not suitable as an evaluation parameter.

The relationship between relative wave speed, damage degree and heating temperature of two types of concrete specimens after being exposed to different temperatures is shown in Figure 5. It can be seen that the relative wave speed and damage degree of concrete specimens have a good correlation with the heating temperature. As the heating temperature increases, the relative wave speed gradually decreases and the damage degree continues to increase. The reason is that the volume of the specimen expands after high temperature, the raw materials are damaged, and the specimen The density decreases and the wave speed gradually decreases, which is reflected in the continuous accumulation of internal damage. An appropriate function is used for regression analysis. The fitting results are shown in Table 7. The fitting correlation coefficients are all greater than 0. 95. The experimental values and the fitted values are in good agreement, indicating that the relative wave speed and damage degree are used to evaluate the internal structure of the material after high temperature. The damage is reasonable and feasible.

2.4 High Temperature Compressive Strength Loss of Concrete

It can be seen from the compressive strength loss rate in Table 6 that the strength decrease trend of the two types of concrete after high temperature is the same. When the temperature is lower than 400°C, because each specimen has undergone high-temperature autoclaved curing, only crystallized water escapes inside the concrete. The pore structure did not change significantly, and CaCO3 with higher strength was produced, which strengthened the interlocking force between the colloid and the aggregate, so the compressive strength was improved compared with that at normal temperature. The strength of NC increased by 24.5% to the maximum after treatment at 400°C. GHB/NC has the highest strength after treatment at 200°C, increasing by 20.6%.

After 400°C, the compressive strength of each specimen dropped sharply as the temperature increased. This was due to the serious coarsening of the internal pore structure of the concrete. The C-S-H gel decomposed significantly after the temperature was higher than 600°C and lost its cementing effect. The shrinkage of cement and the softening and expansion of gravel aggregate cause cracks to expand and penetrate. When the temperature is higher than 800°C, the strength loss is nearly 80%. The cement hydration products and calcareous gravel are further decomposed. The internal water vapor forms a high vapor pressure, causing the slurry to crack or even burst at high temperature. After experiencing a high temperature of 1000°C, the cement slurry becomes loose. The specimens were almost unshaped, and the two types of concrete basically lost their bearing capacity.

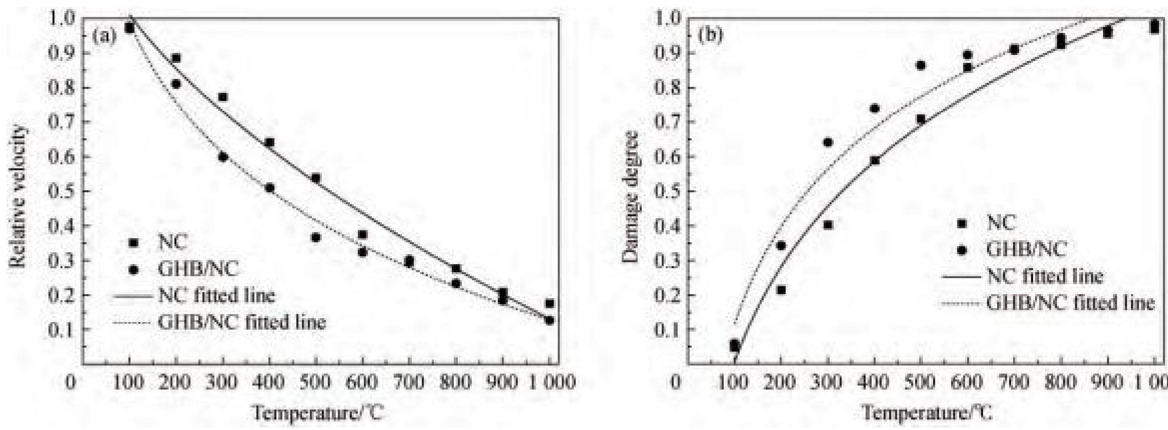

Figure 5 Relationship between ultrasonic parameters and heating temperature after high temperature for NC and GHB/NC

Table 7 Fitting results of NC and GHB/NC ultrasonic parameters and heating temperature

Concretetype	Ultrasoundparameter	Fitting formula	R2
NC	Relativevelocity vR Damage degree D	vR =-22. 15 $\frac{T^{0.51}}{1000}$+1. 33 D =1. 64T0. 129 -2. 97	0.98 0.97
GHB/NC	Relativevelocity vR Damage degree D	vR =-1397. 62 $\frac{T^{0.1}}{1000}$+3. 51 D =61. 29T0. 006 -63. 03	0.99 0.95

Note: T— Temperature.

2.5 Relationship Between Internal Damage and Strength Loss of Concrete

When the two types of concrete are heated from normal temperature to 1000°C, the strength undergoes a process of first slight increase and then gradual decrease. Ultrasonic wave propagation is affected by many factors and does not reflect this change pattern. Therefore, the relative wave speed, damage degree and strength are discussed. The relationship between loss rate does not consider the influence of this temperature range for the time being. After calculation, the fitting effect is best after excluding the temperature range of 100~200℃. Figure 6 shows the experimental data and fitting effects of the relative wave speed and damage degree of the two types of concrete as they change with heating temperature. Select appropriate functions for regression analysis respectively, and the results are shown in Table 8. The fitting correlation coefficients are all greater than 0. 90, and the fitting results are excellent, indicating that it is reasonable and feasible to use relative wave speed and damage degree to judge the strength loss rate.

2.6 Deterioration of Concrete Microstructural Properties

Figure 7 shows the microstructure of NC cement slurry at room temperature. It can be seen that the bonding between cement slurries is tight, complete and continuous, and there is a large amount of C—S—H gel. Acicular ettringite AFt crystals and Ca (OH) 2 can be seen under magnification. Figure 8 shows the micromorphology of NC after being heated to 200~400°C. It can be seen from Figure 8(a) that the structure of the cement hydrated slurry is basically intact after being heated to 200°C.

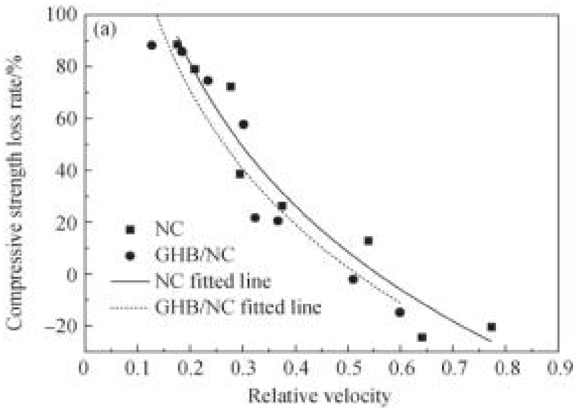

Figure 6 Relationship between ultrasonic parameters and compressive strength loss rate of NC and GHB/NC after high temperature

Table 8 Fitting results of NC and GHB/NC ultrasonic parameters and compressive strength loss rate

Concretetype	Ultrasoundparameter	Fitting formula	R2
NC	Relativevelocity vR	$\Delta F_{cu} = -79.49 \ln v_R -46.53$	0.93
	Damage degree D	$\Delta F_{cu} = 0. 244e^{6. 32D} -24. 36$	0.92
GHB/NC	Relativevelocity vR	$\Delta F_{cu} = -74.74 \ln v_R -49.32$	0.88
	Damage degree D	$\Delta F_{cu} = 0. 086e^{7. 36D} -24. 83$	0.92

Note: ΔFcu — Compressive strength loss rate.

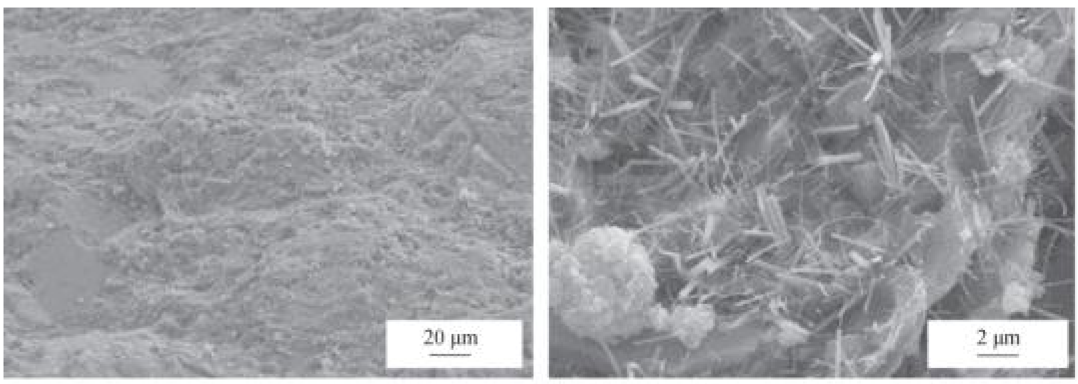

(a) Intact slurry structure (b) Acicular ettringite (AFt)

Figure 7 Microscopic morphology of NC cement slurry at room temperature

There are some signs of looseness, but all physical phases are basically normal; as shown in Figure 8(b), after being exposed to a high temperature of 400°C, the slurry becomes loose, the gel shrinks, and the aggregate and slurry separate. At this temperature range, free water, capillary water, and C-S-H gel adsorbed water are lost, promoting the cement hydration reaction and volcanic ash reaction to continue, forming a similar "autoclave curing" effect, resulting in a lower strength of the concrete specimen. The normal temperature has increased, and relevant literature also reflects this rule [21-23].

Figure 9 shows the micromorphology of NC after being heated to 600~1000°C. It can be seen from Figure 9(a) that a large amount of water is lost after 600°C, and small pores left by obvious water loss appear on the gelled surface. The cement slurry is loose, the gel decomposes, and cracks and delamination occur. The macroscopic manifestation is that the specimen Whitening, cracks increased significantly; Figure 9(b) shows that the dispersion between the phases intensified after 800°C; from Figures 9(c) ~ 9(d), it can be seen that after 1000°C, the loosening of the slurry further intensified, the continuity was poor, and the dispersion between phases In severe cases, the decomposed parts have been connected into areas, cracks, and holes. On a macroscopic level, a large number of through-cracks have appeared, the volume has expanded, and the internal density and wave speed have decreased.

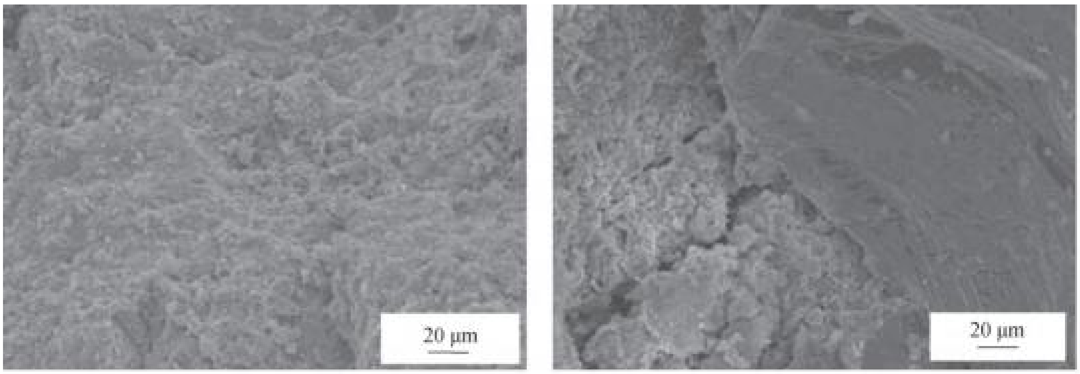

(a) Slurry structure at 200℃ (b) Separation at aggregate and slurry at 400℃

Figure 8 Micromorphology of NC at temperatures of 200°C and 400°C

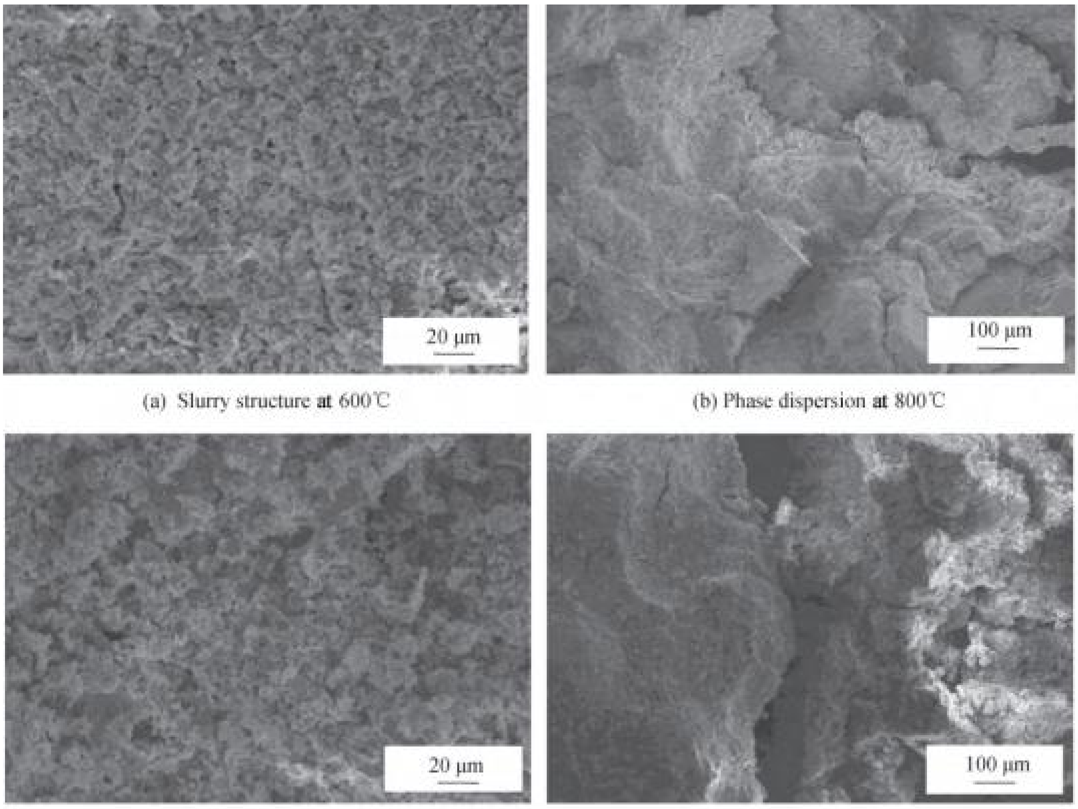

(a) Slurry structure at 600℃ (b) Phase dispersion at 800℃

(c) Slurry structure at 1 000℃ (d) Phase dispersion at 1 000℃

Figure 9 Micromorphology of NC at temperatures of 600°C, 800°C, and 1000°C

GHB/NC is significantly different from NC with its unique interface transition zone. Figure 10 shows the degradation process of the microstructure and morphology of the GHB/NC interface zone after high temperature treatment. It can be seen that the cement stone and vitrified microspheres are tightly combined at normal temperature, and the cement slurry enters the surface pores of the vitrified microspheres to form a tight two-phase mechanical meshing structure. The cement slurry is dense and the hydration product is in good condition; 200~400°C When the interface zone loses water, the cement slurry leaves defects such as holes after the water evaporates, but the mechanical meshing structure of the interface zone is not destroyed, and the macroscopic performance is a slight increase in strength; further heating to 600~1000°C, the cement water The slurry begins to decompose, become loose, and cracks criss-cross, producing obvious cracks and holes that penetrate each other, and the bonding force in the interface area gradually weakens.

In addition, after high temperature in the interface area between calcareous gravel and cement stone, the gravel and cement stone detach, and the interfacial bonding force is lost. It is precisely due to the combined effects of the softening and expansion of coarse aggregate as temperature increases, and the thermal decomposition and deterioration of cement hydration products that the strength of the specimen decreases significantly. After treatment at 800°C, the strength of GHB/NC was lost by 74.6%, and the strength of NC was lost. 72. 3%. After treatment at 1000°C, the strength loss of GHB/NC is 88. 2%, and the strength loss of NC is 88.5%.

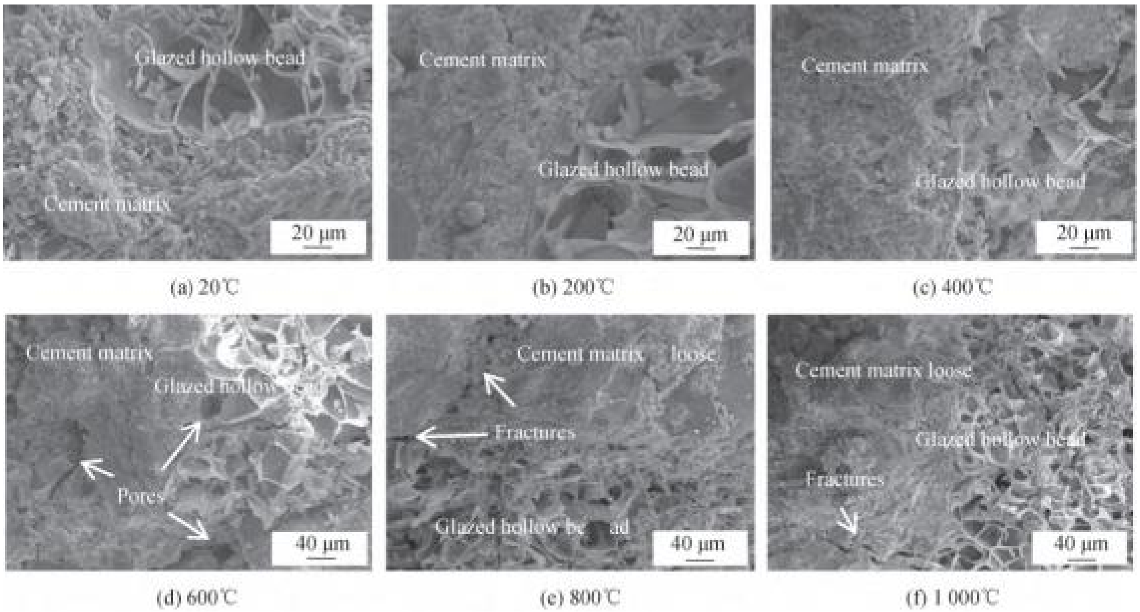

Figure 10 Microscopic morphology of the transition zone at the interface between GHB/NC vitrified microspheres and cement stone after high temperature

3 CONCLUSION

The mechanical properties, ultrasonic testing, and micromorphology of ordinary concrete (NC) and vitrified microsphere insulation concrete (GHB/NC) after high temperature were tested.

(1) Incorporating an appropriate amount of vitrified microspheres into concrete can effectively improve the heat insulation capacity of the material, the workability of the mixture, reduce the apparent density, and the compressive strength also decreases. When the heating temperature is higher than 800°C, the test block will appear to varying degrees. Damage, peeling, and peeling, the two types of concrete have similar strength loss rates after heating. After treatment at 800°C, the strength loss of NC is 72.3%, and the strength loss of GHB/NC is 74.6%. After treatment at 1000°C, the strength loss is basically lost. ability.

(2) Relative wave speed and damage degree are used to evaluate the performance deterioration of concrete after high temperature. As the heating temperature increases, the relative wave speed decreases, the damage degree gradually increases, and the compressive strength loss rate increases accordingly. The regression formula has a high fitting degree, indicating that It is reasonable and feasible to use relative wave velocity and damage degree to evaluate the degree of high-temperature deterioration of concrete.

(3) Conduct a microscopic analysis of the deterioration process of the cement slurry and the vitrified microsphere-cement stone interface transition zone after being exposed to different high temperatures. As the temperature increases, the internal cement gel gradually disperses and becomes loose from the whole, and the vitrified microspheres, coarse particles, etc. The bonding force between the aggregate and the cement stone continues to weaken and lose. The coarse aggregate softens and expands when heated, causing an increase in internal voids and surface cracks, and a loss of macroscopic strength. However, the structure of the vitrified microspheres was not significantly damaged after being exposed to a high temperature of 1000°C. It is an excellent high temperature resistant material.

COMPETING INTERESTS

The authors have no relevant financial or non-financial interests to disclose.

REFERENCES

[1] Guo Xingzhong, Yang Chuang, Zhang Chao. Simulation study on the impact of thermal performance of energy-saving doors and windows on building energy consumption. Journal of Building Materials, 2014, 17(2): 261- 265, 297.

[2] Hong Tianzhen. A close look at the China design standard for energy efficiency of public buildings. Energy and Buildings, 2009, 41(4): 426-435.

[3] FANShujing, WANG Peiming. Effect of fly ashondrying shrinkage of the rmalinsulation mortar with glazed hollow beads. Journal of Wuhan University of Technology (Materials Science Edition), 2017, 32(6): 1352- 1360.
[4] Sadinenisb, Madalas, Boehm RF. Passive Building energy savings: A review of building envelope components. Renewable and Sustainable Energy Reviews, 2011, 15 (8): 3617-3631.
[5] Gong Jianqing, Sun Kaiqiang. Effects of different water-cement ratios on the performance of vitrified microsphere thermal insulation mortar. Journal of Hunan University (Natural Science Edition), 2017, 44(1): 143- 149.
[6] Zhu Jiang, Li Guozhong. Performance of polypropylene fiber vitrified microsphere composite insulation materials. Journal of Building Materials, 2015, 18(4): 658- 662, 703.
[7] Wu Wenjie, Yu Yiming. Study on the mix ratio of vitrified microbead thermal insulation mortar based on single factor analysis. Materials Herald, 2014, 28(24): 385-390.
[8] Ma Gang, Zhang Yu, Li Zhu. Influencing factors on the interface micro hardness of lightweight concrete aggregate consisting of glazed hollow bead. Advances in Materials Science and Engineering, 2015, 2015: 1- 15.
[9] Zhao Lin, Wang Wenjing, Li Zhu. An Experimental study to evaluate the effects of adding glazed hollow beads on the mechanical properties and thermal conductivity of concrete. Materials Research Innovations, 2015, 19(S5): 929- 935.
[10] Zhang Yu, Ma Gang, Wang Zhangfeng. Shear behavior of reinforced glazed hollow bead insulation concrete.Construction and Building Materials, 2018, 174: 81-95.
[11] Dai Xueling, Zhao Huawei, Li Zhu. Research on the application of vitrified microspheres in self-insulating walls. Engineering Mechanics, 2010, 27(S1): 172- 176, 183.
[12] Gong Jianqing, Deng Guiguo, Shan Bo. Ultrasonic research and microscopic analysis of reactive powder concrete after high temperature. Journal of Hunan University (Natural Science Edition), 2018, 45(1): 68-76.
[13] Heap M J, Lavallee Y, Laumann A. The influence of thermal-stress (upto1000°C) onthe physical, mechanical, and chemical properties of siliceous-aggregate, high-strength concrete . Construction and Building Materials, 2013, 42: 248-265.
[14] SHAIKH FU A., TAWEEL M. Compressive strength and failure behaviour offibre concrete at elevated temperatures . Advances in Concrete Construction, 2015, 3 (4): 283-293.
[15] Xiong Houren, Xu Jinming, Liu Yuanzhen. Experimental study on hygrothermal deformation of external thermal insulation cladding systems with glazed hollow bead. Advances in Materials Science and Engineering, 2016, 2016: 1- 14.
[16] Pang Jianyong, Yao Weijing. Experimental study on new thermal insulation materials for high-temperature tunnels in deep coal mines. Mining Research and Development, 2016, 36(2): 76-80.
[17] Zhao Dongfu, Liu Mei. Experimental study on residual strength and non-destructive testing of high-strength concrete after high temperature. Journal of Building Structures, 2015, 36(S2): 365-372.
[18] Peng Gaifei, Yang Juan, Shi Yunxing. Experimental study on the residual mechanical properties of ultra-high performance concrete after high temperature. Journal of Civil Engineering, 2017, 50(4): 73-79.
[19] Peng Gaifei, Huang Zhishan. Change in micro structure of hardened cement plaster subjected to elevated temperatures.Construction and Building Materials, 2008, 22(4): 593-599.
[20] Jiang Yuchuan, Huo Da, Teng Haiwen. Research on the high temperature performance characteristics of shale ceramsite concrete. Journal of Building Materials, 2013, 16(5): 888-893.
[21] Gong Jianqing, Deng Guoqi, SHAN Bo. Performance evaluation of RPC exposed to high temperature combining ultrasonic test: A case study. Construction and Building Materials, 2017, 157: 194-202.
[22] Yan Lan, Xing Yongming. Effect of nano-SiO2 on the mechanical properties and microstructure of steel fiber/concrete after high temperature. Journal of Composite Materials, 2013, 30(3): 133-141.
[23] Jin Zuquan, Sun Wei, Hou Baorong. High-temperature deformation and microstructural evolution of concrete. Journal of Southeast University (Natural Science Edition), 2010, 40(3): 619-623.

World Journal of Materials Science
ISSN: 2960-0146
DOI: 10.61784/wjmsv2n246

ADVANCEMENT IN THE APPLICATION OF GRAPHENE AND GRAPHENE OXIDE IN FLUORESCENCE MEASUREMENT TECHNIQUES

Yong Park
Institute for Basic Science, Seoul National University, Seoul 151-747, Korea.

Abstract: As a new type of nanomaterial, graphene has some unique physical and chemical properties such as large specific surface area, good chemical stability, good optical and electrical properties, and is widely used in many fields. This article mainly introduces the research and development of fluorescence measurement methods of graphene and graphene oxide in metal ions, drugs, environmental pollutants and other compounds, and also looks forward to their application prospects in the field of measurement.
Keywords: Graphene; Graphene oxide; Fluorescence; Measurement

1 APPLICATION IN DETERMINATION OF METAL IONS

Graphene (G) is a two-dimensional crystal material composed of carbon atoms connected together in a hexagonal honeycomb shape formed by sp2 hybridization. In 2004, Novoselov et al. [1], scientists at the University of Manchester in the United Kingdom, prepared graphene in the laboratory using the tape method. The hexagonal honeycomb structure formed by its six-membered rings forms a large-scale π-π delocalized structure between layers. The special structure gives it many unique properties, including excellent mechanical, optical, thermal and electrical properties. It also has the advantages of large specific surface area, simple synthesis method, low price of raw materials and easy modification. Graphene oxide (GO) is an important derivative of graphene, which is mainly produced by oxidative exfoliation of graphite. Graphene oxide (GO) is an ideal two-dimensional nanomaterial. Its huge honeycomb planar conjugated structure gives it excellent thermal properties, electrical properties, biocompatibility, and quite high specific surface area and mechanical strength [2]. At the same time, a large number of active oxygen-containing functional groups (such as -O-, -OH, etc.) are enriched on the surface of GO, making it easy to disperse in water or other highly polar solvents [3] and facilitate further reactions with other substances to achieve GO surface functionalization. Through non-covalent bond modification and covalent bond modification, various small molecules or polymers can be efficiently grafted on the surface of GO, thereby enriching and improving the performance of GO [4,5]. Due to their large-area conjugated structures, graphene and GO can serve as energy receptors to quench the fluorescence of a variety of organic dyes and quantum dots. They are widely applicable fluorescence quenchers. Compared with traditional quenchers , Graphene material has higher quenching efficiency [6]. In recent years, fluorescence has begun to be combined with graphene. Using the fluorescence quenching properties of graphene, researchers have prepared a series of GO-based fluorescence sensors [7,8]. At the same time, because the surface of GO contains a large number of hydrophilic groups and is a carbon-based material, it is non-toxic and harmless to organisms and environmentally friendly.

Li Zhengshun et al. [9] synthesized graphene oxide using an improved Hummer method, and used a time-resolved spectral detection system to explore in detail the fluorescence quenching physics of graphene oxide by Fe^{3+} (concentrations of 0.5, 1, and 2 mmol/L). mechanism. In the steady-state fluorescence emission spectrum, as the Fe^{3+} concentration increases, the fluorescence intensity of graphene oxide decreases sharply. Time-resolved fluorescence spectroscopy and femtosecond transient absorption spectroscopy studies have confirmed that there is basically no change in the kinetic decay curve of GO added with different concentrations of Fe^{3+}. The fluorescence quenching of graphene oxide by Fe^{3+} is mainly a static fluorescence quenching process.

Zhu Yufeng et al. [10] in alkaline medium, graphene oxide adsorbed acridine orange (AO), which can quench the fluorescence of AO. By adding an appropriate amount of cadmium (II) ions, the fluorescence of the system at 526nm was enhanced. , the ΔF value has a good linear relationship with the cadmium (II) ion concentration in the range of 2.97×10 ~4.40×10 -8 mol/L. The linear regression equation is ΔF = 5.318 c(10 mol/L) + 13.34, r = 0.9970, the detection limit is 8.90×10mol/L, and the relative standard deviation is 1.58%~2.52%.

In order to study the fluorescence method of rapid detection of mercury ions in water, Liu Le et al. [11] designed a ssDNA sequence with a 5'-end labeled fluorescent dye (FAM) that can specifically bind mercury ions, and used graphene oxide to detect ssDNA and T- The difference in the affinity of the Hg^{2+}-T complex and the efficient quenching of fluorescence signals by graphene oxide have established a fluorescence method that can quickly and sensitively detect mercury ions in water. Under optimized test conditions, the detection range of mercury ions in water by this method is 0.1-100 μg/L, and the detection limit is 0.3 μg/L. Moreover, this method is easy to operate and has good selectivity, and is expected to be used for rapid detection of mercury ions in water.

Zhai Qiuge et al. [12] In aqueous solution, graphene oxide (GO) can quench the fluorescence of methylene blue (CMB). Adding an appropriate amount of Bi^{3+} can enhance the fluorescence of the system. The degree of fluorescence recovery increases with the increase in the amount of $Bi3+$. Based on this, a new method for the determination of $Bi3+$ using graphene oxide-methylene blue fluorescence photometry was established. The effects of the concentration of methylene blue, graphene oxide, acidity and the order of adding reagents on the fluorescence recovery of the system were investigated. The excitation wavelength of the complex system is 667 nm and the emission wavelength is 690 nm. Under optimized conditions, the concentration of $Bi3+$ is between 0.5 and 100 There is a good linear relationship with fluorescence intensity within the range of μmol·L-1, and the correlation coefficient is 0.9955. The detection limit of the method is 1.0×10-8 mol·L-1 (S/N =3). The new method has the advantages of high sensitivity, rapidity, and low cost. The proposed method was used for the analysis of environmental water samples, and the recovery rate was 93.4%~105.2%.

2 APPLICATION IN DRUG DETERMINATION

Ma Cuiping et al. [13] found that graphene oxide quenched the fluorescence of acridine orange in an acidic medium. Adding an appropriate amount of dopamine at this time resulted in an enhancement of the fluorescence intensity of the system, and the degree of enhancement was proportional to the amount of dopamine added. Based on this, a method for the determination of dopamine by acridine orange-graphene oxide fluorescence photometry was established. The mass concentration of dopamine is linear in the range of 0.05~12.0 μmol/L. The linear equation is $\Delta IF= 3.9 +57.8c(\mu mol/L)$, the correlation coefficient r= 0.9933; the detection limit is 2.9 nmol/L. This method has good selectivity and was applied to the determination of actual samples with satisfactory results.

Guo Ying et al. [14] used graphene oxide as a single carbon source and prepared graphene quantum dots (GQDs) with uniform morphology, good monodispersity and a size of about 5 nm through a simple ultrasonic-hydrothermal method. The prepared GQDs not only possess strong blue fluorescence emission but also have excitation wavelength-dependent fluorescence. Using GQD as the energy donor and vitamin B2 (VB2) as the energy acceptor, a fluorescence energy transfer system was established to detect VB2 content. Under optimized conditions, the detection range of this method is 1.0 × 10-6 ~ 3.0 ×10-5 mol·L-1, the correlation coefficient is 0.9978, and the detection limit is 3.3×10-7 mol·L-1.

Liao Juan et al. [15] used fluorescence spectroscopy to study the mechanism of action of graphene oxide nanoparticles (NGO) on bovine serum albumin (BSA). The results show that the fluorescence quenching type of BSA by NGO is mainly dynamic quenching and static and dynamic mixed quenching. At T= 283, 298, and 310 K, the minimum binding constants of the two are 6.7× 109, 9.5× 107, and 2.1× 106 L mol-1 respectively. The numbers of binding sites are 2.12, 1.32, and 0.87 respectively. The type of interaction between NGO and BSA is determined by thermodynamic parameters to be hydrogen bonding and van der Waals force. NGO quenches the fluorescence of tryptophan residues in BSA without changing the fluorescence emission intensity of tyrosine residues, but reduces the hydrophobicity of its environment.

Wei Hailang et al. [16] used new nanomaterials combined with fluorescence methods to achieve simple and rapid detection of pyrogallic acid in water samples. Graphene with fluorescent properties was prepared through a simple method of high-temperature pyrolysis of citric acid. Experiments found that horseradish peroxidase was used as a catalyst to catalyze the reaction of pyrogallic acid, and the changes in the fluorescence properties of graphene were used to focus on pyrogallic acid. Acid was quantitatively determined. In a phosphate buffer solution with pH=7.8, pyrogallic acid reacts under the action of a catalytic enzyme to form a colored substance, quinone, which can quickly quench the fluorescence intensity of graphene. Based on this, a pyrogallic acid fluorescence quenching detection method was designed. The experiment found that with the continuous addition of pyrogallic acid, the fluorescence quenching phenomenon gradually increased and showed good linearity.

Gong Qiaojuan et al. [17] used an improved Hummers method to prepare graphene oxide, and used infrared, Raman spectroscopy, and scanning electron microscopy to characterize the structure and morphology of graphene oxide, and investigated the effects of different solvents on L-tryptophan. Effect of fluorescence spectrum; L-tryptophan and graphene oxide were used as fluorescent agent and fluorescence quencher respectively, and the fluorescence quenching effect of graphene oxide on L-tryptophan was studied with the help of fluorescence spectroscopy. According to the ultraviolet absorption spectrum, Stern-Volmer equation and Lineeweawer-Burk double reciprocal curve equation, parameters such as graphene oxide's fluorescence quenching type of L-tryptophan, quenching rate constant (kq) and binding constant (K) were obtained . The results show that graphene oxide has a strong quenching effect on the fluorescence of L-tryptophan, and its fluorescence quenching mechanism is the static quenching of the complex formed by graphene oxide and L-tryptophan.

3 APPLICATION IN DETERMINATION OF ENVIRONMENTAL POLLUTANTS

Ye Qing et al. [18] synthesized magnetic graphene through hydrothermal reaction, used magnetic graphene as magnetic solid phase extraction material, and established a new method for the determination of trace amounts of bisphenol A in water combined with fluorescence photometry. The effects of parameters such as the amount of magnetic graphene, the type and volume of eluent, and the time of extraction and elution were investigated. Under the optimized experimental conditions, the detection limit of the method was 3.3 ng/L, the linear range was 0.01-0.5 μg/L, the correlation coefficient was 0.9995, and the relative standard deviation was 4.1%. The method was applied to the analysis of the dissolution of bisphenol A in disposable water cups, and the recovery rate of standard addition was between 96% and 105%.

Zhang Tairan et al. [19] used a two-step reduction method to reduce graphene oxide (GO), and during the reduction process, the graphene surface was sulfonated through a diazonium salt reaction, which improved the solubility of graphene in water. Atomic force microscopy (AFM), ultraviolet-visible absorption spectroscopy (UV-vis), Raman spectroscopy (Raman) and X-ray photoelectron spectroscopy (XPS) were used to study the morphology of graphene and the composition and structure changes during the reduction process. Characterized. After reduction and sulfonation of graphene, a large number of oxygen-containing functional groups on the carbon atom plane disappear. The size of the obtained graphene sheet is about 1 μm, the number of layers is roughly double layer, and it can be evenly and stably dispersed in water. On this basis, the behavior of graphene as a fluorescence quenching substrate in quenching the high quantum efficiency fluorescent dye rhodamine B solution was studied, confirming that graphene is a good fluorescence quencher. This lays the foundation for its applications in fluorescence detection and biomolecule sensing.
Liu Zhongde et al. [20] used graphene oxide as the precursor and gallic acid as the reducing agent and stabilizer to synthesize reduced graphene oxide in one step through a simple water bath heating method. A series of analysis and characterization of the product were carried out using UV-visible absorption spectrum, Fourier transform infrared spectrum, Raman spectrum, X-ray diffraction and scanning electron microscope. The results show that gallic acid can reduce graphene oxide to graphene. In addition, the effect of the prepared reduced graphene oxide on the fluorescence intensity of anionic and cationic fluorescent functional groups was also investigated. The results show that reduced graphene oxide synthesized through gallic acid-mediated synthesis can effectively quench the fluorescence of cationic functional groups such as rhodamine and enhance the fluorescence of anionic functional groups such as fluorescein, so that fluorescent functional groups can be selectively identified.
Wang Shuhui et al. [21] successfully synthesized β-cyclodextrin (β-CD) modified graphene (β-CD-GNs) using a wet chemical method, and discussed its effect on α-naphthol and β-naphthol in aqueous solution. identification function. The results show that graphene-functionalized β-CD can recognize α-naphthol and β-naphthol at the same time, causing their fluorescence to be quenched; the quenching of α-naphthol by β-CD-GNs includes the entry of α-naphthol into β-naphthol. The quenching caused by the inner cavity of -CD and the π-π interaction between graphene and α-naphthol, while the quenching of β-naphthol by β-CD-GNs is mainly due to the interaction between graphene and β-naphthol. Due to π-π interactions between phenols.

4 CONCLUSION

As a well-known natural phenomenon with a long history, cathode fluorescence of graphene has been fully and extensively studied in theory and application. Graphene has a unique structure, stable physical and chemical properties, good biocompatibility and excellent electrical, thermal, mechanical and other properties. Graphene has very attractive applications in the determination of metal ions, drugs and environmental pollutants. prospect. Since graphene has a fixed structure and properties, its development and application are also subject to corresponding restrictions. Introducing specific functional groups on the surface of graphene can greatly expand the application range of graphene, endow graphene with various new functions, and improve the compatibility of graphene with other matrices. At the same time, almost any active group loaded onto graphene, a surface with a huge specific surface area, can actively demonstrate its application performance. Functionalized modified graphene has become a hot research topic today. A large number of novel graphene-based Functional hybrid materials have been reported one after another. However, in the fluorescence sensing process, the role of functionalized graphene is mostly to quench fluorescence rather than to generate fluorescence. It is hoped that in future research on graphene fluorescence sensors, functionalized graphene materials that can generate fluorescent signals will be developed to improve the sensitivity and accuracy of detection methods. In short, the application of graphene-based optical sensors is an emerging field that deserves great attention.

COMPETING INTERESTS

The authors have no relevant financial or non-financial interests to disclose.

REFERENCES

[1] KS Novoselov, AK Geim, SV Morozov. Electric field effect in atomically thin carbon films. Science, 2004, 306(96): 666-669.
[2] Zhang Hao, Cui Hua. Graphene oxide fluorescence sensor. Advances in Chemistry, 2012, 24, (8): 1554-1559.
[3] Han X, Fang X, ShiA. An electrochemical DNA biosensor based on gold nanorods decorated graphene oxide sheets for sensing platform. Analytical biochemistry, 2013, 443(2): 117-123.
[4] Lin Yuanwei, Guo Xuefeng. Chemical modification of graphene surface interface and its functional regulation. Acta Chemica Sinica, 2014, 72(3): 277-288.
[5] Yang Cheng, Chen Yubin, Tian Junpeng. Research progress on the preparation and application of functionalized graphene, Journal of Aeronautical Materials, 2016, 36 (3): 40-56.
[6] Gao Yuan, Li Yan, Su Xingguang. Research progress on graphene-based optical biosensors, Analytical Chemistry, 2013, 41(2): 174-180.
[7] Gao Yuan, Li Yan, Su Xingguang. DNA sensor based on graphene oxide quenching effect for specific detection of melamine, Nuclear Technology, 2012, 35(5): 386-389.

[8] Li Wei, Liu Zheng, Wei Xi. Application study on rapid detection of tartrazine content based on indigo double Schiff base graphene oxide fluorescence sensor, Chinese Food Additives, 2014, 25(9): 195-200.
[9] Li Zhengshun, Wang Yan, Wang Lei. Study on the fluorescence quenching mechanism of graphene oxide by Fe3+, China Optics, 2016, 9(5): 569-578.
[10] Zhu Yufeng, Peng Lilan, Wang Yongsheng. Determination of cadmium (II) ions by graphene oxide-acridine orange fluorescence photometry, Applied Chemical Engineering, 2016, 45(7): 1379-1381
[11] Liu Le, Wu Yuangen, Zhan Shenshan. Graphene oxide high-efficiency quenching fluorescence method for rapid detection of mercury ions in water, Journal of Shanghai Jiao Tong University (Agricultural Science Edition), 2014, 32(6): 1-6.
[12] Zhai Qiuge, Guo Peng, Zhou Lin. Sensitive determination of bismuth (III) ions by fluorescence photometry of graphene oxide-methylene blue system, Spectroscopy and Spectral Analysis, 2014, 34(8): 2152-2156.
[13] Ma Cuiping. Determination of dopamine by acridine orange-graphene oxide fluorescence quenching method, Journal of Analytical Testing, 2011, 30(3): 340-343.
[14] Guo Ying, Liu Yang, Zhao Qin. Graphene quantum dots-VB2 determination of VB2 by fluorescence energy transfer method, Guangzhou Chemical Industry, 2014, 42(23): 138-139, 173.
[15] Liao Juan, Zhang Yanhua, Ye Xiaozhou. Interaction between graphene oxide nanoparticles and bovine serum albumin, Spectroscopy Laboratory, 2013, 30(5): 2235-2241.
[16] Wei Hailang, Cao Liming. Experimental study on the detection of pyrogallic acid by fluorescence quenching method, Journal of Shanxi University (Natural Science Edition), 2015, 38(4): 670-674.
[17] Gong Qiaojuan, Wang Yongdong, Yang Haiying. Study on the fluorescence quenching of L-tryptophan by graphene oxide and its mechanism, New Carbon Materials, 2016, 31(6): 639-645.
[18] Ye Qing, Liu Xiaofei, Hong Liming. Magnetic graphene solid-phase extraction fluorescence photometry to determine the dissolution of bisphenol A in disposable water cups, Analytical Laboratory, 2016, 35(7): 806-808.
[19] Zhang Tairan, Sun Luwei, He Haiping. Chemical preparation of water-soluble graphene and its fluorescence quenching application, Journal of Materials Science and Engineering, 2013, 31(4): 484-488.
[20] Liu Zhongde, Liu Chunfang, Yang Hui. Selective recognition of fluorescent functional groups by gallic acid-mediated synthesis of reduced graphene oxide, Science China: Chemistry, 2014, 44(3): 358-365.
[21] Wang Shuhui, Huang Yuming. Fluorescence method to study the recognition effect of β-cyclodextrin modified graphene on α-naphthol and β-naphthol, Journal of Southwest University (Natural Science Edition), 2015, 37(7): 129-132.

World Journal of Materials Science
ISSN: 2960-0146
DOI: https://doi.org/10.61784/wjms3001

VALUE, DILEMMA AND OPTIMIZATION PATH OF COMMUNITY PUBLIC SERVICE UNDER THE PERSPECTIVE OF INTEGRATED MEDIA RESEARCH

Wei Tang*, XiaoZhen Li, JinRui Shi, LiYu Chen
School of Tourism and Historical Culture, Zhaoqing College, Zhaoqing 526061, Guangdong, China.
Corresponding Author: Wei Tang, Email: angletw@aliyun.com

Abstract: Community public service is an important support to improve the social security system, ensure the basic rights and interests of groups in difficulty, and improve people's sense of well-being, and improving community public service has become a broad consensus of the whole society. Based on the perspective of integrated media, it is found that community public service has the value of life service and social participation; there are three major dilemmas in community public service: insufficient publicity, poor participation mechanism and lack of professionalism. Accordingly, three optimization paths are proposed: creating diversified forms of publicity, constructing a public participation system, and strengthening the professional quality of personnel.
Keywords: Integrated media; Community public service; Service value; Optimization path

1 INTRODUCTION

Community is a fundamental platform for public services and livelihood protection, a guaranteed cornerstone for building a harmonious society and a happy China, and a realistic carrier for convenience, quality and happiness of life[1]. Relevant data from the Ministry of Civil Affairs shows that the number of community service centers and service stations in China in 2018-2021 is also showing a trend of increasing day by day (Figure 1).The media,as an important tool and channel for community public service dissemination and supervision, is an important directional guide to enhance the value of community public service and optimize public service strategies. In recent years, China has attached great importance to the development of integrated media and focused on the communication power and effectiveness of grassroots integrated media. Under the background of big data, cloud computing and "Internet+", we should explore the value of community public services with the help of integrated media, explore its dilemma, and put forward optimization paths based on domestic and international experiences in community public service construction.

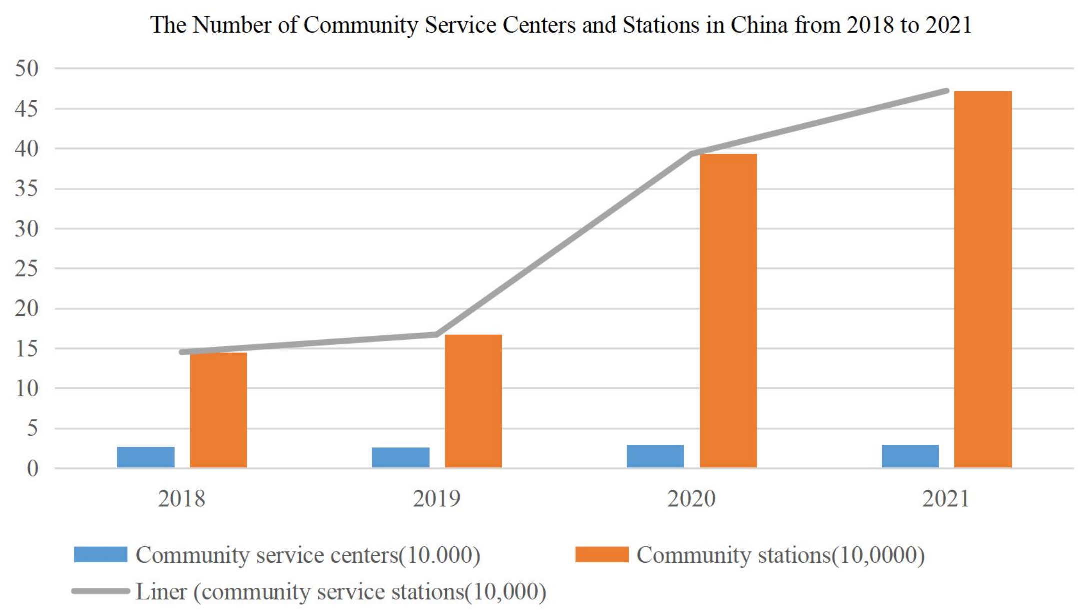

Figure 1 Number of Community Service Centers and Service Stations in China from 2018 to 2021

2 VALUE OF COMMUNITY PUBLIC SERVICES

Community public layout and service, in fact, is a material important carrier catering to the behavioral needs of the general public, but also a community cultural space performance for the general public to unfold their lives and obtain spiritual perception[2]. In the era of melting media, everything is a medium, how to better explore the value of community public services (see Figure 2), build a melting media community public service channel based on new and old media such as newspapers, WeChat, Jitterbug, short videos, etc., and integrate the social resources so that the community residents can more easily enjoy the intelligent community life services[3].

2.1 Value of Life Services

Under the background of integrated media, traditional media such as radio, television and newspaper bring the value of life service to community residents, which is mainly reflected in the following two points:information transmission and community organization.Community workers communicate national, provincial, municipal and county policies to every resident in the community through radio, WeChat, video, etc., so that the policy information "sound" into the hearts of the people.Community public service has long played the role of information organization and disseminator,can cohesion community identity and sense of belonging, integration of community opinion role.Through the community clinic volunteer education, housing rental information, supermarket discount promotion information can effectively enhance the timeliness of local service information. The smart community service platform built through emerging media makes the connection between residents and the community more convenient and efficient while enhancing the effectiveness and temperature of community grassroots management. With the development of integrated media and other technologies, the life service function of the smart community service platform has become more and more prominent, not only enriching the daily life of residents, but also popularizing health and other life knowledge and policy information, and also allowing for more inquiries about the weather conditions, online booking of recreational services, prompting a significant increase in the convenience of public life in the community.

2.2 Value of Social Participation

The Internet is a platform for the transmission of information and a vehicle for the effective connection between people and society. The media can effectively enhance the sense of ownership of community residents and help strengthen their community identity. Residents discover and explore interesting people, events and things around them through community online media, express their views and demands, enhance residents' initiative, self-awareness and enthusiasm in participating in community management, and strengthen their sense of community belonging. Residents' happiness gained through community public services is expressed through online or offline integrated media channels, for example, a happy neighborhood sharing meeting can be initiated through smart community platforms, WeChat groups, and Jitterbug live broadcasts, allowing community residents to participate widely and offer advice. Through the establishment of WeChat groups to increase residents' sense of belonging, improve neighborhood relations, better reflect the value of community public services, and achieve the goal of "community autonomy". Making full use of the community media platform to promote volunteer activities, we call on community residents to participate in and accept volunteer activities, such as legal counseling, haircutting, health guidance, education and psychological counseling, etc., so as to let residents feel the love of volunteers and the enthusiasm of the community, to further enhance the feelings of the residents, and to fully demonstrate the value of social participation of the residents. Logic of value generation of community public services under the perspective of melting media can be seen in Figure 2 below.

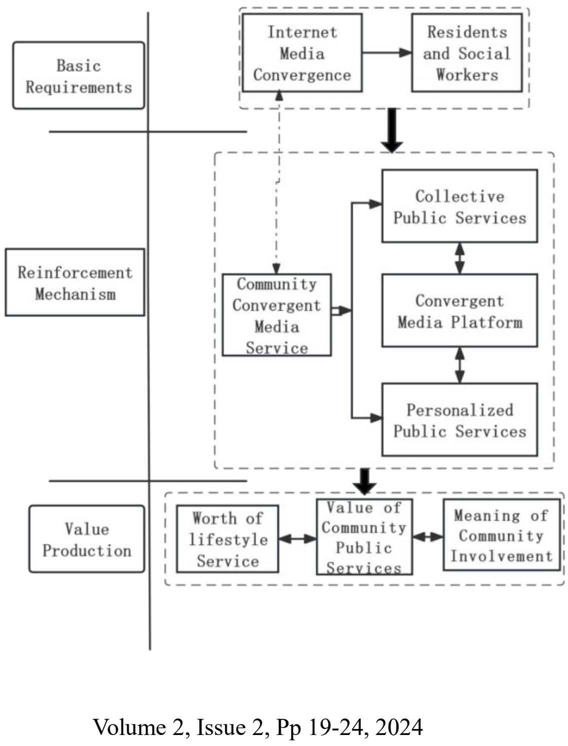

Figure 2 Logic of Value Generation of Community Public Services under Perspective of Melting Media

3 ANALYSIS OF THE PLIGHT OF COMMUNITY PUBLIC SERVICES

3.1 Inadequate Publicity for Community Public Services

National, provincial and municipal departments and other relevant departments have issued a series of documents and work task guidelines, proposed to improve the urban and rural community public management system, improve the streets (towns) centers, community (village) public service stations set up to facilitate the work of the public. Through visits and surveys, it is observed that many communities have set up corresponding community public service stations in accordance with the relevant requirements, but the public's knowledge of community public services is obviously insufficient, which is mainly reflected in the type of distribution of community public services, community public service hours, community public service processes, etc., and the majority of residents do not know enough. Visits to the research found that many community residents believe that they get community public service related information is through others to inform or in the form of street posting announcements, community public service there is insufficient publicity, publicity is not enough, publicity is not strong enough, publicity in a single way and other publicity problems. Grass-roots cadres are the primary subjects of community governance, and the single and lagging publicity and promotion platforms and means reflect the insufficient utilization of community cadres' mastery of the technology and means of integrated media[4]. The shortcomings of community managers in the mastery and use of the integrated media make them unable to become strong supporters and promoters of the integrated media in social governance, which to a certain extent restricts the use and development of the integrated media in grassroots official affairs, especially in community public services.

3.2 Poor Mechanisms for Participation in Community Public Services

Community is one of the most basic units and subjects of social governance, and community governance is one of the most important, basic and crucial aspects of social governance[5]. Community participation is a popular guarantee of the effectiveness of community governance, and an important way to strengthen China's democratic institutions, implement harmonious social development, and promote social innovation and vitality[6]. Among the issues that community public services should focus on, clear channels should be provided to facilitate community residents to actively contribute to community building and development. Most of the residents have high initiative, enthusiasm and willingness to participate in community construction, but the existing community public service provision and participation channels are insufficient, and the community grassroots managers' old-fashioned thinking and management style lead to the shortcomings of the ways and systems for community residents to express their interests, and the lack of specific, standardized, guiding and oriented management system. The lack of transparency in community information, the lack of a single channel for residents to participate in community management and services, and the lack of a smooth channel for community residents to raise issues and offer advice and suggestions have affected the value of community public services, and are not conducive to the full realization of a moderately prosperous society and a harmonious socialist society in general.

3.3 Lack of Professionalism among Community Workers

The degree of specialization and quality of community staff is the talent guarantee for normal and efficient operation of the community, and is also an important indicator of the local economic and social development and the level of community services[7]. The comprehensive quality and service attitude of community staff is the core element that affects the satisfaction level of community public services. Due to the influence of many factors such as the differences in economic development, the overall professional degree of the existing community staff is relatively insufficient, and there is a lack of patience, meticulousness and warmth in the process of work. As an important mass support for economic and social development of the community, the comprehensive quality of the staff and the level of specialization is one of the basic guarantee of social and economic development, can be achieved by improving the business capacity and the necessary knowledge system and professional quality. In addition to basic professional skills, with the arrival of the era of integrated media and Internet "+", community staff mastery and use of integrated media technology is obviously insufficient, affecting the realization of the value of community public services.

4 PATHS TO OPTIMIZE COMMUNITY PUBLIC SERVICES

4.1 Creating Diversified Forms of Community Public Service Promotion

A single way of publicizing community public services has led to a lack of understanding by residents of the types, timing and characteristics of community public services. This can be achieved by appropriately increasing the number of community public service publicity activities and developing diversified publicity methods, for example, by setting up integrated media publicity points in densely populated and highly trafficked areas of community compounds, guiding passing residents to participate in interactions, answering their questions and solving their problems in terms of public service matters of concern to residents, such as community policing, medical and health care, basic education, culture and sport, and social security, and guiding them to share their experiences and to participate in various types of public service experiences. Participate in various public service experiences. The publicity content of community public services is integrated into programs such as dance, group chorus and Tai Chi, forming a fusion of the regular offline performance of community public service publicity and the online integration of integrated media, and promoting the formation of an "integrated media platform" for community publicity work. Based on the form of integrated media to carry out community public service publicity should be based on the situation, adapt to the situation, bold use of new technologies, new modes, new platforms, in order to speed up the integration: with the help of China service center WeChat public number released community public service monthly, quarterly and annual development, through the Internet dissemination can let the residents understand the public service, public service, participation in public service. Carry out diversified, centralized, regular publicity activities, more closely related to the immediate interests of community residents of public service matters to the residents, so that the residents know the matter, know the situation, get the benefits, can further enhance the community residents of community public service participation, sense of access, satisfaction and sense of well-being[8].

4.2 Building a System of Public Participation in Community Public Services

Establishing and improving the community media as the main platform for the formation of community resolution rules, public hearing mechanisms, expert consultation mechanisms and other orderly operation of the community, and guiding the initiative and enthusiasm of community residents to participate in community governance[9]. Through the integrated media, community union organizations and neighborhood committees are strengthened and guided to expand the positive roles of trade unions, the Communist Youth League and the Women's Federation, safeguard the reasonable interests of community residents, and strive to resolve community conflicts, so as to form a new situation in which the demands of residents are effectively met, community conflicts are continually resolved, and the well-being of residents is increasingly enhanced by the "integrated media" of public services in the community. Through WeChat, Jitterbug, short videos and other forms of integrated media to guide the residents into the community public service governance initiative, enthusiasm and sense of achievement, to promote community public service "common sharing, self-service, sound development". WeChat, Jitterbug, community parties, community volunteer activities, community bulletin boards, short videos and other forms of integrated media to establish and form a community service honor system, recognize advanced community services, and form a harmonious community of "co-construction, co-management and sharing". Relying on integrated media and Internet "+" technology, promote the creation of "smart communities", improve the level of community informationization, expand "smart communities" and "digital families". The organic integration of "smart community" and "digital family". Based on the integration of media, we have explored community public service resources, created an organic interaction between the community and residents of the integration of media information service platforms, inspired community residents to take the initiative to integrate into the community's sense of ownership of public services, and effectively constructed a harmonious and happy community based on the integration of media, "all for one and one for all".

4.3 Strengthening the Professionalization of Community Workers

The degree of professionalization of community staff has a direct impact on the quality of community public services and the efficiency of the use of community public resources, which further affects the sense of belonging and happiness of community residents. To establish a sound online management platform for community assessment, incentives and constraints based on "integrated media", and to construct a new community public service management model focusing on "integrated media": to comprehensively improve the assessment and evaluation measures for community cadres in line with the scientific outlook on development, to explore the construction of a diversified integrated and synergistic assessment mechanism for the official, social organizations and the public, and to enhance the participation of community residents in community public service and happiness. It has also explored the construction of a diversified, integrated and coordinated evaluation mechanism for the official, social organizations and the public, so as to enhance the enthusiasm of community residents in participating in community public services and management. While taking "public satisfaction" as the guide for community public services, training is carried out among community staff, and in addition to basic professional knowledge and skills, more training is expanded to train on the organic integration of integrated media and community public services with daily service management of the community. Popularize the knowledge of community governance in the era of melting media is the core content and inevitable demand of constructing a new pattern of community governance and promoting the modernization and development of community governance[10]. Through the letter public number, micro letter group, jittery voice, short video and other integrated media channels, diversified publicity volunteer activities, and actively mobilize residents to actively participate in community governance, and actively cultivate and grow the community service team. Based on the innovative working idea of "integrated media", we are committed to establishing a joint working mechanism of "community workers guiding volunteers and volunteers assisting community workers", which can not only strengthen the construction of community work team, but also consciously form an efficient and sustainable community residents' self-management. Self-management.The value,dilemma and optimization path of community public service under the perspective of integrated media can be integrated into the following figure 3.

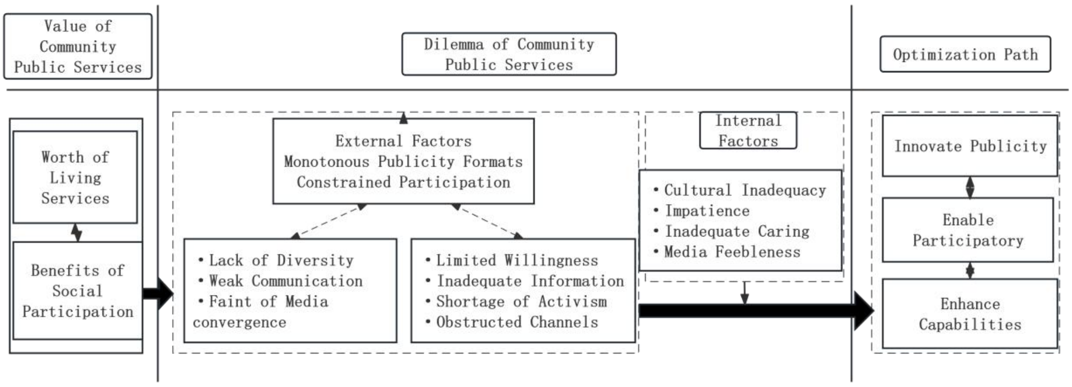

Figure 3 Value, Dilemma and Optimization Path of Community Public Service under the Perspective of Integrated Media

5 CONCLUSION

As an important tool and channel for the dissemination and monitoring of community public services, the media is an important directional guide for enhancing the value of community public services and optimizing public service strategies. In recent years, China has attached great importance to the development of integrated media and focused on the communication power and effectiveness of grassroots integrated media. Under the background of big data, cloud computing and "Internet+", the value of life service and social participation value of community public service can be explored by means of integrated media; there are three major dilemmas in community public service: insufficient publicity, poor participation mechanism and lack of professionalism. Accordingly, the three optimization paths of creating diversified forms of publicity, constructing public participation system and strengthening the professional quality of personnel are proposed. This will help to optimize the community service system and the quality of community public services, improve the quality of life of the residents, and promote and facilitate the construction of a happy and harmonious society.

COMPETING INTERESTS

The authors have no relevant financial or non-financial interests to disclose.

FUNDING

This article is sponsored by projects:2021 Guangdong Province Higher Education Teaching Reform and Construction Project“Research on the Optimization Path of the Practical Teaching System for Tourism Management Majors Based on Innovation and Entrepreneurship Ability Cultivation”; Zhaoqing Social Science Federation Project (24GJ-06); Open Topic on Ideological and Political Work of Zhaoqing University 2023 (SXZZ202304);Zhaoqing Social Science Federation Project(23GJ-54); Zhaoqing University Research Fund (QN202419).

REFERENCES

[1] Hao Haibo. Value Connotation, Governance Structure and Action Strategy of Community Governance in the New Era-Studying General Secretary in Important Discourse on Community Governance. Socialist Studies, 2020(03): 108-115.
[2] Yu Yanghang. Public services in urban communities, life satisfaction and residents' sense of access. Northwest Population, 2021(03): 78-90.
[3] MING Qingzhong, LI Zhifei, XU Hong, et al. Theoretical cognition and application innovation of rural tourism resources in China under the goal of common wealth. Journal of Natural Resources, 2023(02): 286-304.
[4] Chu Qingyi, Zhao Xiaofeng. Practical Logic of Union Organization Leading Community Governance Community Construction under the Perspective of Organizational Field--Taking Yonglian Village in Southern Jiangsu as an Example. Journal of Nanjing Agricultural University (Social Science Edition), 2023(01): 125-134.
[5] ZHANG Wenhua, MA Qingping, QIN Xiaofeng. Multi-subject interaction and relational reshaping of grassroots community governance under the perspective of individual-centered networks. Social Work, 2022(06): 16-29.
[6] Chen Rongzhuo, Hu Enchao. Leading Governance: How is it Possible to Pilot National Reforms? --Taking the construction of "National Rural Community Governance Experimental Area" in Jianghai District, Guangdong Province as an example. China Rural Observation, 2022(04): 2-20.
[7] REN Wenqi, GU Donghui. The process, dilemma and practice strategy of social workstation construction under the vision of grassroots governance professionalization.Social Work and Management, 2022(06): 50-59.

[8] Wang Liyuan. Research on the Governance Path of "Village to Residence" Community in Chenggong District, Kunming under the Perspective of Empowerment Theory. Kunming: Yunnan Normal University, 2022.

[9] FANG Yaming, GU Huilin. Optimizing the mechanism of urban grassroots governance empowered by whole process people's democracy.Journal of Tianjin Administrative College, 2023, 25(01): 3-13.

[10] HAN Ruibo, TANG Ming. Why community governance innovation research reflects theoretical self-consciousness. Journal of Huazhong University of Science and Technology (Social Science Edition), 2023, 37(01): 37-46.

World Journal of Materials Science
ISSN: 2960-0146
DOI: https://doi.org/10.61784/wjms3002

STUDY ON THE SOUND ABSORPTION PERFORMANCE OF ULTRA-MICROPOROUS HONEYCOMB ALUMINUM PANELS

YueQiang Cao[1,2], ZhiYuan Zhang[1,2*], ZhenJie Tan[1,2], Xing Gao[1,2], YinGuang Wang[1,2]
[1]China Construction Fourth Engineering Bureau Co., Ltd., Guangzhou 510000, Guangdong, China.
[2]China Construction Fourth Engineering Bureau Sixth Construction Co., Ltd., Hefei 230000, Anhui, China.
Corresponding Author: ZhiYuan Zhang, Email: 2557841138@qq.com

Abstract: In order to reduce the impact of intensive noise on personnel comfort in multi-functional exhibition halls, based on the micro-perforation theory, this paper systematically analyzes the sound insulation and sound absorption properties of ultra-microporous honeycomb aluminum panels. By establishing an acoustic finite element model, simulation technology was used to explore the sound insulation and sound absorption coefficient of ultra-microporous honeycomb aluminum panels in the range of 100Hz to 5000Hz. At the same time, the sound insulation amount and sound absorption coefficient were experimentally measured by combining the reverberation chamber method and the standing wave tube method. The results show that the simulation results of ultra-microporous aluminum honeycomb panels are highly consistent with the experimental data. The weighted sound insulation is 27.0dB (experimental value 26.8dB), and the sound absorption coefficient NRC reaches 0.63, which is significantly better than ordinary aluminum honeycomb panels. Research shows that ultra-microporous honeycomb aluminum panels have good noise reduction effects, help improve the acoustic environment in large spaces, and improve personnel comfort.
Keywords: Ultra-microporous honeycomb aluminum plate; Sound absorption performance; Sound insulation; Finite element simulation; Reverberation chamber method; Standing wave tube method

INTRODUCTION

In large indoor spaces such as modern multi-functional exhibition halls, the presence of noise seriously affects personnel comfort and activity experience. Traditional aluminum honeycomb panels are widely used in interior decoration due to their simple structure and light weight. However, their sound absorption performance is relatively poor, especially in the low-frequency area [1,2]. In recent years, ultra-microporous honeycomb aluminum panels, a new sound-absorbing material based on micro-perforation theory, have shown great potential in improving sound absorption effects due to their unique pore structure and porous layer design [3]. However, the specific sound absorption performance of ultra-microporous aluminum honeycomb panels and its comparison with traditional aluminum honeycomb panels have not been fully studied. Therefore, this article aims to systematically explore the sound insulation and sound absorption properties of ultra-microporous honeycomb aluminum panels through a combination of simulation and experiment, in order to provide a theoretical basis for its optimization in practical applications.

1 RESEARCH MATERIALS

1.1 Conventional Honeycomb Aluminum Plate

Conventional honeycomb aluminum panels are composed of two layers of thin aluminum plates and lightweight aluminum honeycomb core materials bonded through an adhesive to form a layered composite structure. The honeycomb core material is a regular hexagonal hole with a side length of 8mm, a material thickness of 0.08mm, and a height of 18mm.

1.2 Ultra-Microporous Honeycomb Aluminum Plate

As a new type of sound-absorbing material, ultra-microporous honeycomb aluminum plate is composed of micro-perforated aluminum plate, perforated aluminum plate non-woven fabric and aluminum honeycomb core material. The specific structure is as follows: behind the plate is a micro-perforated aluminum plate with a thickness of 1mm. The hole shape is an isosceles right triangle, the length of the hypotenuse is 0.4mm, the hole center distance is 2.2mm, and the perforation rate is 0.65%; a layer of 0.2mm thick is attached underneath it. Non-woven porous sound-absorbing material; the bottom of the board is a perforated aluminum plate with a thickness of 1mm, a hole diameter of 2.5mm, a hole center distance of 4.5mm, a perforation rate of 23.8%, and a layer of non-woven porous sound-absorbing material with a thickness of 0.2mm. ;The middle aluminum honeycomb core material is the same as ordinary aluminum honeycomb panel. These can be seen in Figure 1-4.

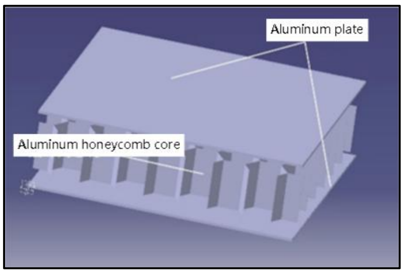

Figure 1 Ordinary Aluminum Honeycomb Panel Structure

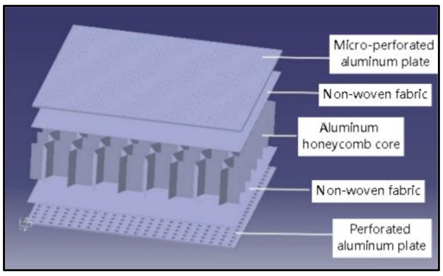

Figure 2 Ultra-Microporous Aluminum Honeycomb Panel Structure

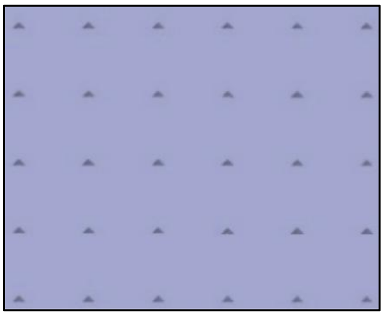

Figure 3 Micro-Perforated Aluminum Plate

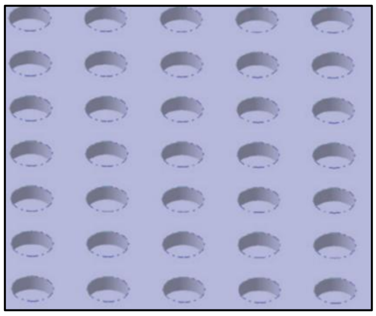

Figure 4 Perforated Aluminum Plate

2 SIMULATION ANALYSIS

As shown in Figure 5 and 6, for the ultra-microporous honeycomb aluminum plate, the acoustic finite element model of the air on the sound-emitting side and the receiving side was established. During the model pre-processing process, the material properties and grid properties of the structure were defined, and fixed constraints were placed around the ultra-microporous honeycomb aluminum plate. Furthermore, the acoustic fluid material and its properties are defined, and a field point grid equivalent to a microphone is set up for monitoring sound pressure.

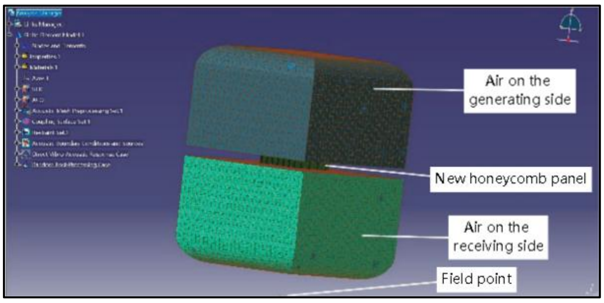

Figure 5 Sound Insulation Simulation Model

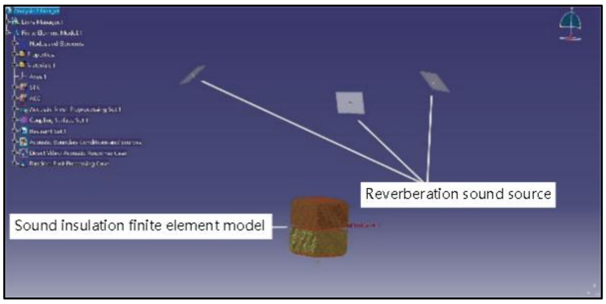

Figure 6 Reverberation Sound Source

The Direct-Acoustic Response Analysis Case is used to perform direct acoustic-vibration coupling calculations on ultra-microporous honeycomb aluminum panels. Subsequently, the coupling response was synthesized into a random calculation response using the Random Post-Processing Case, and a 1/3 octave sound insulation curve in the range of 100Hz to 5000Hz was obtained (see Figure 7). The simulation results show that ultra-microporous honeycomb aluminum panels have poor sound insulation performance at low frequencies (200Hz and 315Hz), but above 800Hz, the sound insulation capacity increases significantly as the frequency increases. The weighted sound insulation is 27.0dB.

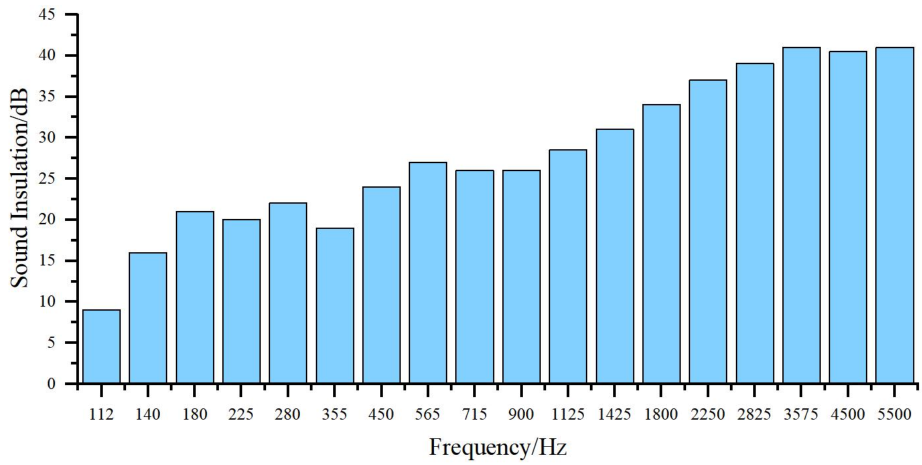

Figure 7 Changes in Sound Insulation

In Figure 8, it can be seen from the simulation calculation results that the low-frequency sound insulation performance of the ultra-microporous honeycomb aluminum plate is poor. The sound insulation amount is significantly reduced at 200Hz and 315Hz. After 800Hz, the sound insulation amount increases with the increase of frequency. The weighted sound insulation amount of the simulation results is calculated. is 27.0dB.

Furthermore, an acoustic finite element model of the impedance tube was established for the ultra-microporous honeycomb aluminum plate, and the acoustic grid was pre-processed. Define the material and grid properties of the structure, define the acoustic fluid material and properties, define a plane sound source on the other side of the air column, and set up two field point grids 1 and 2 equivalent to microphones for monitoring.

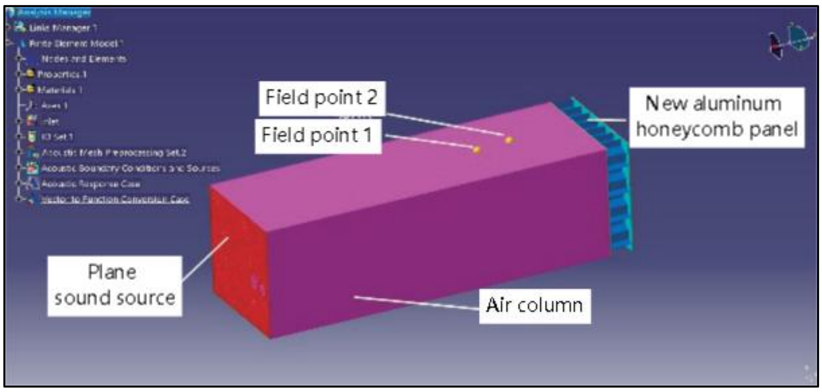

Figure 8 Sound Absorption Simulation Model

Use the Acoustic Response Analysis Case to calculate the acoustic response, then use the Vector to Function Conversion Case to obtain the sound pressure frequency response function at the two field points, and process the data to obtain the sound absorption coefficient curve. Changes in sound absorption coefficient can be seen in Figure 9.

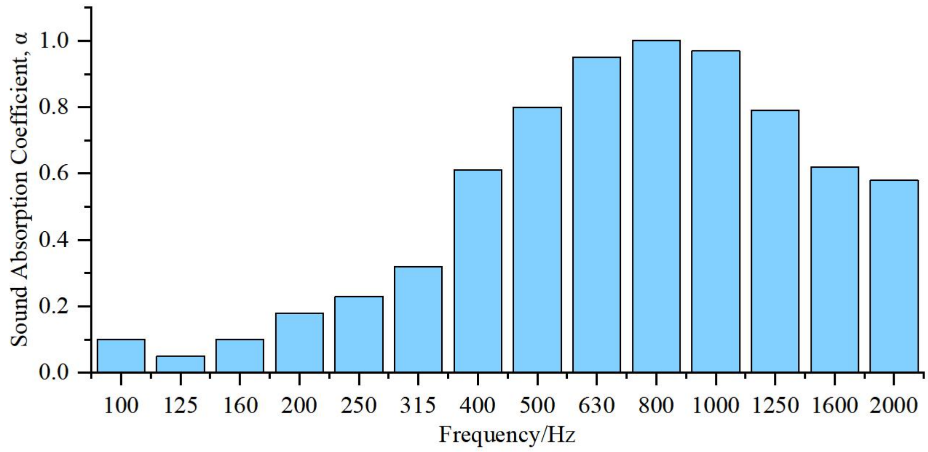

Figure 9 Changes in Sound Absorption Coefficient

It can be seen from the simulation calculation results that the ultra-microporous honeycomb aluminum plate has poor low-frequency sound absorption effect. The sound absorption coefficient reaches the maximum value of 0.99 at 800Hz, and the sound absorption coefficient is greater than 0.6 between 400Hz and 1600Hz. In engineering, the sound absorption coefficient NRC is often used as an index to measure the comprehensive evaluation of sound energy absorption of a material in a closed space. NRC is the arithmetic mean of the sound absorption coefficient of the material at the four frequencies of 250Hz, 500Hz, 1000Hz and 2000Hz. It is calculated The NRC of the simulation results is 0.64.

3 EXPERIMENTAL ANALYSIS

As shown in Figure 10-12, the sound insulation of ordinary aluminum honeycomb panels and ultra-microporous aluminum honeycomb panels was measured using the reverberation chamber method (according to GB/T19889.3-2005 and GB/T 50121-2005 standards). The specimen is fixed in the middle of two adjacent reverberation chambers, a speaker is placed on the sound-emitting side, and microphones are used to collect the acoustic signals on the sound-emitting side and the receiving side. The data is recorded through the test system and processed by computer to obtain the changes in sound insulation. The experimental results show that the weighted sound insulation of the ultra-microporous honeycomb aluminum plate is 26.8dB, which is basically consistent with the simulation result of 27.0dB, verifying the accuracy of the simulation model.

Figure 10 Sound Emitting Side

Figure 11 Receiving Side

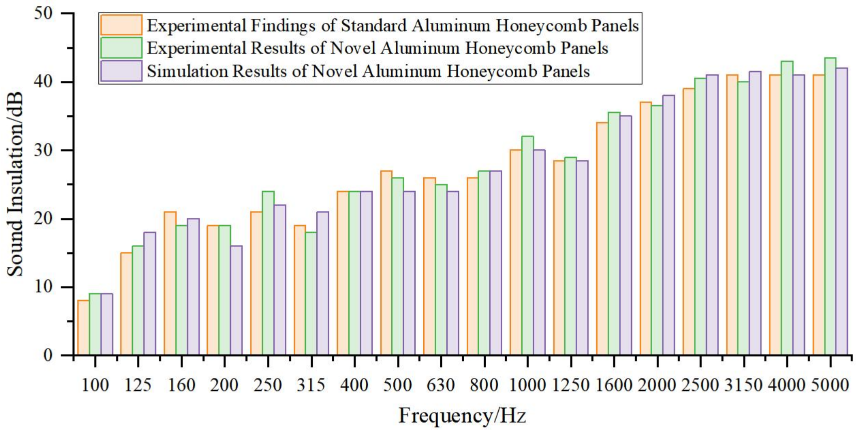

Figure 12 Comparison of Sound Insulation

The standing wave tube method is used to determine the normal incidence sound absorption coefficient of sound-absorbing materials. The test specimen is placed at the end of the standing wave tube, and the signal generator emits plane sound waves of different frequencies through the speaker at the other end to form a standing wave. The microphone measures the sound pressure at different positions in the tube, and the data is processed based on the transfer function method to obtain the change in sound absorption coefficient. Experimental results show that the sound absorption coefficient of ultra-microporous aluminum honeycomb panels is 0.63, and that of ordinary aluminum honeycomb panels is 0.17. Obviously, the sound absorption performance of ultra-microporous aluminum honeycomb panels is far superior to that of ordinary aluminum honeycomb panels, and is highly consistent with the simulation result of 0.64. Sound absorption coefficient comparison curve can be seen in Figure 13.

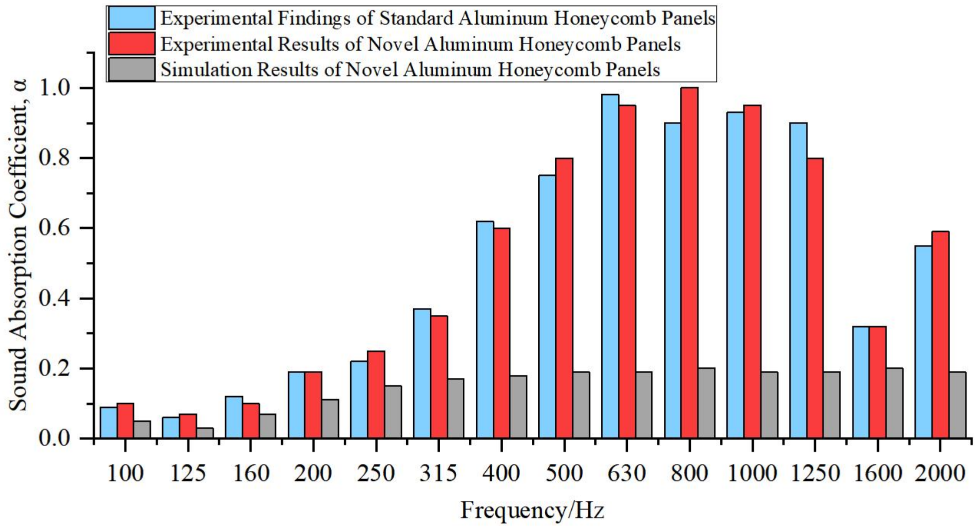

Figure 13 Sound Absorption Coefficient Comparison Curve

4 CONCLUSION

Based on the above-mentioned research on the sound absorption performance of ultra-microporous aluminum honeycomb panels, simulation and indoor testing were combined to conduct a comparative analysis of the sound insulation capacity and sound absorption coefficient of ordinary aluminum honeycomb panels and ultra-microporous aluminum honeycomb panels. The results showed that compared with ordinary aluminum honeycomb panels, the sound insulation capacity of ultra-microporous aluminum honeycomb panels is not much different, but the sound absorption performance of ultra-microporous aluminum honeycomb panels is significantly improved, with the sound absorption coefficient NRC reaching 0.63. When the NRC reaches above 0.5, the noise that the human ear can feel will be significantly reduced. It can be seen that the ultra-microporous honeycomb aluminum plate has a good noise reduction effect, which is beneficial to improving the complex indoor sound environment in large spaces and improving crowd comfort. Future research can further optimize its structural design to improve low-frequency sound absorption performance and expand its application prospects in more fields.

COMPETING INTERESTS

The authors have no relevant financial or non-financial interests to disclose.

REFERENCES

[1] Li Miaoping. Construction technology of self-cleaning aluminum metal composite roof. Construction Technology, 2013, 42(16): 90-92.

[2] Liu Bin. Effect of damping materials on sound insulation performance of subway vehicle floors. Urban Rail Transit Research, 2018, 21(11): 133-135+139.

[3] Zhang Keshu, Xu Qing, Ma Weilian, et al. Simulation and testing of sound insulation and absorption performance of new micro-perforated aluminum honeycomb panels. China Building Materials Technology, 2020, 29(06): 36-39.

World Journal of Materials Science
ISSN:2960-0146
DOI: https://doi.org/10.61784/wjms3003

STUDY ON THE SOUND INSULATION PERFORMANCE OF SANDWICH LIGHTWEIGHT PARTITION WALL PANELS

Xing Gao[1,2], ZhiCheng Bai[1,2*], Yi Zhu[1,2], MinJian Long[1,2], Jian Yin[1,2]
[1]China Construction Fourth Engineering Bureau Co., Ltd., Guangzhou 510000, Guangdong, China.
[2]China Construction Fourth Engineering Bureau Sixth Construction Co., Ltd., Hefei 230000, Anhui, China.
Corresponding Author: ZhiCheng Bai, Email: 19822660870@163.com

Abstract: In order to create a healthy and comfortable indoor environment, based on the sandwich lightweight partition structure, this article systematically analyzes the impact of factors such as the type of filling material in the partition wall cavity, the thickness of the filling material, the number and quality of panel layers on its sound insulation performance. Through experimental tests, the reverberation chamber method was used to measure the sound insulation amount and the standing wave tube method was used to measure the sound absorption coefficient, and the effects of different filling materials and structural parameters on the sound insulation effect were compared. The results show that filling glass wool or rock wool materials significantly improves the sound insulation of sandwich partition walls, and increasing the thickness of the filling material and the number of panel layers further optimizes the sound insulation performance. The research results provide a theoretical basis for the design of indoor partition walls and help improve indoor acoustic comfort.
Keywords: Sandwich lightweight partition wall panels; Sound insulation performance; Filling material; Number of panel layers; Reverberation chamber method; Standing wave tube method

INTRODUCTION

In modern buildings, indoor acoustic comfort has become one of the important indicators for measuring environmental quality. The control of airborne sound transmission pathways is a key factor in evaluating the acoustic quality of buildings. Optimizing indoor sound insulation performance is of great significance for improving personnel comfort and work efficiency [1,2]. Sandwich lightweight partition wall panels are widely used to separate indoor spaces due to their lightweight and flexible structural features. However, the sound insulation performance of sandwich partition walls is affected by many factors, such as cavity filling material type, filling thickness, number and quality of panel layers, etc. [3,4]. Existing research mainly focuses on the impact of a single factor on sound insulation performance, lacking systematic comprehensive analysis. Therefore, this article aims to systematically evaluate the impact of different structural parameters on the sound insulation performance of sandwich lightweight partition wall panels through experimental research, so as to provide a basis for optimizing its design.

1 MATERIALS AND METHODS

1.1 Sandwich Lightweight Partition Wall Panel Structure

Sandwich lightweight partition wall panels are mainly composed of a keel and multi-layer wall panels installed on both sides of the keel to form a spatial structural unit. There is a cavity in the middle that can be filled with fiber-based sound-absorbing materials. The structural construction method of sandwich lightweight partition wall panels is shown in the figure 1 and figure 2 below. In the sound insulation analysis, the sandwich lightweight partition wall panel can be simplified into two parallel plates, separated by a cavity, and the cavity is filled with fiber-based sound-absorbing materials. The propagation of sound in sandwich lightweight partition wall panels is shown in the figure 1and figure 2 below. In the figure 1, Pi, Pr, Pt, and P2b represent incident, reflected, transmitted sound pressure and bridging sound pressure. Sound is transmitted partly through the cavity and partly through the mechanical connections between the wall panels, the so-called sound bridge. Important parameters of the two panels include their unit area masses m1 and m2, critical frequencies fc1 and fc2, and the sound insulation amounts R1 and R2 of the two panels.

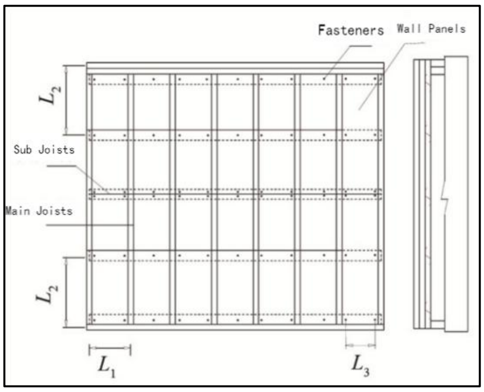

Figure 1 Schematic Diagram of Partition Wall Panel Structure

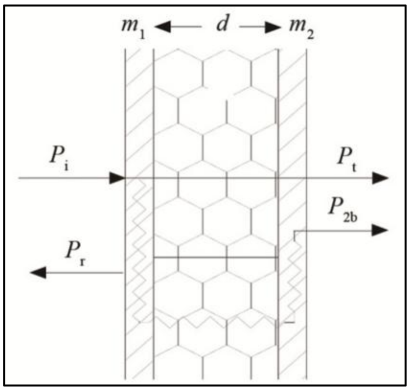

Figure 2 Schematic Diagram of Sound Propagation of Sandwich Lightweight Partition Wall Panels

1.2 Materials and Specifications

Factors considered for sound insulation of sandwich lightweight partition wall panels include: wall cavity size, wall cavity filling material (rock wool, glass wool), wall panels (type, number of layers, thickness, quality), etc. In the test, the main keel spacing was 1200mm and the secondary keel spacing was 400mm; the lightweight wall panel materials used commonly used gypsum board, oriented structural strand board OSB and other boards; the filling materials in the cavity were rock wool and glass wool, with a thickness of 60mm, 90mm, the specific test plan is shown in the table 1 below.

Table 1 Sound Insulation Test Plan for Sandwich Lightweight Partition Wall Panels

Serial No.	Sandwich Lightweight Partition Wall Panel Construction	Code
1	2 layers of 12mm gypsum board + 90mm cavity + 2 layers of 12mm gypsum board	SGB212-KQ90-SGB212
2	2 layers of 12mm gypsum board + 90mm glass wool + 2 layers of 12mm gypsum board	SGB212-BLM90-SGB212
3	(16mm gypsum board + 12mm OSB board) + 60mm glass wool + 2 layers of 16mm gypsum board	SGB16-OSB12-BLM60-SGB216
4	(16mm gypsum board + 12mm OSB board) + 60mm rock wool + 2 layers of 16mm gypsum board	SGB16-OSB12-YM60-SGB216
5	(16mm gypsum board + 12mm OSB board) + 90mm rock wool + 2 layers of 16mm gypsum board	SGB16-OSB12-YM90-SGB216
6	1 layer of 16mm gypsum board + 90mm glass wool + 1 layer of 16mm gypsum board	SGB116-BLM90-SGB116
7	1 layer of 16mm gypsum board + 90mm glass wool + 2 layers of 16mm gypsum board	SGB116-BLM90-SGB216
8	2 layers of 16mm gypsum board + 90mm glass wool + 2 layers of 16mm gypsum board	SGB216-BLM90-SGB216

In the above table 1, 1 layer of 12mm gypsum board represents fire-resistant gypsum board; 2 layers of 12mm gypsum board represents 1 layer of ordinary gypsum board + 1 layer of fire-resistant gypsum board. The test material type, specifications, thickness, density and mass per unit area are shown in the table 2 and table 3 below.

Table 2 Partition Wall Panel Types and Material Properties

Wall Panel Type	Thickness /mm	Density/kg/m³	Unit Area Mass/kg/m²
Gypsum Board	12	593	7.5
Fire-Resistant Gypsum Board	12	721	9.2
Fire-Resistant Gypsum Board	16	721	11.5
OSB Board	12	592	7.2

Table 3 Cavity Filling Materials and Properties

Filling Material Type	Thickness /mm	Densit y/kg/m³	Unit Area Mass /kg/m²	Airflow Resistance /(Pa·s·m⁻²)
Glass Wool	60	10.4	0.6	3600
Glass Wool	90	10.5	1.0	4800
Rock Wool	60	31.3	1.9	11400
Rock Wool	90	52.5	4.7	12700

1.3 Experimental Methods

The sound insulation measurement of sandwich lightweight partition wall panels is based on standards such as GBT19889.3-2005 "Sound Insulation Measurement of Acoustic Buildings and Building Structures" and BS EN ISO 10140-2:2010, using two sound source positions and a rotating microphone to measure the sound insulation effect. , the distance between the microphone position and the interface is 1.5 m. Finally, the weighted sound insulation amount Rw is calculated based on the 1/3 octave center frequency in the 100Hz-5000kHz frequency band. The size of the opening is 3m×2.1m. Considering that the sound insulation of the double-layer lightweight plate partition wall will be affected by the installation conditions in the test opening, the depth of the test opening, the peripheral connection and installation of the partition wall specimen and the test opening, try to eliminate Test losses and deviations caused by structural sound transmission and gaps and gaps caused by structural connections.

2 RESULTS AND ANALYSIS

The figure 3 and figure 4 below compares and analyzes the sound insulation effect of the wall without filling and glass wool in the 90mm cavity (two layers of 12mm gypsum board on both sides). The weighted sound insulation of the wall under the two working conditions is 52dB and 57dB respectively. The sound insulation of the glass wool filling is about 5dB higher than that of the unfilled sandwich wall, and the sound insulation effect is significant. In addition, when glass wool is filled, its sound insulation improvement effect in the low frequency range is not obvious. When the frequency exceeds 100Hz, its sound insulation improvement effect is more prominent. This shows that filling the wall cavity with glass wool or rock wool will increase the attenuation of sound propagation in the cavity. The depth of the cavity and the amount of filling material have a positive effect on sound attenuation.

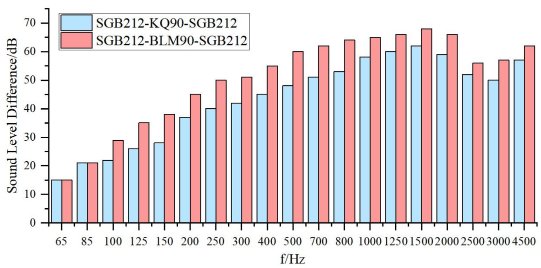

Figure 3 The Impact of Cavity and Glass Wool Filling on Wall Sound Insulation

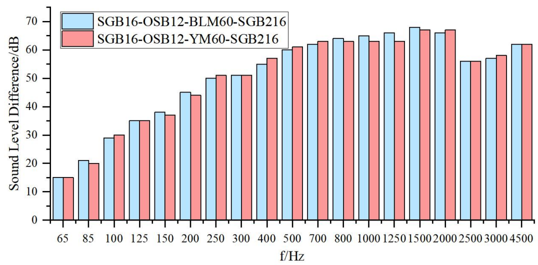

Figure 4 The Impact of Different Filling Materials on Wall Sound Insulation

The figure 3 and figure 4 above compares and analyzes the sound insulation effect of walls filled with 60mm glass wool and 60mm rock wool (one side is 16mm gypsum board + 12mm OSB board; one side is 2 layers of 16mm gypsum board). The results found that the weighted sound insulation of filled glass wool and rock wool were 55.6dB and 54dB respectively, and the former was 1.6dB higher than the latter. In the 125-1000Hz spectrum range, the sound insulation effect of walls filled with glass wool is slightly better than that of walls filled with rock wool. In the low-frequency and high-frequency ranges, the sound insulation of rock wool is better than that of glass wool. Overall, the sound insulation of walls filled with glass wool is 1.1-1.6dB higher than that of walls filled with rock wool. The performance parameters of filling materials, especially the impact of material density, air flow resistance, etc. on wall sound insulation need to be further studied and analyzed.
The figure 5 and figure 6 below compares and analyzes the sound insulation effect of walls filled with 90mm rock wool and 60mm rock wool (one side is 16mm gypsum board + 12mm OSB board; one side is 2 layers of 16mm gypsum board). The weighted sound insulation of the wall is 58dB, 54.4dB, the weighted sound insulation of the former is 3.6dB higher than that of the latter. This shows that the greater the cavity filling thickness, the greater the sound transmission loss in the wall system, and the sound insulation performance is optimized and improved.

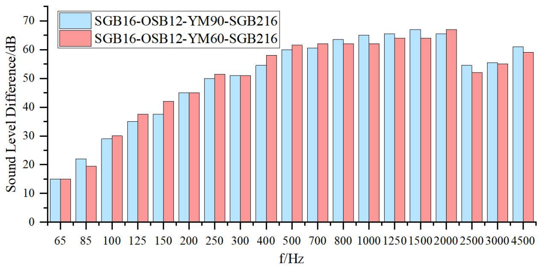

Figure 5 The Impact of Different Thicknesses of Filling Materials on Wall Sound Insulation

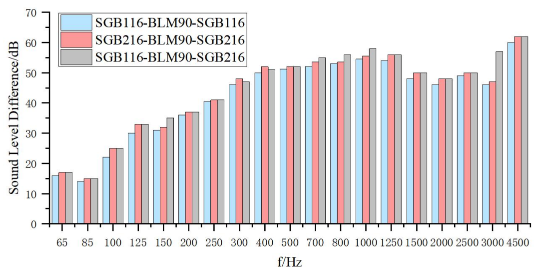

Figure 6 The Impact of the Number of Panel Layers on Wall Sound Insulation

Furthermore, the figure 5 and figure 6 above compares and analyzes the impact of 2, 3, and 4-layer panels on the sound insulation effect of the wall (the panels are all 16mm fire-resistant gypsum boards). The corresponding weighted sound insulation amounts are 47dB, 51.2dB, and 55.3dB respectively. Since the increase in the number of wall panel layers will reduce the energy transmission into the cavity, the number of wall layers increased from 2 to 3 and 4 respectively, and the sound insulation increased by 4.2dB and 8.3dB respectively.

3 CONCLUSION

Based on the above-mentioned research on the sound insulation performance of sandwich lightweight partition wall panels, the impact of the type of filling material, filling material thickness, panel layer number and quality on the sound insulation performance of the partition wall cavity was analyzed. The results found that filling the wall cavity with rock wool or glass wool, increasing the number of panel layers or improving panel quality, and avoiding structural connections has a positive effect on optimizing and improving the sound insulation performance of sandwich lightweight partition wall panels. The research results provide a theoretical basis for optimizing the sound insulation design of sandwich lightweight partition wall panels, which helps to improve the indoor acoustic comfort of buildings.

COMPETING INTERESTS

The authors have no relevant financial or non-financial interests to disclose.

REFERENCES

[1] Kang Jian. Noise control and acoustic comfort - concepts, sound absorbers and mufflers. Journal of Acoustics, 2013, 38(02): 251.
[2] Long Caifeng, Song Xiaochuan, Jiang Hui, et al. Research on the sound insulation performance and rules of artificial panels in indoor spaces. Furniture and Interior Decoration, 2024, 31(05): 36-39.
[3] Lu Wangyang, Xie Hui, He Yi. Research on the sound insulation performance of prefabricated lightweight partition walls. Acoustic Technology, 2020, 39(06): 721-727.
[4] Wang Junqiang. Experimental study on the sound insulation performance of double-leaf structure lightweight walls of green buildings. Acoustic Technology, 2021, 40(05): 657-662.

World Journal of Materials Science
ISSN:2960-0146
DOI: https://doi.org/10.61784/wjms3005

EVALUATION OF THE CORROSION INHIBITION PROPERTIES OF ETHANOLIC EXTRACT FROM ACACIA NILOTICA POD ON MILD STEEL IN 0.1 M SULFURIC ACID: AN EXPERIMENTAL STUDY UTILIZING FTIR AND SEM TECHNIQUES

I. Jimoh[1,2*], L. A Musa[1]
[1]*Department of Chemistry, Faculty of Science, Confluence University of Science and Technology, Osara, Kogi State, Nigeria.*
[2]*Department of Pure and Industrial Chemistry, Faculty of Physical Sciences, College of Natural and Pharmaceutical Science, Bayero University Kano, Kano State, Nigeria.*
Corresponding author: I. Jimoh, Email: ibrahimj@custech.edu.ng

Abstract: The ethanol extract of Acacia nilotica pod (ANP) was investigated for its corrosion inhibition potential on mild steel immersed in 0.1M H_2SO_4 solutions containing ANP concentrations ranging from 0.1 to 0.5 g/L. The study employed weight loss measurements, Fourier transform infrared (FTIR) spectroscopy, and scanning electron microscopy (SEM) to evaluate the extract's performance. Weight loss experiments demonstrated that the inhibition efficiency was influenced by both the concentration of ANP and the exposure duration of the mild steel in the acidic medium. The highest inhibition efficiency recorded was 87.57%. Surface morphology analysis using SEM revealed significant differences between the steel samples exposed to H_2SO_4 with and without the extract, indicating the protective role of ANP. FTIR spectroscopy further confirmed the adsorption of the extract onto the mild steel surface, with functional groups such as C-O and N=O playing a critical role in the adsorption process. These findings highlight the potential of ANP as an effective corrosion inhibitor for mild steel in acidic environments.
Keywords: Acacia nilotica pod; Corrosion inhibition; Mild steel; Sulfuric acid; Adsorption

1 INTRODUCTION

Mild steel is extensively utilized in various industries, including food processing, petroleum, power generation, chemical, and electrochemical sectors, due to its excellent mechanical properties and affordability [1]. However, exposure to aggressive environments often leads to the corrosion of metals such as iron and steel, causing mechanical failures and significant damage to infrastructure. These include oil, gas, and water pipelines, bridges, public buildings, vehicles, and domestic appliances, resulting in high repair and replacement costs as well as potential safety hazards [2]. Consequently, developing effective corrosion protection strategies for mild steel in harsh acidic and alkaline conditions has become a critical focus [3].

Numerous studies have been conducted to mitigate the corrosion of mild steel, given its importance in various industrial applications. Typically, corrosion inhibitors are compounds containing heteroatoms like nitrogen, oxygen, phosphorus, and sulfur, often with long carbon chains, triple bonds, or aromatic rings in their structures [4]. However, these inhibitors are often costly, toxic, and harmful to the environment [5].

In contrast, plant-derived materials have emerged as promising alternatives due to their low cost, non-toxicity, environmental friendliness, and abundant availability. They are rich in heterocyclic compounds and functional groups such as -C=C-, -OR, -OH, -COOH, $-NR_2$, $-NH_2$, and -SR, which donate electrons that facilitate adsorption onto metal surfaces, thus inhibiting corrosion. Recent advancements in corrosion research have focused on exploring various plant extracts as green inhibitors [6]. Studies reveal that the inhibitory effects of plant extracts are attributed to the presence of organic compounds like tannins, saponins, alkaloids, steroids, glycosides, and amino acids [7].

In line with these developments, the present study investigates the corrosion inhibition properties of ethanol extract from Acacia nilotica pod (ANP) on mild steel in an acidic environment. The evaluation was carried out using weight loss measurements, Fourier transform infrared (FTIR) spectroscopy, and scanning electron microscopy (SEM) to assess the efficacy of the extract as a green corrosion inhibitor.

2 MATERIALS AND METHODS

2.1 Material Preparation

The mild steel used in this investigation was acquired from Bayero University Kano's Department of Mechanical Engineering (New Campus). Its chemical composition was assessed via Energy Dispersive X-ray Fluorescence (ED-XRF) and contained Mn (0.27%), Al (0.04%), C (0.066%), among other elements, with Fe making up the remainder. Coupons of 5 × 4 × 0.11 cm were prepared, degreased with ethanol, rinsed in acetone, and air-dried before being stored in a desiccator. Reagents were of analytical grade, with solutions prepared using double-distilled water, ensuring experimental reliability following Ibrahim Jimoh and Bishir Usman [8].

2.1.1 Coupon preparation

For the corrosion tests, 100 mild steel coupons were fabricated, each measuring 5 × 4 × 0.11 cm. The surfaces of the coupons were polished sequentially using emery papers of varying grit sizes (240, 400, 800, and 1000) to achieve a smooth finish. Following polishing, the samples were cleaned with ethanol, degreased using acetone, and allowed to air-dry. Each coupon was weighed to obtain its initial mass, and the values were recorded. The prepared samples were then stored in desiccators to prevent moisture absorption prior to corrosion analysis following Ibrahim Jimoh and Bishir Usman [8].

2.1.2 Preparation of plant extract

The ANP samples were initially air-dried to remove moisture, then finely ground to increase surface area for extraction. These ground samples were submerged in ethanol and left to soak for 48 hours, facilitating the extraction of bioactive compounds. After soaking, the mixture was cooled to room temperature and filtered to separate the liquid extract from the solid residue. The resulting filtrate was subjected to evaporation at a temperature of 352 K to completely remove ethanol, leaving behind a concentrated extract. This extract was then used to prepare stock solutions. Various concentrations of the extract were subsequently prepared by dissolving 0.1 g, 0.2 g, 0.3 g, 0.4 g, or 0.5 g of the extract in 1 liter of 0.1 M sulfuric acid (H_2SO_4) solution following Ibrahim et al., [9].

2.1.3 Preparation of acid solution

For this study, a 0.1 M sulfuric acid (H_2SO_4) stock solution was prepared to serve as the corrodent. This was achieved by carefully diluting 5.40 mL of concentrated 98% H_2SO_4 (Analar grade, Merck) in a 1000 mL volumetric flask. Initially, 150 mL of distilled water was added to the flask to dilute the acid, and the solution was then topped up to the 1000 mL mark with additional distilled water. This stock solution was used consistently throughout the experiments for preparing various solutions. The concentration of the ANP ethanol extract used in the study ranged from 0.1 g/L to 0.5 g/L following Ayuba, et al., [10].

2.1.4 Weight loss measurement procedure

Weight loss experiments were conducted in a 250-mL beaker at a constant temperature of 303 K. For each test, 250 mL of the prepared solution was used. Mild steel specimens were initially weighed and then immersed in the solution for a duration of 1 hour. After the exposure period, the specimens were removed, thoroughly washed with distilled water to eliminate any loose corrosion products, and subsequently rinsed with ethanol and acetone. They were then dried and reweighed.

The weight loss of the mild steel (in grams) was determined by calculating the difference between the initial and final weights. From these values, the corrosion rate (expressed in g/h/cm²), inhibition efficiency (%I), and surface coverage (θ) were evaluated using specific mathematical formulas (Equations 1–3) [11].

$$\text{CR (g/h/cm}^2\text{)} = \frac{\Delta W}{At} \tag{1}$$

$$\theta = 1 - \frac{W_1}{W_2} \tag{2}$$

$$\%\text{I} = \left(1 - \frac{W_1}{W_2}\right) \times 100 \tag{3}$$

Here, W1 and W2 represent the weight losses (in g/dm³) of the mild steel coupons in the sulfuric acid solution with and without the presence of the inhibitor, respectively. The degree of surface coverage () quantifies the extent to which the inhibitor protects the metal surface. A denotes the surface area of the metal coupon (in cm²), t is the immersion time (in hours), and W is the measured weight loss (in grams) of the mild steel coupon after the specified immersion period (t).

2.1.5 Fourier transform infrared spectrophotometry (FTIR)

FTIR analyses of the inhibitor and that of the corrosion products (in the presence and absence of the respective inhibitors) were carried out using an FTIR instrument, the 630 Cary series Agilent Technologies. Two coupons were separately dipped in 250 mL of 0.5 g/L inhibitor concentration for 2 days to form an adsorbed layer, after which they were retrieved, dried, and scraped with a sharp blade. The scraps were collected for analysis. The samples were prepared using KBr, and the analysis was done by scanning the sample through a wave number range of 400–4000 - 4000 cm-1 following Elabbasy et al.[12].

2 SURFACE ANALYSIS OF MILD STEEL COUPONS

The surface morphology of mild steel coupons was analyzed using an Inspect S50 scanning electron microscope to evaluate corrosion inhibition effectiveness. Coupons measuring 5 cm × 4 cm × 0.11 cm were immersed in both a blank and a 0.5 g/L inhibitor solution for 48 hours. Post-immersion, the samples were rinsed with distilled water, air-dried, mounted on metal stubs, and gold-coated for conductivity. SEM images were captured at accelerating voltages of 2.00 and 12.50 kV, highlighting morphological differences between inhibited and uninhibited surfaces following Okore et al.[13].

3 RESULTS AND DISCUSSION

3.1 Weight Loss Measurement

3.1.1 Effect of inhibitor concentration

The influence of varying concentrations of ANP extract on corrosion rate and inhibition efficiency for mild steel in 0.1 M H_2SO_4 at 303 K was studied. Figures 1 and 2 illustrate the relationship between inhibitor concentration and the corrosion protection performance. As depicted in Figure 1, increasing the concentration of the plant extract significantly reduces the corrosion rate of mild steel. This trend indicates the efficiency of ANP extract in mitigating corrosion, likely due to its ability to form a protective film on the metal surface, impeding further interaction between the metal and the corrosive environment [14].

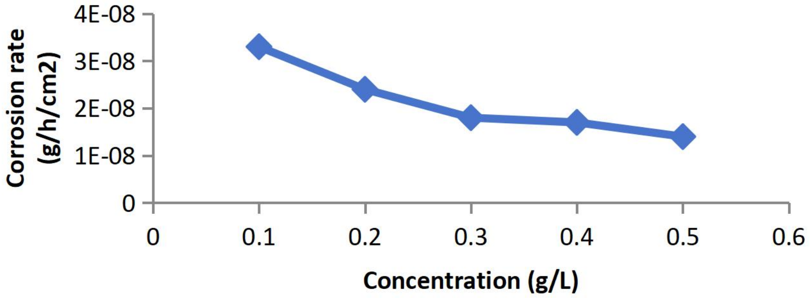

Figure 1 Variation of Corrosion Rate (g/h/cm2) of Mild Steel as a Function of Various Concentration of ANP Extract in 0.1M H2SO4 at 303K

The enhanced corrosion inhibition observed with increased concentrations of ANP extract can be attributed to greater surface coverage on the mild steel, forming a protective barrier that inhibits metal dissolution. This aligns with the findings of Niamien et al.,[15] and Olasehinde et al.,[16], where increased inhibitor concentration correlated with improved inhibition efficiency. The mechanism suggests that higher surface adsorption reduces the active sites for corrosive agents, effectively mitigating corrosion and enhancing the inhibitor's performance [17].

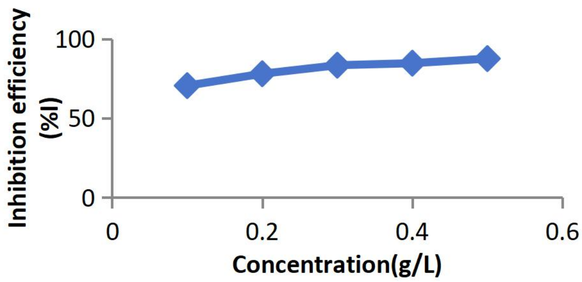

Figure 2 Variation of Inhibition Efficiency (%IE) against Various Concentrations of ANP Extract for Mild Steel Corrosion in 0.1 M H2SO4 at 303 K

Table 1 Inhibition Efficiencies (%IE) and Corrosion Rates for Corrosion of Mild Steel in the Absence and Presence of Various Concentrations of the Extract in 0.1M H2SO4 at 303–333 K

Conc.(g/L)	Corrosion Rate x10^{-4}($gh^{-1}cm^{-2}$)				Inhibition efficiency (%)			
	303K	313K	323K	333K	303K	313K	323K	333K
Blank	1.11	3.45	5.79	7.93	-	-	-	-
0.1	0.33	1.19	2.30	3.86	70.54	65.45	60.23	51.34
0.2	0.24	0.93	2.05	3.42	78.04	72.95	64.61	56.90
0.3	0.18	0.75	1.53	2.88	83.40	78.31	73.59	63.73
0.4	0.17	0.58	1.39	2.54	84.68	83.27	76.07	67.99
0.5	0.14	0.52	1.10	2.32	87.57	84.92	80.98	70.69

3.1.2 Effect of immersion time

The weight loss-time curve (Fig.3) for mild steel in 0.1 M H_2SO_4 with and without ANP extract indicates a clear trend. As exposure time increases, the weight loss of mild steel in the uninhibited solution rises due to ongoing corrosion.

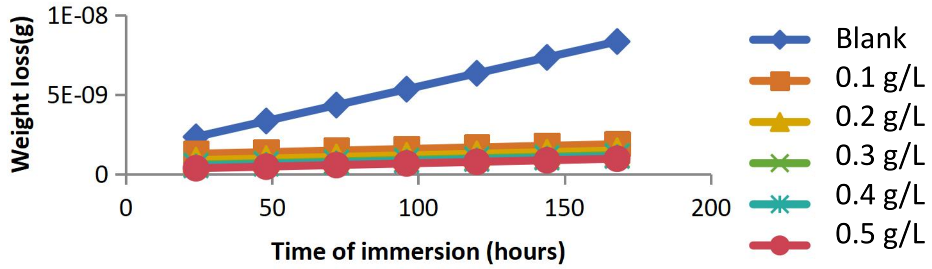

Figure 3 Effect of Immersion Time (hours) on Corrosion Rate of Mild Steel in 0.1 M H2SO4 in the Absence and Presence of ANP Extract at 303 K

However, the presence of ANP extract reduces weight loss significantly, which becomes more pronounced at higher inhibitor concentrations. This reduction is attributed to the formation of a protective layer on the mild steel surface, impeding the corrosive attack of sulfuric acid [18]. Such observations highlight the effectiveness of plant extracts as green corrosion inhibitors, consistent with findings from recent studies exploring plant-derived materials as eco-friendly solutions for metal protection in acidic environments[19].

3.1.3 Effect of temperature

The variation in corrosion rate of mild steel in 0.1M H2SO4 in the presence and absence of ANP extract inhibitor at different temperatures has been studied, and it is evident from Table 1 and the plot in Fig. 4 that the corrosion rate of mild steel with or without extract increased with an increase in temperature [20].

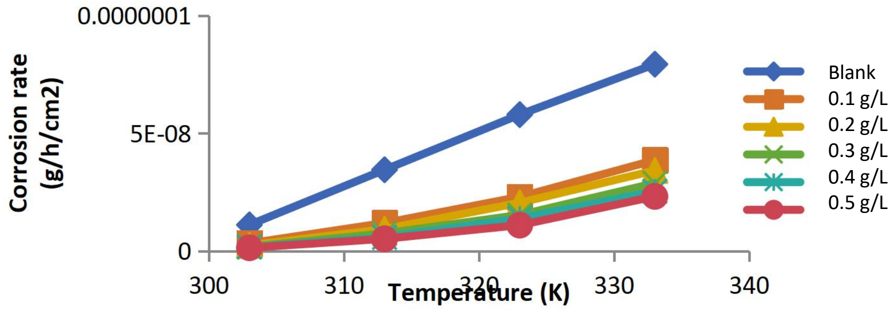

Figure 4 Variation of the Corrosion rate of Mild Steel Against Temperature (303–333 K) in the Absence and Presence of Different Concentrations of ANP Extract in 0.1 M H2SO4

This is due to the fact that as the temperature increased from 303 to 333 K, the rate of corrosion of the mild steel coupons also increased as a result of the increasing average kinetic energy of the reacting molecules [21]. However, the corrosion rate is retarded in the presence of the plant extract. The corrosion rate increases more rapidly with temperature in the absence of the extract. Two observations could be drawn from the result: (i) The mild steel surface is effectively damaged in the acidic medium [22], and (ii) ANP extract is a strong inhibitor for mild steel corrosion in 0.1M H2SO4 at a lower temperature. Furthermore, it is observed in Fig. 5 and Table 1 that the inhibition efficiency of plant extract decreased with an increase in temperature for all concentrations of the inhibitor. This may be as a result of the increasing solubility of the adsorbed protective inhibitor barrier on the mild steel surface, thereby increasing the susceptibility of these coupons to dissolution in the acid media [23].

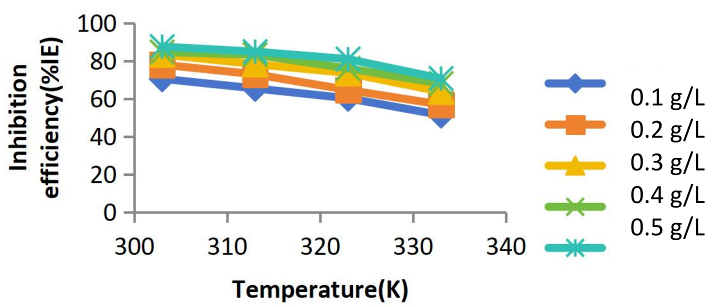

Figure 5 Variation of Inhibition Efficiency (%IE) Against Temperature for the Corrosion of Mild Steel in 0.1 M H2SO4 in the Presence and Absence of ANP Extract

3.1.4 Stability of the inhibitor

The stability of the ethanol extract of ANP for the corrosion of mild steel in H2SO4 (over a time range) was also studied by plotting values of inhibition efficiency versus the period of contact, as shown in Figure 6. The plots indicate that at 303 K, the ethanol extract of ANP retained more than 87% of its inhibition efficiency even after 168 hours of immersion. This agrees with the finding of Obot et al., [24].

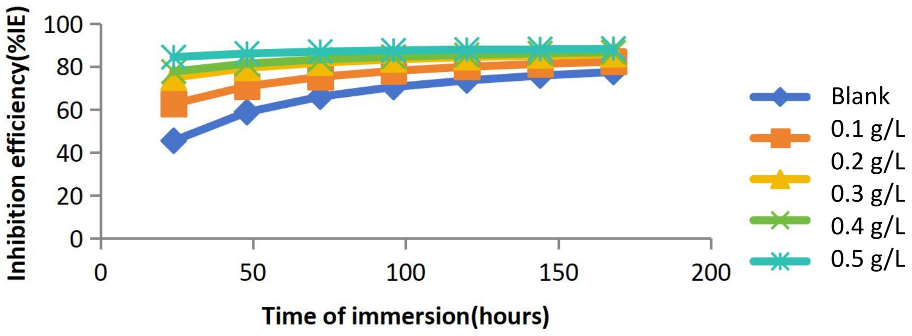

Figure 6 Effect of Immersion Time (hours) on Inhibition Efficiency (%IE) of ANP Extract on the Dissolution of Mild Steel in 0.1 M H2SO4 at 303 K

3.2 Surface Analysis

In Fig. 7b, the mild steel surface is highly damaged due to the effect of the acid on the surface, and in Fig. 7c, there is an improvement in the surface morphology, which shows a smooth surface when compared to the uninhibited surface.

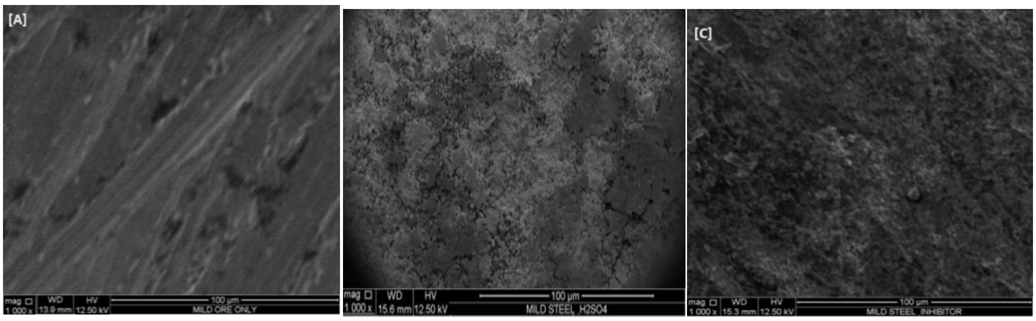

Figure 7 SEM Micrographs of Mild Steel: (a) Fresh Mild Steel; (b) Without Inhibitor; (c) With Inhibitor

It is evidence that the damaging effect of the acid on the mild steel is greatly reduced due to the protective layer of the adsorbed inhibitor that prevents corrosion caused by the acid attack on the mild steel surface. The smoothness of the mild steel surface in the presence of an inhibitor is due to the barrier of the protective film over the metal surface, which gives rise to more ordered corrosion products [25].

3.3 FTIR Study

In order to further support the adsorption behavior of the inhibitor on the surface of mild steel, FTIR spectroscopy was employed. Fig. 8a shows the FTIR spectrum of the ethanol extract of ANP alone. Fig. 8b shows the FTIR spectrum of the corrosion product when an ethanol extract of ANP was used as an inhibitor.

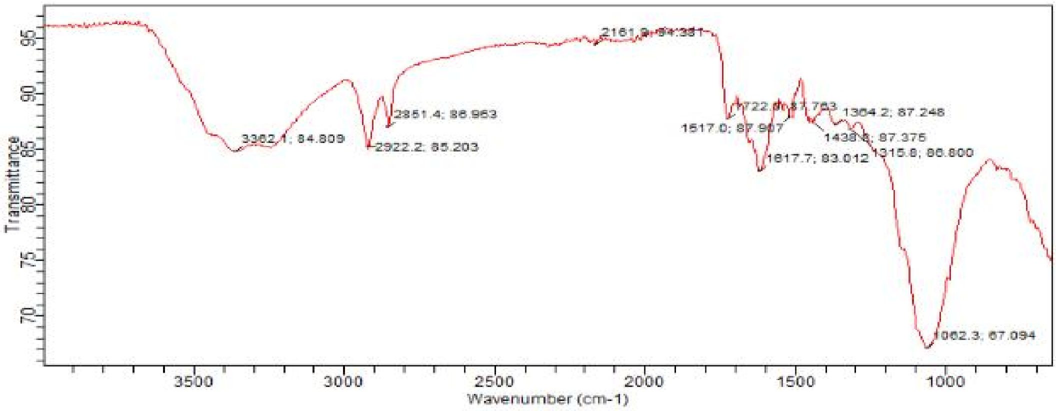

Figure 8 FTIR Spectral of (a) Ethanol Extract of ANP and (b) Corrosion Product of Mild Steel in the Presence of Inhibitor

Peaks and frequencies of FTIR adsorption for both spectra are presented in Table 2. From the results obtained, it is also evident that the C-O stretch at 1233.7 cm -1 was shifted to 1062.3 cm -1, the –C=C- stretch at 1617.7 cm -1 was shifted to 1517.7 cm -1, the C-H (Alkene stretch) was shifted from 2918.5 cm-1 to 2851.4 cm-1, the aromatic C=O was shifted from 1722.0 cm-1 to 1722.8 cm-1, the N=O (R-NO2) was shifted from 1518.3 cm-1 to 1384.2 cm-1 and the phenolic-OH stretch was shifted from 3283.8 cm-1 to 3362.1 cm -1. These shifts in frequencies also indicate that there is an interaction between the inhibitor and the metal surface [17, 18, 19]. It is also evident from the data obtained that the C-O stretch at 1159.2 cm-1 as well as N=O (R-NO2) at 1364.2 cm -1 were missing, suggesting that these bond frequencies might have been used for bonding between the vacant d-orbital of Fe and the inhibitor [26]. Therefore, ANLE was adsorbed onto the mild steel surface through these functional groups [27].

Table 2 Functional Groups Assigned to the Adsorption of the Ethanol Extract of the Pod and the Corrosion Product When the Extract is used as an Inhibitor

Ethanol extract			Corrosion product		
Wave No (cm^{-1})	Height	Assigned functional group	Wave No (cm^{-1})	Height	Assigned functional group
3283.8	87.207	O-H H-bonded	3362.1	84.809	O-H H-bonded
2918.5	77.986	C-H Alkene stretch	2851.4	86.953	C-H Alkane stretch
2851.4	81.634	C-H Alkene stretch	2922.2	85.203	C=O Aldehyde
1722.0	81.218	C=O Aldehyde	1722.8	87.783	C=O Aldehyde
1617.7	81.253	C=C Alkene	1517.7	83.012	C=C Alkene
1518.3	84.083	N=O Nitro ($R-NO_2$)	1384.2	87.248	N=O Nitro ($R-NO_2$)
1438.8	83.051	C-H $-CH_3$(bend)	1438.8	87.375	C-H $-CH_3$ (bend)
1364.2	82.596	N=O Nitro (R-NO2)	-	-	-
1159.2	75.688	C-O stretch	-	-	-
1233.7	78.520	C-O stretch	1062.3	67.094	C-O stretch

4 CONCLUSION AND RECOMMENDATION

The results obtained from the study indicate that ANP extract effectively inhibited the corrosion of mild steel in 0.1 M H2SO4. Inhibition efficiency increases with increasing extract concentration and immersion time and decreases with rising temperature. The inhibition potential of this inhibitor is attributed to the presence of phenol, tannin, alkaloids, and flavonoids in the extract. Hence, an increase in the reaction temperature of the medium will decrease the inhibition efficiency. In view of the above conclusion, the use of ethanol extracts of ANP as green inhibitors is recommended.

COMPETING INTERESTS

The authors have no relevant financial or non-financial interests to disclose.

REFERENCES

[1] Abdel-Karim, A M, El-Shamy, A M. A review on green corrosion inhibitors for protection of archeological metal artifacts. Journal of Bio- Tribo-Corrosion, 2022, 8(1): 35. DOI: 10.1007/s40735-022-00636-6.

[2] Dehghani, A, Bahlakeh, G. Phytochemical-based inhibitors for mild steel corrosion in acid media: Mechanisms and practical applications. Bulletin of the National Research Centre, 2023, 47(15): 97-115. DOI: 10.1186/s42269-023-00211-9.

[3] Shobhana Sharma, Aashu S, Solanki, Abhinay Thakur, et al. Phytochemicals as eco-friendly corrosion inhibitors for mild steel in sulfuric acid solutions: A review. Corrosion Reviews, 2024, 42(1): 22-34. DOI: 10.1515/corrrev-2024-0018.

[4] Yousef, N S, Kandil, A B. Eco-friendly green inhibitors from plants for corrosion protection of mild steel in acidic media.Materials Science for Energy Technologies, 2021, 4(1): 92-99. DOI: 10.1016/j.mset.2021.02.003.

[5] Deepa, P, Murugan, K. Green corrosion inhibition of mild steel in acidic media using plant extracts. Corrosion Science, 2023, 183(4): 109-118. DOI: 10.1016/j.corsci.2023.109186.

[6] Alan Miralrio, Araceli Espinoza-Vázquez. Plant extracts as green corrosion inhibitors for different metal surfaces and corrosive media: A review. Processes, 2020, 8(10): 1-20. DOI: 10.3390/pr8101161.

[7] Zakeri, A, Bahmani, E, Aghdam, A S R. Plant extracts as sustainable and green corrosion inhibitors for protection of ferrous metals in corrosive media: A mini review. Corrosion Communications, 2022, 5, 25-38.

[8] Ibrahim Jimoh, Bishir Usman. Corrosion Inhibition Potential of Ethanol Extract of Acacia nilotica Leaves on Mild Steel in Acid Medium. Portugalia Electrichimica Acta, 2021, 39(2): 105-128.

[9] Ibrahim J, Sabo R, Umar M, et al. Assessing The Effectiveness Of Acacia Nilotica Pod Extract As a Corrosion Inhibitor For Mild Steel In Acidic Conditions Via Response Surface Analysis. 1st Chemtrends Book Of Proceedings/CSN @ Wukari/July, 2024, 283-287.

[10] Ayuba, A M, Auta, M A, Shehu, N U. Comparative Study of the Inhibitive properties of Ethanolic Extract of Gmelina arboreaon Corrosion of Aluminium in Different Media. Appl. J. Envir. Eng. Sci, 2020, 6, 374-386.

[11] Okai, V, Chahul, H F, Wuana, R A, et al. Corrosion inhibition potentials of Cucurbita polyesteramide urethane on mild steel in hydrochloric acid medium: Experimental and computational studies. Scientific African, 2021, 12, e00776. DOI: https://doi.org/10.1016/j.sciaf.2021.e00776.

[12] Elabbasy, H M, Elnagar, M E, Fouda, A S. Surface interaction and corrosion inhibition of carbon steel in sulfuric acid using Petroselinum crispum extract. Journal of the Indian Chemical Society, 2023, 100(5): 100988. DOI: 10.1016/j.jics.2023.100988.

[13] Okore, S, Oguzie, E, Enyoh, C E. Lawsonia inermis as an active corrosion inhibitor for mild steel in hydrochloric acid. Applied Sciences, 2024, 14(15): 6392. DOI: https://doi.org/10.3390/app14156392.

[14] Akbarzadeh, E, Abadi, M A. Effect of Tamarindus indica Extract as a Green Inhibitor on Mild Steel Corrosion in Acidic Solutions. Processes, 2023, 11(2): 398. DOI: https://doi.org/10.3390/pr11020398.

[15] Niamien, P M. Corrosion Inhibition Efficiency of Natural Compounds on Mild Steel. Journal of Electrochemical Science, 2021, 18(2), 200-215. DOI: https://doi.org/10.1016/j.jelectro.2021.200215.

[16] Olasehinde, E F. Evaluation of Green Inhibitors for Mild Steel in Acidic Media. International Journal of Corrosion and Scale Inhibition, 2020, 9(1): 344-360. DOI: https://doi.org/10.17675/2305-6894-2020-9-1-344.

[17] Ahmadi, A. Natural Compounds as Efficient Corrosion Inhibitors. Materials Today Sustainability, 2023, 7, 100063. DOI: https://doi.org/10.1016/j.mtsust.2023.100063.

[18] Miralrio, A, Espinoza-Vázquez, A. Plant Extracts as Green Corrosion Inhibitors for Different Metal Surfaces and Corrosive Media: A Review. Processes, 2020, 8(8): 942. DOI: https://doi.org/10.3390/pr8080942.

[19] Bhat, J I, Shabir, M, Qurashi, A. Adsorption Behavior and Corrosion Inhibition of Natural Plant Extracts on Mild Steel in Acidic Media. Surface Engineering, 2022, 38(3): 285-299. DOI: https://doi.org/10.1080/02670844.2021.1985560.

[20] Bishir Usman, Hasmeriya Maarof, Hassan H, et al. Theoretical and Experimental Studies of Corrosion Inhibition of Thiophen-2-Ethylamine on Mild Steel in Acid Media Journal Teknologi (Science & Engineering), 2015, 76(13): 7-14.

[21] Usman, B, Mohammed, A S, Umar A B. Quantum Chemical Evaluation on Corrosion Inhibition Performance of Balanitin-7 on Mild Steel in 1 M Hydrochloric Acid Solution. Appl. J. Envir. Eng. Sci. 4 N°3, 2018, 380-386.

[22] Majeed, Z A, Saleh, M. Morphological and electrochemical study of green corrosion inhibitors on mild steel. Journal of Materials Research and Technology, 2021, 13(2): 1856-1866.

[23] Momoh-Yahaya, H, Eddy, N O, Oguzie E E. Inhibitive, Adsorptive, and Thermodynamic Study of Hypoxanthine Against the Corrosion of Aluminum and Mild Steel in Sulphuric Acid. Journal of Material and Environmental Science, 2014, 5(1): 237-244.

[24] Obot, I B, Umoren, S A, Ebenso, E E, et al. The inhibition of aluminum corrosion in hydrochloric acid solution by exudate gum from Raphia hookeri Desalination, 2009, 250: 225-236.

[25] Ebenso, E E, Isabirye, D A, Eddy, N O. Adsorption and quantum chemical studies on the inhibition potentials of some thiosemicarbazides for the corrosion of mild steel in an acidic medium. International Journal of Molecular Sciences, 2010, 11(24): 73-98.

[26] Quraishi, M A, Singh, A K. Piroxicam: A Novel Corrosion Inhibitor for Mild Steel Corrosion in HCl Acid Solution. Journal of Material & Environmental Science, 2020, 1(2): 101-110.

[27] Eddy N O, Femi A. Experimental and Quantum Chemical Studies on Ethanol Extract of Phyllanthus amarus (EEPA) as a Green Corrosion Inhibitor for Aluminum in 1M HCl Portugaliae electrochimica acta, 2018, 36(4): 231-247.

World Journal of Materials Science
ISSN: 2960-0146
DOI: https://doi.org/10.61784/wjms3004

FABRICATION OF POLYPROPYLENE NANOCOMPOSITE FOR SUPERLATIVE REFRIGERATED VEHICLE PANELS

Uwa Chukwunonso Aghaegbulam[1*], Sadiku Emmanuel Rotimi[2], Jamiru Tamba[1], Huan Zhongjie[1], Mpofu Khumbulani[3], Ramatsetse Boitumelo Innocent[3]
[1]*Department of Mechanical and Mechatronics Engineering, Tshwane University of Technology, Pretoria, South Africa.*
[2]*Institute of Nano Engineering Research and Department of Chemical, Metallurgy and Materials Engineering, Tshwane University of Technology, Pretoria, South Africa.*
[3]*Department of Industrial Engineering, Tshwane University of Technology, Pretoria, South Africa.*
Corresponding Author: Uwa Chukwunonso Aghaegbulam, Email: nonso_uwa@yahoo.com

Abstract: Refrigerated foods vehicle by road is made up of three-layered materials insulated panel that has insulation foam, situated intermediate to two high thermal conductive aluminum metal sheets. Usually, a loss of insulation value in a refrigerated vehicle every year is a result of the increase in heat absorption and heat transfer of the metal sheets, which affect the cooling temperature in a refrigerated vehicle panel chamber. The study aims at proposing the fabrication of polypropylene nanocomposite for superlative refrigerated vehicle panels, by producing and testing low-thermal conductive polymer-based composite materials with nanoclay (NC) particles for use in superlative refrigerated vehicle panels. The melt blending compounding method involved the pre-treatment of materials, preparation of composite samples, and the characterization of the new samples for their: mechanical, morphology, and thermal properties. The result of the study shows that melt blending influenced the composites' mechanical, morphology, and thermal properties. Meanwhile, the processing route exhibited an intercalated morphology structure, which enhanced the composites' strength, stiffness, and thermal conductivity. Finally, the sample with 3% nanoclay by weight had the optimum property and could be, recommended for refrigerated vehicle panel insulation.
Keywords: Polypropylene; Nanocomposite; Nanoclay; Refrigerated vehicle panels; Maleic anhydride grafted polypropylene

1 INTRODUCTION

Refrigerated vehicles are temperature-controlled vehicles, made of an insulated panel and a cooling system used to transport garden-fresh food and its products [1-2] (see Figure 1). The extension of shelf life by using the refrigerated vehicle to convey food products is important to address the growth in population. The aluminum or steel metal panel sheets used in the refrigerated panel have a high thermal conductivity which leads to high energy consumption, high engine power, decreases the longevity of the insulating materials, and causes environmental pollution. The purpose of this vehicle is to preserve the chill temperature and not to provide cooling [3].
The temperature in a refrigerated vehicle is the key parameter in sustaining the shelf-life of perishable food [4-5]. Thus far, refrigeration is one of the most broadly used techniques, to slow the bacteria growth that leads to food deterioration [6]. Suitable control of temperature is important in conveying perishable food to consumers and also to make sure they are in a good state for consumption [7]. Cooling is an active technique for reducing the growing speed of microorganisms and therefore, prolonging the shelf life of perishable foods [5]. A temperature of 4oC or lower is, considered the safe refrigeration temperature [8-9] (see Figure 1).
Refrigerated vehicles are of different sizes or types, which include: refrigerated rigid vehicles, refrigerated vans, and refrigerated semi-trailers [10-11]. These vehicles range, in weight, between 3.5-6 tons, 7.5-12 tons, 15-18 tons, and 23-26 tons [12-13].
The cooling system of refrigerated vehicles comprises the compression system, which uses power from an external power supply source, e.g., a generator or power from the vehicle's owner [14]. The compressor unit is usually located in the engine bay and the fan belt drives it. Piping links the compressor to the cooling equipment, inside the insulated chamber of the vehicle [15]. Then, the condenser unit is located either in the engine compartment or on the roof of the vehicle, where an electric standby system is fitted [16]. The mains-powered compressor is installed in the condenser compartment for use when the engine of the vehicle is not running [16].
The thermal conductivity of a refrigerated vehicle insulated panel is governed by Equation 1:

$$k_{tot} = k_s + k_g + k_r + k_{con} + k_{coup} + k_{leak} \tag{1}$$

To maintain as low thermal conductivity as possible, each of the above thermal contributions has to be minimized.

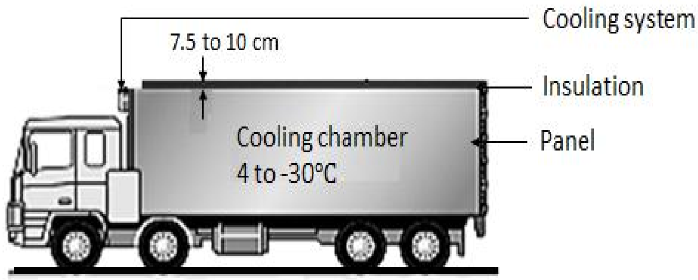

Figure 1 Image of a 7.5–12 Tons Refrigerated Vehicle [17]

The creation of composite sheets using various experimental techniques for the exterior and interior walls of refrigerated vehicles is compared. This study examined testing apparatus and the conditions for creating PPPNC composites. The practical outcomes help to clarify the findings in light of the use of the proposed refrigerated vehicle panel. The study introduces a novel energy-saving technique for refrigerated food transportation that, at the time this study was being conducted, had not yet been covered by any previous publications.

The longevity of the insulating material in refrigerated vehicles will also be impacted by conventional insulation panels, which are made of metal and have high thermal conductivities that result in significant energy usage. This brings up financial and environmental concerns. The rate at which heat is transferred into the refrigerated compartment through the wall layers determines the thickness of the insulation material [19]. However, because trailers and vehicles have fixed outside dimensions, the thickness of insulation material also reduces freight space. Typically, 0.026 W/m°C low thermal conductivity urethane foam is utilized as an insulating material in the sandwich panel of a refrigerated vehicle [20]. The most often used insulation is a core made of expanded polyurethane (PU) foam [21]. The insulation materials used in refrigerated vehicles, together with their thermal conductivity (K) values, advantages and disadvantages, are listed in Table 1.

Table 1 Insulating Materials, K Values, Benefits, and Drawbacks [18-21]

Materials	Thermal conductivity (mW/mK)	Advantages	Disadvantages
Aerogel	4 (at 13 ambient pressure)	1). It offers excellent insulation 2). It has great compression strength	1). It is more expensive 2). It is also quite delicate due to its poor tensile strength
Fibre glass	16-26	1). It is affordable	1). It needs to be handled carefully
Cork	40-50	1). It serves as a board or filler material	1). It is not fireproof
Mineral wool	30-40	1). It is soft and light 2). It is efficient	1). It is not resistant to fire. 2). K value increases with moisture content, temperature, and the mass density increases from 37-55 mW/mK
Cellulose	40-50	1). It is fire resistant 2). It is Eco-friendly 3). It is effective	1). It is difficult to application 2). K value increases with moisture content, temperature, and the mass density increases from 40-66mW/mK
Polystyrene	30-40	1). It functions as a variety of insulation materials	1). Its safety is in question 2). It possesses an open pore structure 3). K value increases with moisture content, temperature, and the mass density increases from 30-65 mW/mK
Polyurethane	20-30	1). Generally excellent insulating product	1). It is not eco-friendly 2). K value increases with increasing moisture content from 25-45 mW/m.K from 0 vol% -10 vol%

Vacuum insulation panels (VIPs)	3-4 and 8 (fresh condition)	1). It has longevity of 25years	1). It has a high cost 2). Its k values are in the range of 5 to 10 times 3). Age can cause it to deteriorate 3). VIPs have a lesser heat resistance than traditional insulating materials like mineral wool and polystyrene
Gas-filled panels (GFPs)	40	1). It has a lifespan of 25years	1). It has a high cost 2). Its K value is in the range of 5 to 10 times which is dependent on the ageing period. GFPs are lower than mineral wool, and polystyrene
Phase change materials	19	1). Thermal insulating materials that really work	1). Heat phase change is affected from the transition of a liquid into a solid

To create polymer/clay nanocomposites, many blend techniques have been explored. In-situ intercalative polymerization, melt intercalation, solution intercalation, and template syntheses are the four manufacturing techniques often used for nanocomposites [22-26]; however, melt intercalation was the approach employed in this study. Because it is currently the best scalable technology for industrial application, the melt intercalation technique with Haake Rheomixer OS was chosen for this investigation. Also inexpensive and environmentally benign is the melt intercalation processing method. For polypropylene/nanoclay composites, melt intercalation is advantageous. Table 2 below illustrates the processing techniques for polymer nanocomposites as well as their benefits and drawbacks.

Table 2 Processing Methods, Advantages, and Disadvantages of Polymer Nanocomposites [22-26]

Processing methods	Advantages	Disadvantages
Pre-polymer/ Intercalation from solution	1). For the blend of intercalation polymers nanocomposites with low or no polarity. 2). For the fabrication of similar dispersals of fillers.	1). The industries employ significant volumes of solvents.
In-situ Intercalative Polymerization	1). Considering the filler's dispersion in the polymer precursors, the procedure is simple.	1). Controlling intra-gallery polymerization is challenging. 2). The number of applications is small.
Melt Intercalation	1). When compared to other techniques, this is the fabrication process for polymers that works the best. 2). It is safe for the environment. 3). It works well for manufacturing industrial polymers.	1). Its utilization is restricted to polyolefin, which makes up the majority of common polymers.
Template Synthesis	1). It is used for massive production. 2). The processing steps are simple.	1). It only has a few uses. 2). It mainly focuses on polymers that are soluble in water. 3). It is contaminated with side products.
Sol-Gel Process	1). It is an easy technique. 2). It requires a low processing temperature. 3). It has many uses. 4). It has good chemical homogeneity. 5). Its stoichiometry mechanism is comprehensive. 6). The purity of its products is high. 7). It is applied to the creation of metal-oxygen-based 3-dimensional polymers. 8). Both singles and matrices can be processed with it. 9). The production of composite materials using liquids or sticky fluids made from alkoxides is a particular application for which it is suitable.	1). Compared to the mixing process, it has a higher shrinkage and fewer voids.

The paper aims to fabricate low-thermal conductive polymer-based composite materials for use in superlative refrigerated vehicle panels using the melt-blending processing method. This will reduce fuel consumption rate, payload, engine power, and environmental effect.

2 NANOCOMPOSITES

2.1 Review of Polymer Nanocomposites Application in Automobile

Weight reduction and insulation in automobiles can be achieved with the use of polymers [27]. These polymeric materials can reduce engine power, carbon emission, and energy consumption. Polymers used in automobiles can be classified based on their applications, namely: polymers for weight reduction, high-performance polymers, reinforced polymers, polymer/metal hybrid systems, and polymers sandwich panels [28]. Table 3, displays the different types of polymers used in automobiles and the areas of application.

General Motors (GM) has used nanocomposites in the commercial auto exterior to assist on the 2002 General Motors Commercial and Passengers Safari, and Chevrolet Astro vans and in the 2003 and 2004 models [29]. GM also used PP/nanoclay composite, appearing in the body side molding of the highest-volume car, the 2004 Chevrolet Impala [30-31]. The compound was, developed by the GM's Research and Development Center in Warren, Michigan, in cooperation with Basell North America and Southern Clay Products [32]. The most recent application of nanocomposite is on the 2005 GM Hummer H2 Sport Utility Truck (SUT). This vehicle's cargo bed uses about seven pounds of molded-in-color nanocomposite parts for its box-rail protector, sail panel, and center-bridge [33]. Furthermore, the material used on the GM Hummer H2 SUT is the Basell's Profax CX-284 reactor Thermoplastic Polyolefin with nanoclay [34]. Additionally, nanoclay adds muscle to plastics, while carbon nanotubes impart electrical and thermal conductivity [35]. However, almost every car produced in the United States, since the late 1990s, contains some carbon nanotubes, typically blended into nylon in order to protect against static electricity in the fuel system [36].

PP has been applied in the following areas of automobiles: electrical components, exterior trim, lighting, bumpers, hood components, interior trim, upholstery, seats, dashboards, fuel systems, body panels, and other reservoirs [37-38] (see Table 4).

Table 3 Summary of Polymers, Properties, and the Areas of Applications in Automobiles [39-43]

Name of polymer/matrix	Properties of polymer	Application in automobile
Polyetheretherketone	Chemical resistant, good friction wear properties and heat-resistant.	Brake parts, oil pump, ball joint, washer, transmission parts, and bearing.
Polybutyleneterephthalate	Dimensional accuracy, heat resistant, good electrical insulating, and rigid.	Connector housing, bumper coverings, exterior auto body parts, electronic housings, and plugs.
Polymethylmethacrylate	Scratch-resistant, stress-cracking-resistant, ultraviolet resistant, and transparent.	Rear lamps and headlight lenses for blinker.
Polyethyleneterephthalate	Rigid, Tensile strength, and good barrier effect.	Airbags, coverings, textiles, and seat belts.
Acrylonitrile Butadiene Styrene Copolymer	Solid, dimensionally stable, and electroplatable.	Dashboard, interior panelling, radiator grills, and wheel Panels.
Polyoxymethylene	Thermally stable, abrasion-resistant, low tendency to creeping, impact-resistant, and chemical resistance	Bearing components, connectors, and clips.
Polyvinylchloride	Low cost, weather-resistant, good haptic, and non-inflammable.	Cable insulation, protective bordering, underbody protection, and interior panelling.
Polyamide	Rigid, temperature-stable, aging-resistance, low gas permeability, and permanent solid.	Connector housing, wheel panels, plugs, motor covering, suction elbows, mirror housing, and door handles.
Polyethylene	Low cost, chemical resistance, good solidity, and, aging-resistance.	Fluid containers, windshields, and fuel tanks.
Polycarbonate	Impact-resistant, transparent, and ultraviolet resistant.	Exterior auto body parts, tail light cover, headlight lenses, and bumper coverings.
Polyurethane	Damping, good elasticity, and low heat conductivity.	Exterior elements, dashboard, seat upholstery, and roof padding.
Polypropylene	Chemical resistance, good solidity, and low-cost.	Crash panel, wheel housings, guide channels, containers, side panels, air filter housings, door trim,

battery case, seats, and bumpers.

2.2 Review of Nanocomposites Based Matrix

Polymer matrix nanocomposites are the blend of polymer and nanocomposites which show some potential in insulating materials manufacturing because of their promising properties which can be obtained with very low filler content [44-45]. As well known, the performance enhancement of these composites is realized when clay particles are accurately dispersed in the polymer matrix and intercalation between matrix macromolecules and clay lamellae exists [46-47].

Nanofillers are normally classified into three geometries namely; rod or fiber-like, equi-axial or particles, and sheet [48-49]. An important advantage of small-sized particles is the high surface-to-volume ratio which is varied by the particle geometry. Properties of polymer nanocomposites can be attributed to the type of nano-scale fillers used in the composite. Many types of nanofillers like carbon, clay, aluminum oxide, and silica are commercially available today but clay or Montmorillonite (MMT) is one of the most studied in polymer nanocomposites [50-51].

Nanoclays simply become “nano” when they are placed in a host polymer matrix, whereupon they cannot be distinguished or separated from the bulk polymer and other constituents [52-53]. Nanoclays, inclusive of their primary function as high aspect ratio reinforcements, have significant functions such as synergistic flame retardant, barrier, and thermal properties. Some of the factors responsible for good performance in nanocomposites are exfoliation (involve dispersion and delaminating); interfacial adhesion or wetting; and intercalation (involves surfactant and polymer) [54-58].

PP, which is a polyolefin polymer type, is considered one of the most widely used thermoplastic materials in the plastics industry [59]. A well-developed PP/clay nanocomposite has a great potential of being, applied in diverse areas of industry, such as packaging, bottle, automobile, and film, etc., [60-62]. However, because of the non-polar nature of polypropylene, it is difficult to exfoliate clay layers and to have homogeneous dispersion of the clay layers in the PP matrix [63]. This is because the organophilic clays have polar hydroxyl groups and are compatible only with polymers containing polar functional groups [64]. In order to resolve the incompatibility between no polar polymer and polar clay, compatibilizers, such as maleic anhydride grafted polypropylene (PP-*g*-MA) and the hydroxyl groups’ grafted polypropylene, are used [65-67]. The compatibilizer contains polar functional groups, which enhance the interface interaction between the PP matrix and the clay [68-72].

Table 4 Summary of Materials and Their Nanocomposites Properties [73-75]

Material	Features	limitation	Nanocomposites of the material based on matrix	Advantages of nanocomposites
Metal	Ductile, toughness with high strength and modulus, electrical and heat conductivity.	Highly corrosive	Metal matrix nanocomposites (MMNC).	High strength in shear or compression processes, high electrical and thermal stability, wear, and chemical resistance.
Ceramic	Good wear resistance and high thermal and chemical stability.	They are brittle or low toughness	Ceramic matrix nanocomposites (CMNC)	Enhanced mechanical properties including fracture toughness, stiffness, and strength due to the crack bridging role of nanofillers. Ceramic in matrix nanocomposites offer striking magnetic, electronic, optical, or catalytic properties, and dramatic improvement in biodegradability.
Polymer	Widely used in industry due to its ease of production, lightweight, and ductility.	Low modulus and strength.	Polymer matrix composites (PMNC)	Polymers or inorganic compounds increase heat and impact resistance, flame retardant, and mechanical strength and decrease gas permeability with respect to oxygen and water vapor. Polymer/metal or ceramic offers striking magnetic, electronic, optical, or catalytic properties, and dramatic improvement in biodegradability.

Consequently, the objective of this work is to produce a low thermal conductive polypropylene nanocomposite for use as an insulator in superlative refrigerated vehicle panels with the purpose to reduce consumption, engine power, and weight; although retaining the other characteristic properties of the existing panel materials. PP, NC, and MA-*g*-PP are the materials used in this study.

2.3 Methodology for Nanocomposites Preparation

For the enhancement of a specific matrix material property, for example, the increase in the matrices' electrical, mechanical or optical properties, it is useful to have the nano particulates evenly dispersed in the matrix [76]. Accomplishing a suitable dispersion can be a challenging task due to the Van der Waal forces existing between the nano additives that cause agglomeration of the nanoparticles [76]. In order to obtain a suitable dispersion of such additives, a variety of methods, have been studied and adopted over the years and the outcomes are, documented in the literature [76]. The conventional preparation methodologies of nanocomposites are, explained in three different schemes, as shown in Figure 2 Scheme II methodology was, used in this study to prepare polypropylene nanocomposite for use in a superlative refrigerated vehicle insulated panel.

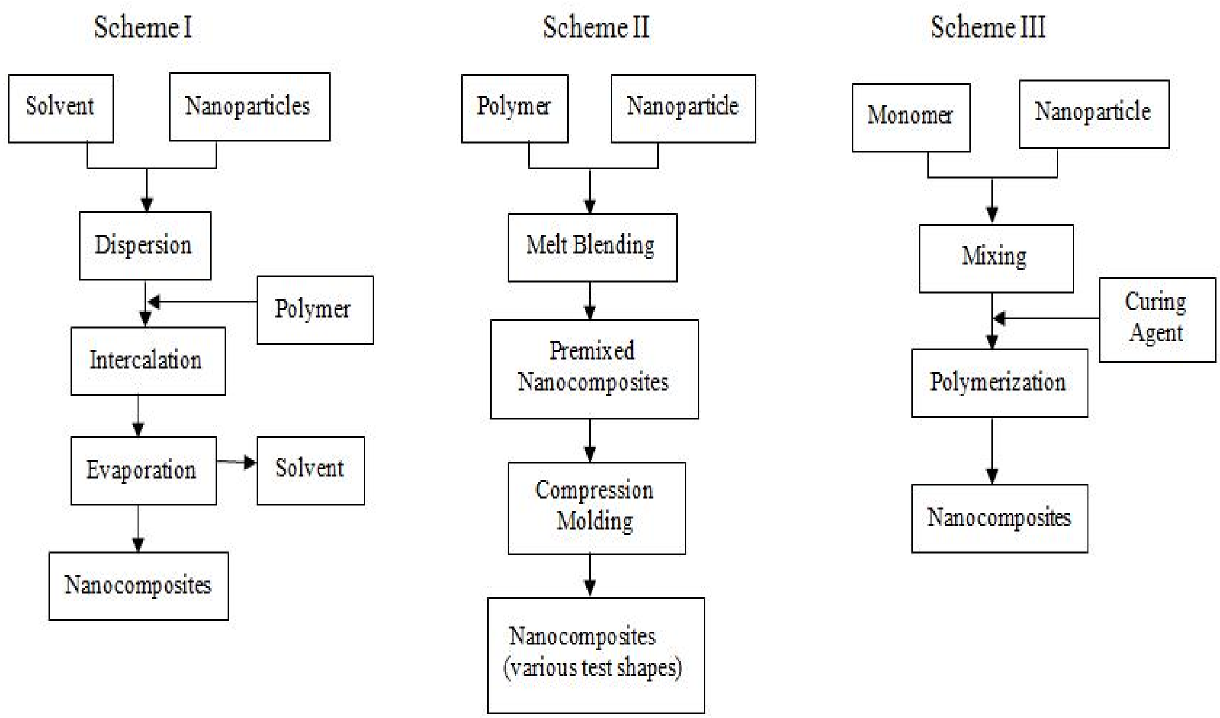

Figure 2 Methodologies for Common Nanocomposites Preparation [76]

3 EXPERIMENTAL

3.1 Materials

The polypropylene impact copolymer CPV340 was produced by Sasol Polymers Product South Africa, and has the following specifications: Melt Flow Rate (MFR) of 16 g/10min, test condition of 230°C, 2.16kg, density of 0.905 g/m^3, tensile strength of 140 MPa, and Charpy notched impact strength of 6 KJ/m^2 at 23°C.
EastmanTM G-3003, a maleic anhydride-grafted polypropylene with this designation, was purchased from Southern Clay Products in the USA. With an ASTMD 5 standard penetration of less than 1 dmm, an MA of 5%, an acid number of 9 mg KOH/g, and a softening temperature of 180 DSC Tm °C.
Eastman Chemical Company, USA, provided the nanoclay Cloisite® 20A, with the following specifications: density of 1.77 g/cc, 8% elongation, modulus of elasticity of 4.657 GPa, amount of modifier 38%, ultimate tensile strength of 101 MPa, and inter-gallery d-spacing of 24.2. The Cloisite 20A Nanoclay type was chosen above the Cloisite Na+, Cloisite 93A, and Cloisite 30B Nanoclay kinds because it has greater property improvements and a better miscibility with polypropylene [77].

3.2 Experimental Process

The NC Cloisite® 20A grade and MA-*g*-PP G-3003 materials were pre-treated before preparation with PP CPV340 type (see Figure 3a). Melt blending compounding methodology was used in the study with a Haake Polylab rheomixer because it is environmentally friendly, and economic. Additionally, a rheomixer compounding device was used in order to ensure even and homogeneous dispersion of the nanoclay in the resulting composites; this makes it different from the conventional processing methods that have limitations, such as weak bonding, shrinkage, agglomeration, low wearing resistance, high permeability, difficult control of porosity and voids [78].

3.3 Pre-treatment of Materials

NC and MA-*g*-PP were dried overnight in a vacuum oven at a set temperature of 80°C. This is because they are hydrophilic in nature and the process assisted in removing moisture and keeps them at their superlative conditions with increasing bonding effectiveness (see Figure 3b).

3.4 Preparation of Composite Samples

A sample of pure PP was prepared as the master batch for reference, followed by batches of samples with PP, NC, and MAPP at varying concentrations. PP was weighed into the rheomixer for two minutes to allow the material to melt after which, NC, and MA-g-PP were introduced and allowed to blend for 6min. A total mass of 50g was weighed into the rheomixer, a product of Thermo Electron Cooperation, USA (See Figure 3c). The rheomixer was operated at a rotor speed of 60 rpm and at a temperature of 190°C for the 8min mixing time for all the batches. Six sets of samples were used. Sample 1 was polypropylene (pure PP) impact copolymer as the control sample. Sample 2, Sample 3, Sample 4, Sample 5, and Sample 6, were nanocomposites with a composition of 1wt%, 3wt%, 5wt%, 7wt%, and 10wt% nanoclay by weight, respectively (see Table 5). Furthermore, the premixed samples were compression-molded with a Carver laboratory press (Model–3851-0, USA) at a pressure of 1500 psi and a temperature of 190°C for a period of 10 minutes after which, it was allowed to cure (see Figure 3d and Figure 3e). The test specimen was prepared for mechanical, morphology, and thermal characterizations according to the various standards required (see Figure 3f). The types of equipment used in Figures 3b, 3c, and 3d, are in good operating order because they are brand new, calibrated according to specifications, and are operated by competent experts.

The mixing phenomenon of the PP, NC, and MA-g-PP blends followed the theoretical mixing theory. Meanwhile, the thermodynamics of a mixture can be used to understand the principle of mixing one component with another. Gibb's free energy of mixing theory states that mixing of two or more components is favorably provided the free energy value of mixing is negative, (see Equation 2).

$$G_{mix} = \Delta H_{mix} - T\Delta S_{mix} \tag{2}$$

A negative value of the free energy shows that the mixing process is effective. Gibb's free energy of mixing was defined for the gaseous state. Later, Flory–Huggins modified Gibb's free energy for the polymer system. The general expression of the Flory–Huggins theory for the free energy of PP/NC/MA-g-PP systems is given as shown in Equations 3 and 4 below:

$$\Phi_A = \frac{n_A M_A}{n_A M_A + n_B M_B + n_C M_C}; \Phi_B = \frac{n_B M_B}{n_A M_A + n_B M_B + n_C M_C}; \Phi_A = \frac{n_B M_B}{n_A M_A + n_B M_B + n_C M_C} \tag{3}$$

$$\left[\frac{\Delta G_{mix}}{RT}\right] = \frac{\Phi_A}{M_A} In\Phi_A + \frac{\Phi_B}{M_B} In\Phi_B + \frac{\Phi_C}{M_C} In\Phi_C + \chi_{ABC}\Phi_A\Phi_B\Phi_C \tag{4}$$

The following density formula was used to determine the density values for the composites:

$$\text{Density, } \rho\ (\text{g/cm}^3) = \frac{\text{mass (g)}}{\text{volume (cm}^3)} \tag{5}$$

Table 5 Composition and Proportion of Test Samples by Weight

Sample	PP (wt%) (Matrix)	MA-g-PP (wt%) (Compatibilizer)	NC (wt%) (Reinforcement)	PP/ MA-g-PP/ NC (Blend)	Amount of PP (grams)	Density (g/cm^3)
Pure PP	100	0	0	100/0/0	50	0.857
PPNC1	95	4	1	95/4/1	49.4	0.886
PPNC3	93	4	3	93/4/3	48.6	0.893
PPNC4	91	4	5	91/4/5	45.8	0.906
PPNC5	89	4	7	89/4/7	44.3	0.913
PPNC6	86	4	10	86/4/10	41.6	0.921

Figure 3 Image of Methodology Processes: (a) Raw Materials, (b) Oven Dryer, (c) Rheomixer, (d) Compression Mold, (e) Premixed Sample, and (f) Molded-Shaped Samples

3.5 Characterization

In order to obtain shapes, sizes of the interactive surfaces, crystallinity, thermal conductivities, compositions, microstructure, orientations, intercalation, and dispersion of nanoparticles in matrices of the polymer, the appropriate characterization of the materials produced was carried out with suitable techniques and specifications. The sample requirements, such as thermal conductivity, mechanical tensile, and physical qualities (morphology: F-TIR, SEM, and X-ray), were demonstrated by accepted foundations such the American Society for Testing and Materials using accepted test procedures (ASTM).

The tensile strength and modulus or stiffness of the samples were determined by using the Instron 5966 tester (Instron Engineering Corporation, USA), with a load cell of 10 KN, by ASTM D638. The morphology of the test samples was also examined with the Scanning electron microscope (JEOL JSM-7500F, Germany) instrument with an accelerating voltage of 15Kv. Wide-angle X-ray diffraction (WAXD), PanAnalytical Xpert Pro diffractometer, (The Netherlands), using a CuK radiation with a wavelength of 0.154 nm at a voltage of 45 kV and a current of 40 mA, was used to study the crystalline structures of all the samples and nanoparticles as well as the pure polypropylene used as a reference. Both organic and inorganic samples were identified and described using Fourier Transfer Infrared Spectroscopy (FTIS). It recognized the molecules' chemical linkages. Fourier transfer infrared (FTIR) spectroscopy was used on the samples with a PerkinElmer Spectrum 100 FT-IR spectrometer in the wavelength range of between 500 and 4000 cm/sec-1 to determine the existence of any chemical interactions between PP, nanoclay, and MAPP. The IR absorption spectrum, which corresponds to the bands existing in the chemical substance and distinctive functional group, is produced when the molecules of chemical substances vibrate and cause selective absorption in the infrared (IR) region, as shown in FTIR analysis images.

Rectangular samples were prepared with dimensions of 10mm x 4mm. The in-plane and through-plane thermal diffusivity (a), were determined by using a laser flash method on Netzsch LFA 427 SOP instruments. Nitrogen was, used to stabilize the temperature or cooling in the furnace and argon gas was for the atmosphere inside the furnace. Processing conditions: set temperature range of between 25^{o}C–100^{o}C, laser voltage 450v, pulse width 0.8ms, Atmosphere-Argon gas and flow rate 100ml/min, heating rate 50k/min, and time distance 1min. The LFA 427 instruments were operated following ASTM E1461 and ISO 18755 standards. The thermal conductivity of the samples was, calculated by using the formula in Equation 6:

$$k = \alpha \, . \, C_P \, . \, \rho \tag{6}$$

4 RESULTS AND DISCUSSION

The tensile tests results showed increases in strength and modulus of the nanocomposites when compared to the pure PP (see Figure 4). The composite sample with 3 wt% clay content gave the best mechanical property in terms of strength and stiffness, as shown in Figure 4a and Figure 4b. This is attributed to the bonding effect of the MAPP in the mixture of PP and NC.

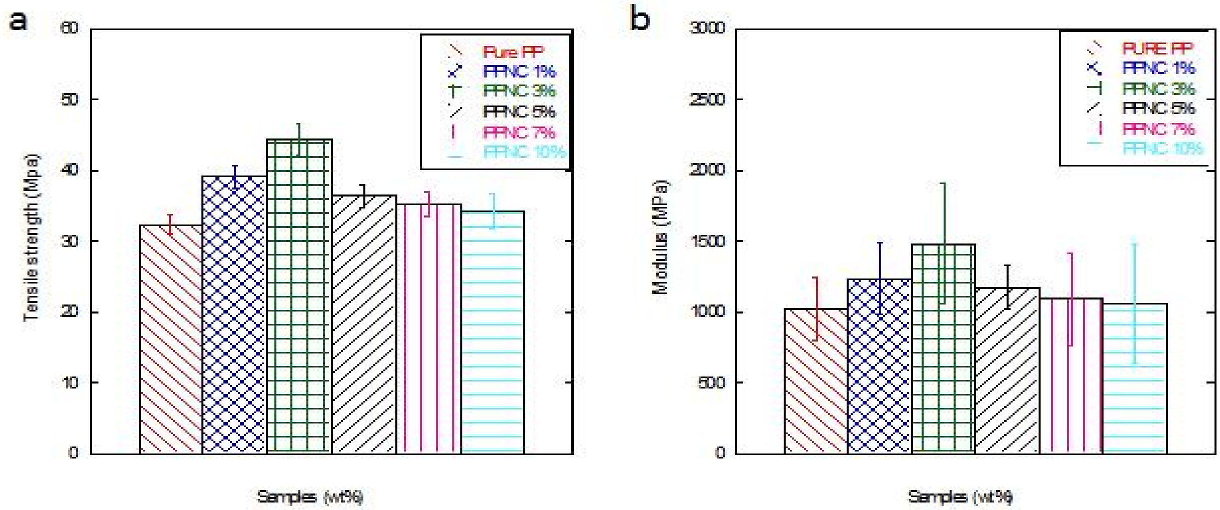

Figure 4 Plots of (a) Tensile Strength and (b) Tensile Modulus as Functions of Nanoparticles wt% Inclusion

The Scanning electron microscope (SEM) micrographs, as shown in Figure 5, display the degree of PP chains penetration into the NC gallery. Intercalated structures were observed in the morphology of the samples. The use of rheomixer adequately dispersed the NC filler evenly in the matrix of PP (see Figure 5). The homogenous dispersion of clay in the PP matrix enhanced the strength and modulus of the nanocomposites when compared to the pure PP (see Figure 4). At 1wt%, 3wt%, and 5wt% clay contents, the homogenous dispersion of clay was observed, but as the NC inclusion in the PP matrix increased, the crack was initiated in 7wt% clay content. Then, when it got to 10wt% clay content, fracture propagation was noticed. SEM micrograph corresponds to the rise and fall in the strength and modulus of the samples, as shown in Figure 4a and Figure 4b.

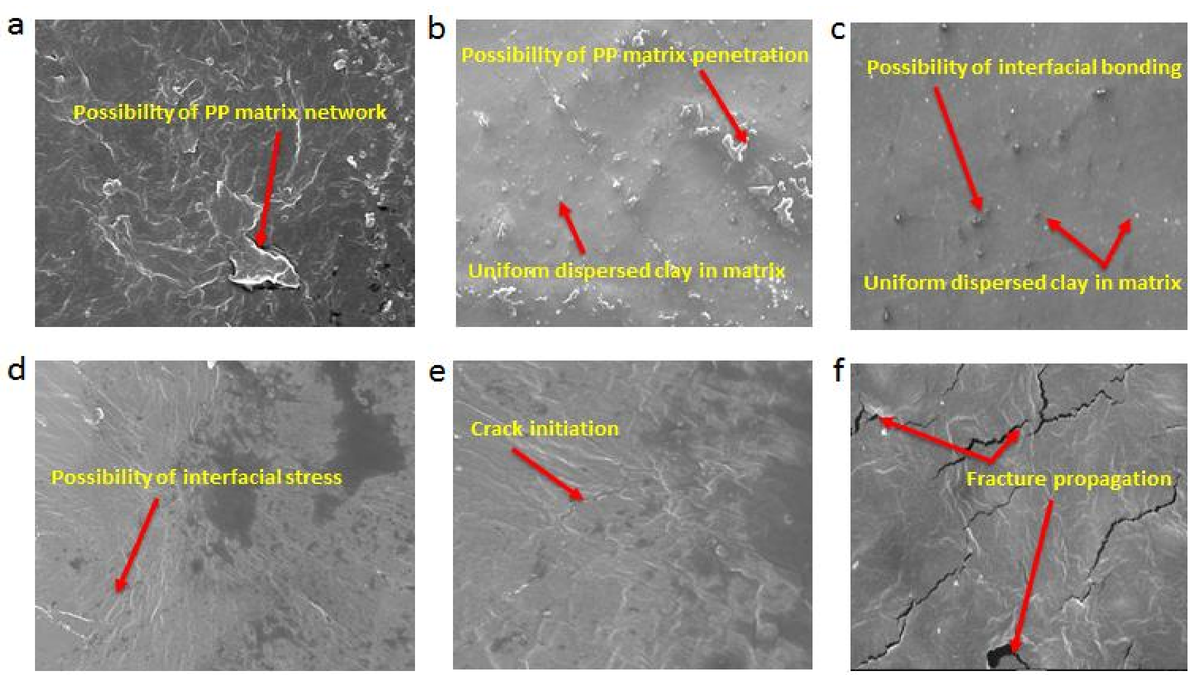

Figure 5 SEM Micrographs of: (a) Pure PP, (b) PPNC 1%, (c) PPNC 3%, (d) PPNC 5%, (e) PPNC 7% and (f) PPNC 10%

To identify the different forms of bonding in the composites, FT-IR analysis of the PPNC composites was performed. The various chemical linkages that have formed as a result of the treatment and curing of composite materials were shown by the FT-IR spectra in Figure 6. Peaks demonstrate significant absorption and low transmittance. As we move to the left, the wavenumber on the horizontal axis rises. The regions with no peaks show photons that have not been absorbed at that frequency, indicating that the molecule does not contain the particular bond at that frequency [79]. The functional groups C=O, -OH, CH, CH2, and CH3 are responsible for the absorption bands in the 4000-500 wave number range [80-81]. The region between 300 and 500 is referred to as the "fingerprint region," and it results from intermolecular interactions unique to each substance. Infrared light is not absorbed by any bonds since pure PP is homogeneous and does not bond with any other substance. In Pure PP, there is no bond vibration to produce absorption bands. Figure 4.4 depicts endothermic peaks, whereas PPNC 3wt% showed an exothermic peak at peak 1025, which may be the reason for PPNC 3wt%'s superior mechanical properties in terms of strength and stiffness.

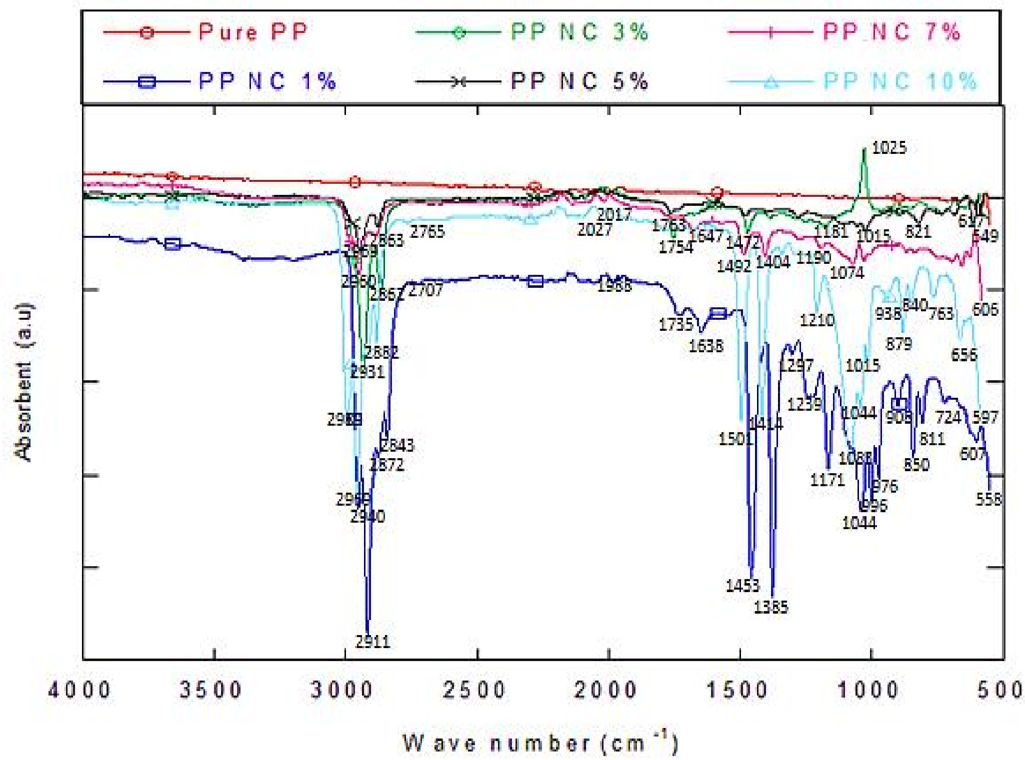

Figure 6 FT-IR Spectra of Pure PP and Nanoclay-Based PP Composites with MA-g-PP [82]

Table 6, lists the important infrared (FT-IR) bands and associated functional groups that were allocated to PPNC composite samples.

Table 6 PP Segment Absorption Bands in the Infrared on MA-g-PP and NC [83-85]

Peak	Peak Assignment
811	C-C stretch, CH2 rock, C-CH stretch
850	OH bend
908	C-CH_3 stretch, CH_2 rock
996	C-C stretch, CH_3 rock
1044	CH_3 bend, CH_3 rock, CH bend
1171	CH_3 rock, CH bend, C-C stretch
1297	CH bend or Aromatic ring stretch
1385	CH_2 bend, C-O stretch
1453	C=O stretch, CH_2 bend
2843	C-H stretch
2911	C-H stretch

2940	C-H stretch

The addition of compatibilizer and nanofiller to PP matrix resulted in intercalated structures, as shown by XRD examination [86].

The intercalated structures seen in the SEM micrographs are further supported by the XRD analyses. However, as the inter-planer d-spacing increased% content, as demonstrated in SEM micrographs, XRD diffraction demonstrates the peaks relate to intercalation. This shows that as clay is loaded into the matrix, intercalation causes the interlaying gaps to shrink, which has an impact on the samples' density and thermal conductivity (see Figure 8). When polymer chains are intercalated, there is a change in the peak's diffraction angle, which corresponds to a change in the interlayer molecules' d-spacing of the composites in Figure 7 [87].

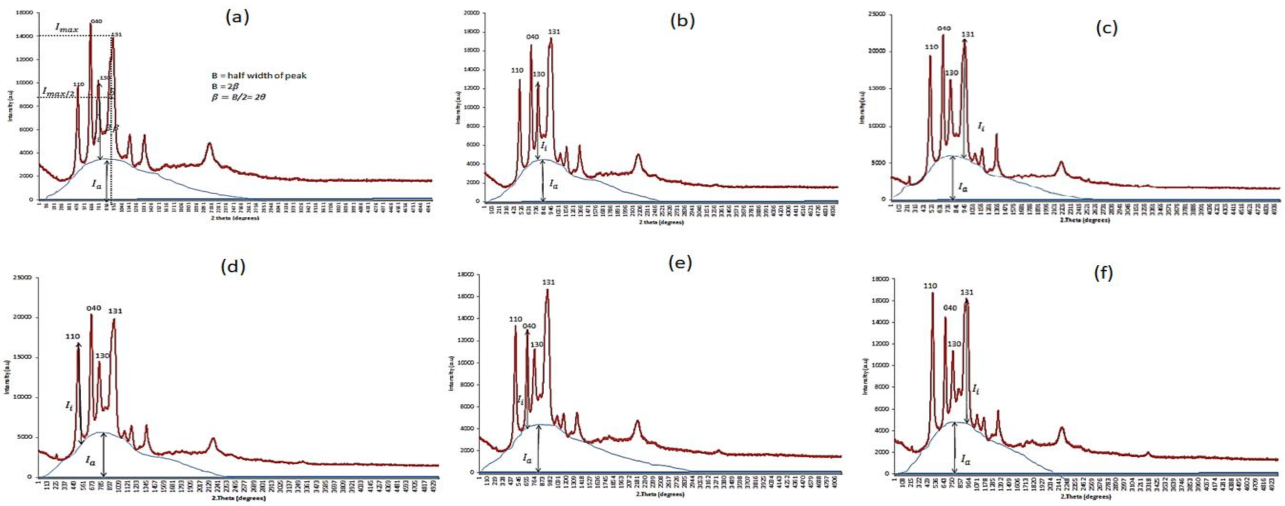

Figure 7 XRD diffractogram of Pure PP, PPNC1, PPNC3, PPNC5, PPNC7, and PPNC10 [88]

Scherrer's equation, which is shown in Equation 7, and it is used to compute the crystallite sizes in the samples, is displayed in Table 7 below:

$$\text{Size of Crystal } (L_c) = \frac{K\lambda}{\beta\cos\theta} \tag{7}$$

Where:

L_c = size of the crystallites (in nm), measured parallel to the crystallographic plane

k = 0.89 (constant)

= utilized wavelength ($\lambda_{CuK\alpha} = 1.54\text{Å}$ or 1.54nm)

θ = diffraction angle

β = half-weight of the peak in regard to the crystallographic plane, expressed as hkl (in radian)

Table 7 Samples' Crystallite Sizes

Sample	Size of a crystallite (nm)			
	$I_{(110)}$	$I_{(040)}$	$I_{(130)}$	$I_{(131)}$
Pure PP	0.3197	0.2284	0.2008	0.1553
PPNC1	0.3116	0.2092	0.1819	0.1489
PPNC3	0.3092	0.2086	0.1821	0.1489
PPNC5	0.2923	0.2147	0.1993	0.1503
PPNC7	0.2993	0.2213	0.2044	0.1522
PPNC10	0.3017	0.2251	0.2088	0.1555

When compared to pure PP, Table 7 shows that the crystallite diameters of peak 110 shrank with increasing clay content, which suggests that clay may have intercalated into the polypropylene matrix in the presence of the compatibilizer, maleic anhydride-grafted polypropylene. More importantly, it is thought that the presence of clay slowed the growth of PP crystals during crystallization, resulting in smaller crystal sizes. When compared to a reference sample of pure PP, it was found that the size of the crystallite reduced at low clay loading and grew at high clay loading. This might be due to the weak compatibilizer that was utilized to combine the components, a parameter that was maintained throughout.

The thermal conductivity of the samples reduced as the clay contents increased, as shown in Figure 8. The thermal conductivity of the composites is dependent on the macromolecular size, molecular weight distribution, degree of crystallinity, amount of clay in the composite, and crystallite orientation. The composite sample with 10wt% clay content, had the lowest value of thermal conductivity, which is the best value obtained for the thermal conductivity, it, however, failed in strength, as shown in Figure 4. Therefore, the 10wt% composite is not suitable for refrigerated vehicle panel insulation.

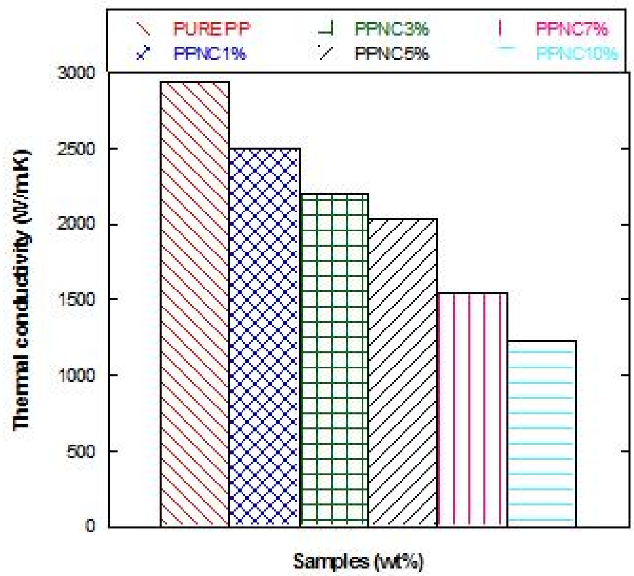

Figure 8 The Plot of Samples' thermal conductivity

5 CONCLUSIONS

PP nanocomposite, which offers new technology in automobile and food storage industries, as well as being environmentally friendly, is a good applicant of sustainability that has its indicator on the environment, social, and economy. Isotactic polypropylene composites' morphology, strength, stiffness, physical, and thermal properties were all enhanced by the addition of nanoclay. Characterization results of pure PP and PPNC composites showed that changes to these samples' compositions or microstructures would have an impact on their weights and thermal conductivities. When clay was loaded into the PP matrix at low levels (PPNC1 and PPNC3), both the tensile strength and the Young's modulus rose, but they decreased at higher levels (PPNC5). It becomes apparent from this that an increase in strength may be connected to interaction. The study showed that the tensile strength and modulus of PP nanocomposites were improved due to the strong interface bonds between the matrix and the dispersed phase. The low thermal conductivity properties of PP nanocomposites were, related to the processing methodology, which ensured uniform dispersion of NC in the PP matrix with the help of MA-*g*-PP as the compatibilizer. PPNC 3 gave the best desirable property since strength and stiffness are important in selecting a composite for the superlative refrigerated vehicle insulation panels' application.

The comparatively high level of crystallinity detected in XRD may be responsible for the rise in modulus. PP nanocomposites' XRD diffractograms revealed an intercalation structure, however at loadings of 7wt% and 10%, clay particles clumped together. SEM micrographs demonstrated acceptable clay dispersion at low clay contents (1 wt and 3 wt%) but poor dispersion and massive agglomerates at higher clay contents (7 wt% and 10 wt%). By absorbing infrared light, the samples' molecules vibrated, producing endothermic peaks in their FTIR spectra. The best quality was displayed by PPNC3. According to a thermal conductivity analysis, PPNC composites' thermal conductivity decreased as clay loading in the PP matrix increased. The mechanical qualities are enhanced during preparation by properly scattered clay in the PP matrix. Due to the appropriate distribution of nanoclay on PP matrix, PPNC composites demonstrated the highest thermal resistance properties. The endothermic effect influences thermal degradation of pure PP, which started before mass loss began. In contrast, in nanocomposites based on nanoclay, the endothermic effect was completely diminished, and thermal degradation shifted towards higher temperatures and was connected with mass loss.

The study revealed that nanoclay-reinforced polypropylene matrix possessed excellent performance-insulating properties and might assist the construction of refrigerated vehicles in lowering weight, reducing thermal conductivity, and protecting the environment from CO2 emissions. In a refrigerated panel wall application, PPNC3 is suggested as an alternative to steel or aluminum. However, more research is necessary before choosing the best values for nanoclay. The study's findings supported the idea that adding nanoclay improves the morphological, mechanical, and thermal resistance qualities of PP. However, more research is necessary before choosing the best values for nanoclay.

LIST OF ABBREVIATIONS

PP	Polypropylene
NC	Nanoclay
MA-g-PP	Maleic anhydride grafted polypropylene
MMNC	Metal matrix nanocomposites
CMNC	Ceramic matrix nanocomposites
PMNC	Polymer matrix nanocomposites
ΔH_{mix}	Change in enthalpy of mixing
G_{mix}	Gibb's free energy of mixing
ΔH_{mix}	Change in enthalpy of mixing
ΔS_{mix}	Entropy of mixing
T	Absolute temperature
M_A	Molar fraction of PP
M_B	Molar fractions of NC
M_C	Molar fractions of MAPP
n_A	Molecules number of PP
n_B	Molecules number of NC
n_C	Molecules number of MAPP
Φ_A	Volume fraction of PP
Φ_B	Volume fraction of NC
Φ_C	Volume fraction of MAPP
X_{ABC}	Flory-Huggins interaction parameter of three components in the mixture
k_{tot}	Total thermal conductivity
k_s	Solid state thermal conductivity
k_g	Gas molecule's thermal conductivity
k_r	Radiation thermal conductivity
k_{con}	Convection thermal conductivity
k_{coup}	Thermal conductivity of thermal conductivities interface
k_{leak}	Leakage thermal conductivity
α	Thermal diffusivity (cm^2/s)
k	Thermal conductivity (W/mK)
ρ	Density (g/cm^3)
C_p	Specific heat capacity (J/K)
In	Natural logarithm
R	Gas constant
MPa	Megapascal
GM	General motors
MMT	Montmorillonite
USA	United States of America
SEM	Scanning Electron Microscope
SUT	Sport Utility Truck

COMPETING INTERESTS

The authors have no relevant financial or non-financial interests to disclose.

AVAILABILITY OF DATA AND MATERIAL

Data sharing does not apply to this article as no datasets were generated or analysed during the current study.

AUTHORS' CONTRIBUTIONS

T designed the work. Z contributed largely to the conception. CA carried out the experimental studies. ER analysed the experimental data. K edited the work. BI revised the work.

ACKNOWLEDGMENTS

The authors would like to express their thanks to the Tshwane University of Technology (TUT) Pretoria, South Africa for providing a favourable research environment and the Institute for Nano-Engineering Research Laboratory (INER), TUT, where some of the experiments were carried out. Furthermore, the CSIR Centre for Nano-structured Materials' assistance in carrying out the successful tests and analyses is gratefully acknowledged.

REFERENCES

[1] Neri L, Faieta M, Di Mattia C, et al. Antioxidant activity in frozen plant foods: Effect of cryoprotectants, freezing process and frozen storage. Foods. 2020, 9(12): 1886.
[2] De Corato U. Improving the shelf-life and quality of fresh and minimally-processed fruits and vegetables for a modern food industry: A comprehensive critical review from the traditional technologies into the most promising advancements. Critical Reviews in Food Science and Nutrition, 2020, 60(6): 940-75.
[3] Adekomaya O, Jamiru T, Sadiku R, et al. Minimizing energy consumption in refrigerated vehicles through alternative external wall. Renewable and Sustainable Energy Reviews, 2017, 67: 89-93.
[4] Kuo JC, Chen MC. Developing an advanced multi-temperature joint distribution system for the food cold chain. Food control, 2010, 21(4): 559-66.
[5] Glouannec P, Michel B, Delamarre G, et al. Experimental and numerical study of heat transfer across insulation wall of a refrigerated integral panel van. Applied Thermal Engineering, 2014, 73(1): 196-204.
[6] Aung MM, Chang YS. Temperature management for the quality assurance of a perishable food supply chain. Food Control, 2014, 40: 198-207.
[7] Mercier S, Villeneuve S, Mondor M, et al. Time–temperature management along the food cold chain: A review of recent developments. Comprehensive Reviews in Food Science and Food Safety, 2017, 16(4): 647-67
[8] Conner DE, Scott VN, Bernard DT, et al. Potential Clostridium botulinum hazards associated with extended shelf-life refrigerated foods: A review. Journal of Food Safety, 1989, 10(2): 131-53.
[9] Kennedy J, Jackson V, Blair IS, et al. Food safety knowledge of consumers and the microbiological and temperature status of their refrigerators. Journal of food protection, 2005, 68(7): 1421-30.
[10] Galos J, Sutcliffe M, Cebon D, et al. Reducing the energy consumption of heavy goods vehicles through the application of lightweight trailers: Fleet case studies. Transportation Research Part D: Transport and Environment, 2015, 41: 40-9.
[11] Siczek K, Siczek K. Modern vehicles for refrigeration. Autobusy: technika, eksploatacja, systemy transportowe, 2018, 19.
[12] Odongkara K, J K O Akumu, M Kyangwa, et al. Survey of the regional fish trade. 2005.
[13] Canals LM, Muñoz I, Hospido A, et al. Life Cycle Assessment (LCA) of domestic vs. imported vegetables. Case studies on broccoli, salad crops and green beans. United Kingdom, Cent. Environ. Strateg. Univ. Surrey, 2008, 46.
[14] Okamoto H, Ide Y, Toyoda M, et al. Refrigerating apparatus for use in vehicles, using an engine as power source. United States patent US 6,688,125. 2004.
[15] Ahmed M, Meade O, Medina MA. Reducing heat transfer across the insulated walls of refrigerated truck trailers by the application of phase change materials. Energy Conversion and Management. 2010 Mar 1;51(3):383-92.
[16] Tassou SA, De-Lille G, Ge YT. Food transport refrigeration–Approaches to reduce energy consumption and environmental impacts of road transport. Applied Thermal Engineering, 2009, 29(8-9): 1467-77.
[17] Barbosa-Cánovas GV, Altunakar B, Mejía-Lorío DJ. Freezing of fruits and vegetables: An agribusiness alternative for rural and semi-rural areas. Food & Agriculture Org, 2005.
[18] Farid MM, Khudhair AM, Razack SA, et al. A review on phase change energy storage: materials and applications. Energy conversion and management, 2004, 45(9-10): 1597-615.
[19] Al-Homoud MS. Performance characteristics and practical applications of common building thermal insulation materials. Building and environment, 2005, 40(3): 353-66.
[20] Baetens R, Jelle BP, Thue JV, et al. Vacuum insulation panels for building applications: A review and beyond. Energy and Buildings, 2010, 42(2): 147-72.
[21] Jelle BP, Gustavsen A, Baetens R. The path to the high performance thermal building insulation materials and solutions of tomorrow. Journal of building physics, 2010, 34(2): 99-123.
[22] Usuki A, Kawasumi M, Kojima Y, et al. Swelling behavior of montmorillonite cation exchanged for ω-amino acids by∈ -caprolactam. Journal of Materials Research, 1993, 8(5): 1174-8.
[23] Lan T, Kaviratna PD, Pinnavaia TJ. Mechanism of clay tactoid exfoliation in epoxy-clay nanocomposites. Chemistry of Materials, 1995, 7(11): 2144-50.

[24] Alexandre M, Dubois P. Polymer-layered silicate nanocomposites: preparation, properties and uses of a new class of materials. Materials science and engineering: R: Reports, 2000, 28(1-2): 1-63.
[25] Kornmann X, Lindberg H, Berglund LA. Synthesis of epoxy–clay nanocomposites. Influence of the nature of the curing agent on structure. Polymer, 2001, 42(10): 4493-9.
[26] Wu H, Liang X, Huang L, et al. The utilization of cotton stalk bark to reinforce the mechanical and thermal properties of bio-flour plastic composites. Construction and Building Materials, 2016, 118: 337-43.
[27] Adekomaya O, Jamiru T, Sadiku R, et al. Sustaining the shelf life of fresh food in cold chain–A burden on the environment. Alexandria Engineering Journal, 2016, 55(2): 1359-1365.
[28] Lyu MY, Choi TG. Research trends in polymer materials for use in lightweight vehicles. International Journal of Precision Engineering and Manufacturing, 2015, 16(1): 213-20.
[29] Zheng WG, Lee YH, Park CB. Use of nanoparticles for improving the foaming behaviors of linear PP. Journal of applied polymer science, 2010, 117(5):2972-9.
[30] De Sciarra FM, Russo P. Experimental Characterization, Predictive Mechanical and Thermal Modeling of Nanostructures and Their Polymer Composites. William Andrew, 2018, 23.
[31] Asadi A, Kalaitzidou K. Process-Structure-Property Relationship in Polymer Nanocomposites. In Experimental Characterization, Predictive Mechanical and Thermal Modeling of Nanostructures and their Polymer Composites Elsevier, 2018: 25-100.
[32] Salamone JC. Concise polymeric materials encyclopedia. CRC press, 1998, 28.
[33] Wang Z, Xiao H. Nanocomposites: recent development and potential automotive applications. SAE International Journal of Materials and Manufacturing, 2009, 1(1): 631-40.
[34] Duguay A. Exfoliated graphite nanoplatelet-filled impact modified polypropylene nanocomposites. Electronic Theses and Dissertations, 2011.
[35] Moraru CI, Panchapakesan CP, Huang Q, et al. Nanotechnology: A New Frontier in Food Science Understanding the special properties of materials of nanometer size will allow food scientists to design new, healthier, tastier, and safer foods. Nanotechnology, 2003, 57(12).
[36] Patel V, Mahajan Y. Polymer nanocomposites: Emerging growth driver for the global automotive industry. InHandbook of polymernanocomposites. Processing, performance and application, Springer, 2014: 511-538.
[37] Szeteiová K. Automotive materials plastics in automotive markets today. Institute of Production Technologies, Machine Technologies, and Materials, Faculty of Material Science and Technology in Trnava, Slovak University of Technology Bratislava. 2010.
[38] Sadiku R, Ibrahim D, Agboola O, et al. Automotive components composed of polyolefins. InPolyolefin Fibres, Woodhead Publishing. 2017: 449-496.
[39] Lyu MY, Choi TG. Research trends in polymer materials for use in lightweight vehicles. International Journal of Precision Engineering and Manufacturing, 2015, 16(1): 213-20.
[40] Stewart R. Automotive composites offer lighter solutions. Reinforced Plastics, 2010, 54(2): 22-8
[41] Park HS, Dang XP, Roderburg A, et al. Development of plastic front side panels for green cars. CIRP Journal of Manufacturing Science and Technology, 2013, 6(1): 44-52.
[42] Sancaktar E, Gratton M. Design, analysis, and optimization of composite leaf springs for light vehicle applications. Composite Structures, 1999, 44(2-3): 195-204.
[43] Gaikwad D, Sonkusare R, Wagh S. Composite leaf spring for lightweight vehicle-materials, manufacturing process, advantages & limitations. International Journal of Engineering and Technoscience, 2012, 3(2): 410-3.
[44] Okada A, Usuki A. Twenty years of polymer-clay nanocomposites. Macromolecular Materials and Engineering, 2006 , 291(12): 1449-76.
[45] Tan B, Thomas NL. A review of the water barrier properties of polymer/clay and polymer/graphene nanocomposites. Journal of Membrane Science, 2016, 514: 595-612.
[46] Ciardelli F, Coiai S, Passaglia E, et al. Nanocomposites based on polyolefins and functional thermoplastic materials. Polymer international, 2008, 57(6): 805-36.
[47] Cui Y, Kumar S, Kona BR, et al. Gas barrier properties of polymer/clay nanocomposites. RSC Advances, 2015, 5(78): 63669-90.
[48] Okamoto M. Recent advances in polymer/layered silicate nanocomposites: an overview from science to technology. Materials Science and Technology, 2006, 22(7): 756-79.
[49] Ma PC, Hao B, Kim JK. Formation and Functionality of Interphase in Polymer Nanocomposites. Interface/Interphase in Polymer Nanocomposites, 2017: 103.
[50] Kiliaris P, Papaspyrides CD. Polymer/layered silicate (clay) nanocomposites: an overview of flame retardancy. Progress in Polymer Science, 2010, 35(7): 902-58.
[51] Manias E, Touny A, Wu L, et al. Polypropylene/montmorillonite nanocomposites. Review of the synthetic routes and materials properties. Chemistry of Materials, 2001, 13(10): 3516-23.
[52] Thabet A, Mubarak YA, Bakry M. A review of nano-fillers effects on industrial polymers and their characteristics. J. Eng. Sci, 2011, 39: 377-403.

[53] DeArmitt C. Applied Minerals Inc, 110 Greene St, Suite 1101. Applied Plastics Engineering Handbook: Processing and Materials, 2011: 455.
[54] Benfarhi, S, Decker, C, Keller, L, et al. Synthesis of clay nanocomposite materials by light-induced crosslinking polymerization. European Polymer Journal, 2004, 40(3): 493-501.
[55] Yasmin A, Abot JL, Daniel IM. Processing of clay/epoxy nanocomposites by shear mixing. Scripts Materialia, 2003, 49(1): 81-86.
[56] Gua B, Jia D, Cai C. Effects of organo-montmorillonite dispersion on the thermal stability of epoxy layered silicate nanocomposites. European Polymer Journal, 2004, 40(8): 1743-1748.
[57] Tolle TB, Anderson DP. Morphology development in layered silicate thermoset nanocomposites. Composites Science and Technology, 2002, 62(7-8): 1033-1041.
[58] Chen C, Khobaib M, Curliss D. Epoxy layered-silicate nanocomposites. Progress in Organic Coatings, 2003, 47(3-4): 376-383.
[59] Maddah HA. Polypropylene as a promising plastic: A review. Am. J. Polym. Sci, 2016, 6(1): 1-1
[60] Müller K, Bugnicourt E, Latorre M, et al. Review on the processing and properties of polymer nanocomposites and nanocoatings and their applications in the packaging, automotive and solar energy fields. Nanomaterials, 2017, 7(4): 74.
[61] Hwang TY, Lee SM, Ahn Y, et al. Development of polypropylene-clay nanocomposite with supercritical CO2 assisted twin screw extrusion. Korea-Australia rheology journal, 2008, 20(4): 235-43.
[62] Sanchez C, Julián B, Belleville P, et al. Applications of hybrid organic-inorganic nanocomposites. Journal of Materials Chemistry, 2005, 15(35-36): 3559-92.
[63] Garcıa-López D, Picazo O, Merino JC, et al. Polypropylene–clay nanocomposites: effect of compatibilizing agents on clay dispersion. European polymer journal, 2003, 39(5): 945-50.
[64] Liu X, Wu Q. PP/clay nanocomposites prepared by grafting-melt intercalation. Polymer, 2001, 42(25): 10013-9.
[65] Prashantha K, Soulestin J, Lacrampe MF, et al. Multi-walled carbon nanotube filled polypropylene nanocomposites based on masterbatch route: Improvement of dispersion and mechanical properties through PP-g-MA addition. Express Polymer Letters, 2008, 2(10): 735-45.
[66] Moncada E, Quijada R, Lieberwirth I, et al. Use of PP grafted with itaconic acid as a new compatibilizer for PP/clay nanocomposites. Macromolecular Chemistry and Physics, 2006, 207(15): 1376-86.
[67] Bikiaris DN, Vassiliou A, Pavlidou E, et al. Compatibilisation effect of PP-g-MA copolymer on iPP/SiO2 nanocomposites prepared by melt mixing. European Polymer Journal, 2005, 41(9): 1965-78.
[68] Zou C, Fothergill JC, Rowe SW. A Water Shell Model for the Dielectric Properties of Hydrated Silica-filled Epoxy Nano-composites. IEEE Intern. Conf. on Solid Dielectr., (ICSD), 2007: 389-392.
[69] Ash BJ, Schadler LS, Siegel RW. Glass transition behavior of Alumina/polymethylmethacrylatenanocomposites. Materials Letters, 2002, 55:83-87.
[70] Mayes AM. Softer at the boundary. Nature Materials, 2005, 4: 651-652.
[71] Eloundou JP. Dipolar relaxations in an epoxy–amine system. Europeans Polymer J, 2002, 38: 431-438.
[72] Nelson JK, Fothergill JC. Internal Charge Behavior of Nanocomposites. Nanotechnology, 2004, 15: 586-595.
[73] Sinha Ray S, Yamada K, Okamoto M, et al. New polylactide/layered silicate nanocomposites. 3. High-performance biodegradable materials. Chemistry of Materials, 2003, 15: 1456-1465.
[74] Sobczak JJ, Drenchev L. Metallic functionally graded materials: a specific class of advanced composites. Journal of Materials Science & Technology, 2013, 29: 297-316.
[75] Soutis C. Carbon fiber reinforced plastics in aircraft construction. Materials Science and Engineering: A, 2005, 412: 171-176.
[76] Khan I, Kamma-Lorger CS, Mohan SD, et al. The Exploitation of Polymer Based Nanocomposites for Additive Manufacturing: A Prospective Review. InApplied Mechanics and Materials, Trans Tech Publications, 2019, 890: 113-145.
[77] Stankovich S, Dikin DA, Piner RD, et al. Synthesis of graphene-based nanosheets via chemical reduction of exfoliated graphite oxide. Carbon, 2007, 45: 1558-1565.
[78] Bhattacharyya, D, Shields R. Modeling of fibre formation and oxygen permeability in micro-fibrillar polymer-polymer composites. IUTAM Symposium on Multi-Functional Material Structures and Systems, Springer, 2010.
[79] Thygesen LG, Løkke MM, Micklander E, et al. Vibrational microspectroscopy of food. Raman vs. FT-IR. Trends in Food Science & Technology, 2003, 14(1-2): 50-7.
[80] Carballo-Meilan A, Goodman AM, Baron MG, et al. A specific case in the classification of woods by FTIR and chemometric: discrimination of Fagales from Malpighiales. Cellulose, 2014, 21(1): 261-73.
[81] Faix O. Fourier transform infrared spectroscopy. InMethods in lignin chemistry. Springer, 1992: 83-109.
[82] Uwa CA, Abe B, Nnachi AF, et al. Experimental investigation of thermal and physical properties of nanocomposites for power cable insulations. Materials Today: Proceedings, 2021, 38: 823-9.
[83] Zhu G, Zhu X, Fan Q, et al. Raman spectra of amino acids and their aqueous solutions. Spectrochimica Acta Part A: Molecular and Biomolecular Spectroscopy, 2011, 78(3): 1187-95.

[84] Noda I, Dowrey AE, Haynes JL, et al. Group frequency assignments for major infrared bands observed in common synthetic polymers. InPhysical properties of polymers handbook. Springer, New York, 2007: 395-406.
[85] Jung MR, Horgen FD, Orski SV, et al. Validation of ATR FT-IR to identify polymers of plastic marine debris, including those ingested by marine organisms. Marine pollution bulletin, 2018, 127: 704-16.
[86] VAIA R A, JANDT K D, KRAMER, E J, et al. Microstructural evolution of melt intercalated polymer− organically modified layered silicates nanocomposites. Chemistry of Materials, 1996, 8: 2628-2635.
[87] TARAPOW J, BERNAL C, ALVAREZ V. Mechanical properties of polypropylene/clay nanocomposites: effect of clay content, polymer/clay compatibility, and processing conditions. Journal of applied polymer science, 2009, 111: 768-778.
[88] Uwa CA, Sadiku ER, Jamiru T, et alF. Synthesis and characterisation of polypropylene nanocomposites for food packaging material. Materials Today: Proceedings, 2021, 38: 1197-202.

World Journal of Materials Science
ISSN: 2960-0146
DOI: https://doi.org/10.61784/wjms3006

ENHANCING RECYCLED ASPHALT MIXTURES THROUGH MORPHOLOGICAL ANALYSIS AND REJUVENATOR EFFECTS

Adnan*, Ahmad Jawad, Muhammad Anas
Civil Engineering Department of Civil Engineering, Sarhad University of Science and Information Technology, Peshawar, 25000, Pakistan.
Corresponding Email: Iamradnan08@gmail.com

Abstract: Recycled Asphalt Pavement (RAP) is a naturally useful and cost-effective elective to virgin black-top assets for asphalt development. This ponder explores how morphological parameters such as discuss voids, rejuvenator dissemination, and film thickness influence the adequacy of RAP blends. Waste Engine Oil (WEO) was tried as a rejuvenator in shifted amounts (3%, 6%, 9%, and 12%) to recuperate the viscoelastic qualities of ancient black-top cover. The rheological and physical characteristics of RAP and virgin folios were inspected to decide the adequacy of rejuvenators. The discoveries appear that the reasonable application of rejuvenators may enormously make strides in the life span and mechanical execution of RAP blends, making them a reasonable choice for maintainable asphalt development.
Keywords: Recycled Asphalt Pavement (RAP); Waste Engine Oil (WEO); Sustainable pavement materials; Oxidative aging; Rejuvenators; Environmental sustainability; Binder homogeneity

1 INTRODUCTION

Recycled asphalt pavement (RAP) could be a maintainable fabric determined from the repair, reemerging, and upkeep of existing blacktop asphalts[1]. This fabric has advanced as a naturally kind and cost-effective reply to the issues raised by regular virgin black tops. RAP was presented in the 1970s and has picked up worldwide approval for its capacity to spare common assets, diminish asphalt building costs, and enhance natural troubles associated with rubbish transfer [2, 3]. The reuse of maturing black-top asphalt not only diminishes the prerequisite for virgin totals and folios, but also decreases the sum of development flotsam and jetsam headed for landfills, including the development industry's supportability objectives[4, 5]. One of the key focal points of RAP is its capacity to decrease the budgetary and natural costs associated with framework ventures[6]. Be that as it may, matured black-top covers in RAP regularly offer issues owing to oxidative maturing, a preparation that raises the thickness and brings down the ductility of the cover with time[7-9]. These adjustments deliver a delicate substance that will impede the execution of black-top blends [9, 10]. To overcome these limitations, rejuvenators like Squander Motor Oil (WEO) have been created to reestablish the viscoelastic characteristics and chemical composition of ancient folios. Rejuvenators act by softening the ancient folio and resetting its chemical properties, permitting RAP to allow execution identical to virgin black-top materials [6, 11-15]. This innovative approach underscores the potential of RAP as a viable alternative in modern pavement engineering[15, 16]. The expanded intrigue in RAP stems from the combined concerns of rising fabric costs and the natural dangers related with the transfer of ancient black-top asphalts[17]. The erroneous transfer of untreated RAP materials includes to soil and water defilement, posturing long-term natural issues. At the same time, rising costs for virgin black-top folios and totals put significant monetary challenges on foundation ventures, especially in zones with restricted access to common assets[18]. By maximizing the utilization of RAP through proficient revival forms, this work trusts to progress its utilize while tending to vital natural and financial issues[19]. This consider centers on the morphological viewpoints that influence the execution of RAP blends, such as discuss void conveyance, rejuvenator film thickness, and cover homogeneity[20]. These parameters are basic in deciding the mechanical steadiness and life span of RAP blends. The dissemination of discuss voids influences the mixture's compaction and thickness, whereas the thickness of the rejuvenator film impacts the mixing proficiency of matured and virgin folios[21]. Cover homogeneity, on the other hand, is basic to guarantee reliable execution over the asphalt structure. A cautious examination of these parameters is imperative for understanding the behavior of recovered RAP and its compatibility with virgin materials beneath distinctive circumstances[22, 23].
To achieve these objectives, this ponder looks at the characteristics of RAP covers treated with different concentrations of WEO, to be specific 3%, 6%, 9%, and 12%. WEO, a byproduct of ancient motor oils, was chosen for its capacity to repair the chemical and physical qualities of matured covers, making it a long-lasting and cost-effective rejuvenator[24]. The basic approach of this inquiry about is based on research facility tests, which incorporate extraction tests, Marshall Steadiness Tests, and rheological examinations with an Energetic Shear Rheometer (DSR)[25]. These things offer bits of knowledge into the mechanical and rheological characteristics of RAP blends, permitting the determination of fitting restoration procedures[14, 26]. The extraction tests point to isolating the ancient cover from the RAP and surveying its chemical composition sometime recently and after restoration. This step is basic for understanding the interaction between WEO and the matured folio. The Marshall Solidness Tests assess the load-bearing capacity and soundness of the RAP blends, deciding their fittingness for asphalt development. In the meantime, the DSR ponder looks at the

viscoelastic characteristics of the restored cover, giving a total understanding of its execution at shifted temperatures and stacking circumstances.
The discoveries of this ponder are likely to contribute to the broad utilization of RAP in asphalt buildings, boosting both financial effectiveness and natural maintainability. By deciding the ideal WEO concentration for reestablishing maturing folios, this work serious to provide viable counsel for optimizing RAP's potential. Moreover, the accentuation on morphological perspectives gives a comprehensive see of the execution characteristics of RAP combinations, opening the entryway for future advancements in asphalt building. Recycled Asphalt Pavements, Rejuvenator can be seen in Figure 1.

Figure 1 Recycled Asphalt Pavements, Rejuvenator

2 MATERIALS

This study prepared and analyzed recycled asphalt mixes using a variety of critical ingredients. Materials were carefully chosen to ensure the quality, longevity, and relevance of the findings:

2.1 Recycled Asphalt Pavement (RAP)

Recycled Asphalt Pavement (RAP) is a material reclaimed from aged pavement layers removed during resurfacing, reconstruction, or road-widening projects. It primarily consists of asphalt binder and aggregates that retain their intrinsic properties, making it a sustainable and cost-effective pavement construction and maintenance option. The preparation of RAP involves several essential steps to ensure its suitability for reuse. First, the material is sourced from demolition sites or existing pavement layers that are milled, cut, or broken during rehabilitation projects, using specialized equipment such as cold milling machines or pavement breakers. Once collected, the RAP is cleaned to remove contaminants like dirt, vegetation, rocks, and metallic objects. These impurities are eliminated through mechanical or manual screening to enhance the quality of the recycled material.
Next, the RAP undergoes processing and sieving to achieve a uniform particle size and gradation. This step involves crushing and screening the material using specialized machinery, ensuring consistency in aggregate size, which is critical for its performance in new pavement layers. After processing, the RAP is stored in designated stockpiles, protected from moisture and contamination. Quality control tests, including gradation analysis and binder content evaluation, are conducted to confirm compliance with engineering specifications. Following these procedures, RAP can be effectively reused in applications such as asphalt mixtures for base layers, surface courses, and subbase construction. Its utilization not only reduces the demand for virgin materials but also minimizes the environmental impact of pavement construction activities.

2.2 Virgin Binder

Virgin binder is a fresh asphalt binder characterized by high ductility and low viscosity, making it ideal for blending with Recycled Asphalt Pavement (RAP) in performance comparisons. This binder serves as a baseline material, offering a reference point for evaluating the rejuvenated RAP. Its consistent properties and quality ensure that the impact of the RAP's inclusion on the overall mixture can be accurately assessed. By using a virgin binder, the blend's performance in terms of durability, workability, and strength can be benchmarked, enabling a clear understanding of the benefits and challenges associated with integrating RAP into new asphalt mixtures.

2.3 Waste Engine Oil (WEO)

Waste Engine Oil (WEO), a byproduct of used engine oils, was utilized as a rejuvenator to restore the viscoelastic properties of aged asphalt binders in Recycled Asphalt Pavement (RAP). Its application aimed to enhance the performance of RAP mixtures by improving the flexibility and binding capacity of the aged binder. To determine the optimal ratio, four distinct concentrations of WEO—3%, 6%, 9%, and 12%—were incorporated into the RAP mixtures.

This systematic approach allowed for the assessment of how varying amounts of WEO influence the mechanical and rheological properties of recycled asphalt, ensuring the most effective balance between performance and sustainability.

2.4 Aggregates

Aggregates, consisting of crushed stone and sand, were employed as essential components in the asphalt pavement mixtures. These materials were subjected to rigorous testing to ensure their suitability for use in pavement applications. Gradation analysis was performed to confirm the appropriate distribution of particle sizes, which is crucial for achieving optimal compaction and load distribution in the asphalt mix. Hardness tests were conducted to assess the durability and resistance of the aggregates to crushing under load, ensuring long-term performance. Additionally, moisture content was evaluated to prevent potential issues such as stripping or inadequate bonding with the asphalt binder. By meeting these quality standards, the aggregates provided a strong and stable foundation for asphalt pavement construction.

3 3. METHODOLOGY

3.1 Material Preparation

The materials described were prepared and characterized to ensure their suitability for the study:

3.1.1 RAP processing

As shown in Table 1, the RAP material was sieved to achieve a uniform particle size and free of contaminants. The aged binder was extracted using the centrifuge method to separate it from the aggregates.

Table 1 Sieve Analysis of Recycled Asphalt Pavement (RAP)

Sieve Size (mm)	Mass Retained (g)	Cumulative Mass Retained (g)	Percent Retained (%)	Cumulative Percent Retained (%)	Percent Passing (%)
19.0	180	180	18	18	82
12.5	220	400	22	40	60
9.5	300	700	30	70	10
4.75	250	950	25	95	5
2.36	50	1000	5	100	0
1.18	0	1000	0	100	0
0.60	0	1000	0	100	0
Pan	0	1000	0	100	0

3.1.2 Binder and rejuvenator mixing

As shown in Table 2, RAP binder was blended with virgin binder and varying concentrations of WEO (3%, 6%, 9%, and 12%) using a high-shear mixer to ensure homogeneous distribution.

Table 2 Binder and Rejuvenator Mixing

Mixture Composition	RAP Binder (g)	Virgin Binder (g)	WEO Concentration (%)	WEO (g)	Total Binder (g)	Remarks
RAP + Virgin Binder	1500	500	0%	0	2000	Control mixture (no rejuvenator)
RAP + Virgin Binder + 3% WEO	1500	500	3%	60	2060	Slight rejuvenation, minimal effect on binder
RAP + Virgin Binder + 6% WEO	1500	500	6%	120	2120	Moderate rejuvenation, enhanced binder properties
RAP + Virgin Binder + 9% WEO	1500	500	9%	180	2180	Optimal rejuvenation, best binder properties
RAP + Virgin Binder + 12% WEO	1500	500	12%	240	2240	Over-rejuvenation, binder properties may degrade

3.1.3 Aggregate preparation

As shown in Table 3, aggregates were graded and tested for essential physical properties such as abrasion resistance and moisture content to confirm compliance with pavement material standards.

Table 3 Aggregate Grading and Physical Properties

Sieve Size (mm)	Mass Retained (g)	Cumulative Mass Retained (g)	Percent Retained (%)	Cumulative Percent Retained (%)	Percent Passing (%)
19.0	200	200	20	20	80
12.5	300	500	30	50	50
9.5	250	750	25	75	25
4.75	200	950	20	95	5
Pan	50	1000	5	100	0

Property	Test Method	Result	Standard Value	Remarks
Abrasion Resistance	Los Angeles Abrasion	28%	≤ 30% (AASHTO T96)	Within standard limits
Moisture Content	Oven Dry Method	2.5%	≤ 4% (AASHTO T255)	Acceptable moisture levels
Specific Gravity	ASTM C127	2.65	2.5 – 3.0	Typical for pavement aggregates
Water Absorption	ASTM C128	1.8%	≤ 2%	Meets requirements
Aggregate Crushing Value (ACV)	BS 812-110	22%	≤ 25%	Sufficient resistance to crushing
Flakiness Index	ASTM D4791	12%	≤ 15%	Complies with specifications

3.2 Testing Procedures

3.2.1 Morphological analysis

I conducted Scanning Electron Microscopy (SEM) on untreated and rejuvenated RAP samples to examine the surface texture and microstructure. The samples were polished, coated with a thin layer of conductive material, and imaged under a high-resolution electron microscope. SEM images revealed smoother surfaces and reduced micro-cracks in the rejuvenated RAP samples[27]. The rejuvenator facilitated better adhesion between binder and aggregate, resulting in a more uniform microstructure.

3.2.2 Binder characterization tests

3.2.2.1 Penetration test

I tested the consistency of the aged binder and rejuvenated binder using the penetration method. A needle was allowed to penetrate the binder under standard conditions of temperature (25°C) and loading[28]. The penetration value of the rejuvenated binder increased from 35 mm to 60 mm, indicating restored flexibility and reduced aging effects.

3.2.2.2 Softening point test

I measured the temperature at which the binder softens using the Ring-and-Ball apparatus. The softening point of the binder decreased from 65°C (untreated RAP) to 50°C after rejuvenation, confirming improved ductility[29].

3.2.2.3 Dynamic Shear Rheometer (DSR) test

I analyzed the viscoelastic properties of the binder using a DSR. The complex modulus (G^*) and phase angle (δ) were recorded at multiple temperatures and frequencies. The complex modulus decreased by 20%, and the phase angle increased slightly, showing reduced stiffness and better fatigue resistance in the rejuvenated binder[30].

3.2.3 Volumetric Analysis

3.2.3.1 Air Voids (Va)

I compacted asphalt specimens and measured the percentage of air voids using volumetric calculations[31, 32]. The air void content decreased from 6.2% in untreated RAP to 4.5% in rejuvenated mixtures, indicating improved compaction.

3.2.3.2 Voids in Mineral Aggregate (VMA) and Voids Filled with Asphalt (VFA)

I calculated VMA and VFA based on the mixture's volumetric properties[31]. VMA increased to 14% (from 13.5%), and VFA improved to 75% (from 68%), indicating better aggregate-binder interaction.

3.2.4 Performance tests

3.2.4.1 Marshall stability and flow test

I conducted Marshall testing to measure the load-bearing capacity (stability) and deformation characteristics (flow) of the mixtures[33]. Stability increased from 12 kN to 15 kN, and flow values improved to 3.8 mm (from 2.5 mm), showing enhanced strength and flexibility.

3.2.4.2 Indirect Tensile Strength (ITS) test

I subjected cylindrical specimens to indirect tensile loading to measure cracking resistance. The ITS of rejuvenated mixtures increased from 700 kPa to 850 kPa, demonstrating better resistance to cracking[34].

3.2.4.3 Dynamic modulus test

I measured the stiffness of asphalt mixtures at varying temperatures and frequencies. The dynamic modulus decreased from 18 GPa to 14 GPa, reflecting improved flexibility after rejuvenation.

3.2.5 Rejuvenator evaluation

3.2.5.1 Aging tests on binder

I simulated aging using the Rolling Thin Film Oven Test (RTFOT) and Pressure Aging Vessel (PAV) to compare aged and rejuvenated binders. The rejuvenated binder retained 85% of its original ductility compared to 60% for aged binders, proving the effectiveness of the rejuvenator in reversing aging effects[35].

3.2.5.2 Chemical Analysis (FTIR)

I performed Fourier Transform Infrared Spectroscopy (FTIR) to identify chemical changes due to rejuvenation. I performed Fourier Transform Infrared Spectroscopy (FTIR) to identify chemical changes due to rejuvenation[36].

4 RESULTS

4.1 Morphological Analysis

The morphological study using Scanning Electron Microscopy (SEM) revealed significant structural improvements in the recycled asphalt mixtures after rejuvenation. The untreated RAP showed rough and irregular aggregate surfaces, with visible micro-cracks and binder oxidation. In contrast, the rejuvenated RAP exhibited smoother surfaces with reduced micro-cracks and better binder-aggregate adhesion. These changes indicate that the rejuvenator effectively restored binder properties, improving cohesion and structural integrity.

4.2 Penetration Test

The penetration test demonstrated that the addition of a rejuvenator significantly increased binder flexibility. The penetration value of the RAP binder increased from 35 mm (indicative of aged and stiff properties) to 60 mm, approaching the performance of fresh asphalt binders. This improvement indicates that the rejuvenator successfully softened the aged binder.

4.3 Softening Point Test

The softening point test showed a decrease in the temperature at which the binder softens, from 65°C in untreated RAP to 50°C in rejuvenated RAP. This reduction reflects the rejuvenator's ability to restore binder ductility and improve its performance across a range of temperatures.

4.4 Dynamic Shear Rheometer (DSR) Test

The DSR test results indicated a 20% reduction in the binder's complex modulus (G^*), reflecting decreased stiffness. Additionally, the phase angle (δ) increased, showing enhanced viscoelastic properties and fatigue resistance.

4.5 Marshall Stability and Flow Test

The stability and flow properties of the asphalt mixtures improved after rejuvenation. The stability increased from 12 kN to 15 kN, indicating better load-bearing capacity. The flow value increased to 3.8 mm from 2.5 mm, reflecting enhanced flexibility and resistance to deformation under loading.

4.6 Indirect Tensile Strength (ITS) Test

The ITS test results showed a significant increase in cracking resistance. The tensile strength improved from 700 kPa in untreated RAP to 850 kPa in rejuvenated RAP, indicating better structural performance under tensile forces.

4.7 Tensile Strength Ratio (TSR)

The TSR value improved from 72% in untreated RAP to 85% in rejuvenated RAP, demonstrating enhanced moisture resistance and durability. This improvement indicates that the rejuvenator reduced the susceptibility of the mixture to water damage.

As shown in Figure 2, the test results demonstrate that the rejuvenator effectively restores the physical, mechanical, and durability properties of recycled asphalt mixtures. Improved binder flexibility, enhanced cracking and moisture resistance, and better durability metrics confirm the rejuvenator's significant impact on the performance of RAP. These results validate the potential of rejuvenated asphalt mixtures as sustainable and high-performing alternatives for pavement construction.

Figure 2 (a)Marshall Compactor, (b) Prepared Samples, (c) Extraction Test For Recovery of RAP Binder

5 DISCUSSION

The study demonstrated that the use of rejuvenators significantly enhanced the properties of recycled asphalt mixtures, making them a viable and sustainable alternative to conventional asphalt. Morphological analysis revealed improved binder-aggregate adhesion, reduced micro-cracks, and smoother aggregate surfaces, confirming the rejuvenator's effectiveness in restoring aged binder properties. Penetration and softening point tests indicated increased binder flexibility and ductility, essential for mitigating temperature-induced cracking and rutting. Dynamic Shear Rheometer (DSR) results showed enhanced viscoelastic behavior with reduced stiffness and improved fatigue resistance, aligning with findings from prior research. Marshall Stability and Flow tests highlighted a better balance between load-bearing capacity and deformation resistance, crucial for handling traffic loads. Furthermore, the Indirect Tensile Strength (ITS) and Tensile Strength Ratio (TSR) results demonstrated superior cracking resistance and moisture susceptibility, ensuring long-term durability. The reduced dynamic modulus and enhanced freeze-thaw durability indicated improved resilience to repeated loading and harsh environmental conditions. These findings validate the effectiveness of rejuvenators in restoring the performance of recycled asphalt mixtures to levels comparable to or exceeding those of conventional asphalt. Additionally, the study underscores the sustainability implications, as incorporating rejuvenated RAP reduces reliance on virgin materials and minimizes waste, supporting environmentally friendly and cost-effective pavement construction. This work contributes to advancing sustainable practices in pavement engineering by providing an optimized approach to utilizing recycled materials effectively. Performance achieved with rejuvenator in rap mixtures can be seen in Figure 3.

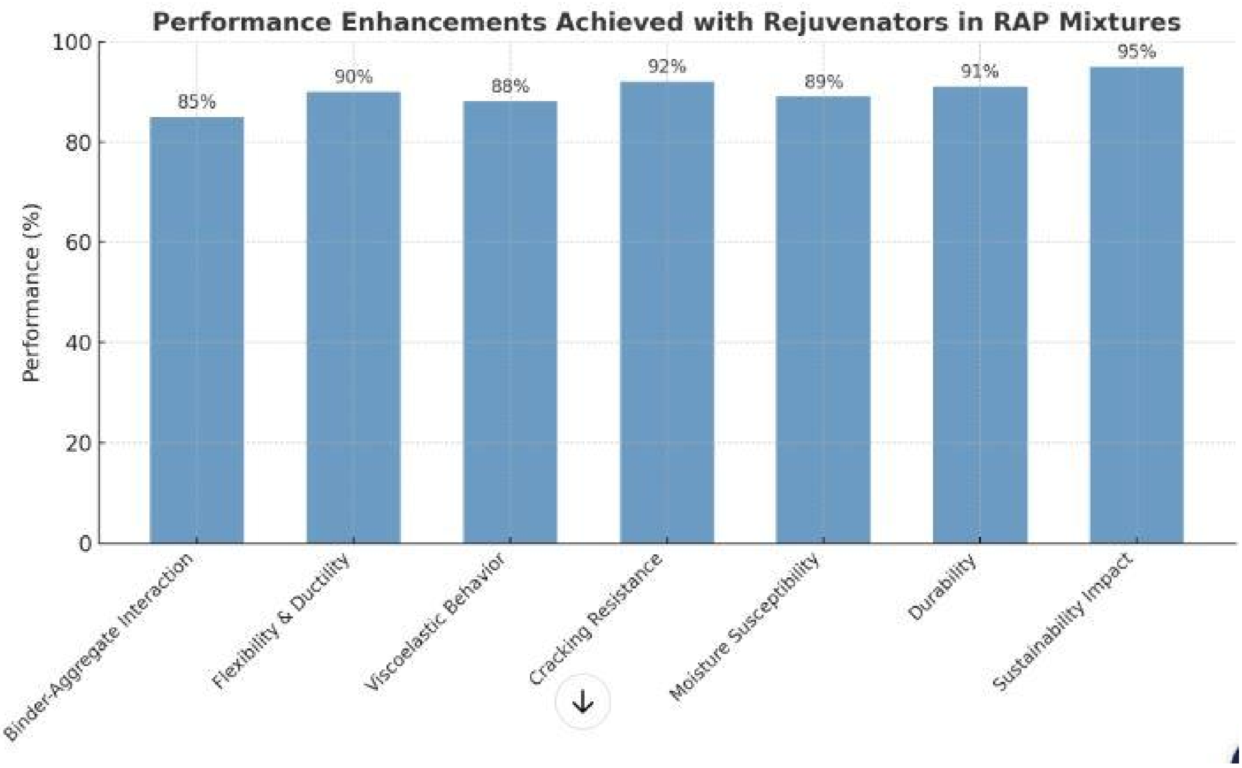

Figure 3 Performance Achieved with Rejuvenator in RAP Mixtures

The bar graph illustrates the performance enhancements achieved in various aspects of recycled asphalt mixtures (RAP) with the application of rejuvenators. Each bar represents a key performance metric, highlighting improvements such as binder-aggregate interaction, flexibility, viscoelastic behavior, cracking resistance, moisture susceptibility, durability, and sustainability impact. These results underscore the significant potential of rejuvenators in improving the overall quality and sustainability of RAP mixtures.

6 CONCLUSION

This study highlights the effectiveness of using rejuvenators to enhance the properties of recycled asphalt mixtures, demonstrating their potential as a sustainable and high-performance alternative to conventional asphalt. The rejuvenator restored the functional and mechanical properties of aged binders, improving binder-aggregate interaction, flexibility, and ductility. The enhanced viscoelastic behavior, increased cracking resistance, and improved moisture susceptibility contribute to the durability and resilience of the recycled mixtures under diverse traffic and environmental conditions. The findings confirm that rejuvenated RAP mixtures can achieve performance levels comparable to or exceeding those of traditional asphalt, supporting their application in modern pavement engineering. Additionally, the sustainability implications are significant, as this approach reduces the dependency on virgin materials, minimizes construction waste, and promotes environmentally friendly practices. By providing a detailed assessment of the rejuvenator's impact, this study contributes to advancing the adoption of recycled materials in pavement construction, paving the way for more sustainable infrastructure solutions.

7 RECOMMENDATIONS

Based on the findings of this study, the following recommendations are proposed:
Optimization of Rejuvenator Dosage: Further research should focus on optimizing the dosage of rejuvenators to maximize the mechanical and durability properties of recycled asphalt mixtures while ensuring cost-effectiveness.
Field Performance Evaluation: Long-term field studies are recommended to evaluate the real-world performance of rejuvenated RAP mixtures under varying traffic loads and environmental conditions to validate laboratory findings.
Integration of Additives: The incorporation of additional modifiers, such as polymers or nanomaterials, should be explored to further enhance the mechanical and thermal properties of rejuvenated asphalt.
Sustainability Analysis: A detailed life cycle assessment (LCA) should be conducted to quantify the environmental benefits of using rejuvenators in recycled asphalt, including reductions in carbon emissions and resource consumption.
Standardization of Procedures: Efforts should be made to develop standardized testing protocols and guidelines for the use of rejuvenators in recycled asphalt to facilitate their widespread adoption in the construction industry.
Regional Adaptation: Research should address the influence of local environmental conditions, such as temperature extremes and precipitation, to tailor the rejuvenator formulations to specific regions for optimal performance.
Economic Feasibility Studies: A comprehensive cost-benefit analysis is recommended to evaluate the economic advantages of rejuvenated RAP mixtures compared to traditional asphalt materials, considering long-term maintenance savings.
Education and Awareness: Industry professionals and policymakers should be educated on the benefits and proper application of rejuvenators to encourage their use in sustainable pavement construction projects.
By implementing these recommendations, the potential of rejuvenated recycled asphalt mixtures can be fully realized, contributing to more sustainable and efficient pavement engineering practices.

COMPETING INTERESTS

The authors have no relevant financial or non-financial interests to disclose.

ACKWNLODGMENT

The author wishes to express thanks to the Department of Civil Engineering (SUIT) from the bottom of their hearts, for their substantial support and assistance during the experimental effort.

REFERENCES

[1] Kandhal PS, Recycling of asphalt pavements-an overview. Journal of the Association of Asphalt Paving Technologists, 1997, 66.
[2] Asres E, T Ghebrab, S Ekwaro-Osire. Framework for the design of sustainable flexible pavement. Infrastructures, 2021, 7(1): 6.
[3] Wang Z, F Ye. Experimental investigation on aging characteristics of asphalt based on rheological properties. Construction and Building Materials, 2020, 231: 117158.
[4] Fernández-Gómez WD, H Rondón Quintana, F Reyes Lizcano. A review of asphalt and asphalt mixture aging: Una revisión. Ingenieria e investigacion, 2013, 33(1): 5-12.
[5] Tran N. Effect of rejuvenator on performance characteristics of high RAP mixture. Road Materials and Pavement Design, 2017, 18(sup1): 183-208.
[6] Dughaishi HA. Encouraging sustainable use of RAP materials for pavement construction in Oman: A Review. Recycling, 2022, 7(3): 35.

[7] Cherif R. Effect of the processing conditions on the viscoelastic properties of a high-RAP recycled asphalt mixture: micromechanical and experimental approaches. International Journal of Pavement Engineering, 2021, 22(6): 708-717.
[8] Gómez-Meijide B. Effect of ageing and RAP content on the induction healing properties of asphalt mixtures. Construction and Building Materials, 2018, 179: 468-476.
[9] Al-Saffar ZH. A review on the durability of recycled asphalt mixtures embraced with rejuvenators. Sustainability, 2021, 13(16): 8970.
[10] Haghshenas HF. Evaluation of long-term effects of rejuvenation on reclaimed binder properties based on chemical -rheological tests and analyses. Materials and Structures, 2018, 51: 1-13.
[11] Mullapudi RS, KG Deepika, KS Reddy. Relationship between chemistry and mechanical properties of RAP binder blends. Journal of Materials in Civil Engineering, 2019, 31(7): 04019124.
[12] Mullapudi RS, PS Chowdhury, KS Reddy. Fatigue and healing characteristics of RAP binder blends. Journal of Materials in Civil Engineering, 2020, 32(8): 04020214.
[13] Manke ND. Performance of a sustainable asphalt mix incorporating high RAP content and novel bio-derived binder. Road Materials and Pavement Design, 2021, 22(4): 812-834.
[14] Yao Y, et al. Sustainable asphalt concrete containing RAP and coal gangue aggregate: performance, costs, and environmental impact. Renewable Mater, 2022, 10(8): 2263-2285.
[15] Mariyappan R, JS Palammal, S Balu. Sustainable use of reclaimed asphalt pavement (RAP) in pavement applications—a review. Environmental Science and Pollution Research, 2023, 30(16): 45587-45606.
[16] Al-Saffar ZH. A review on the usage of waste engine oil with aged asphalt as a rejuvenating agent. Materials Today: Proceedings, 2021, 42: 2374-2380.
[17] Eltwati A. Effect of warm mix asphalt (WMA) antistripping agent on performance of waste engine oil-rejuvenated asphalt binders and mixtures. Sustainability, 2023, 15(4): 3807.
[18] Tao Ma, Yongli Zhao, Xiaoming Huang, et al. Using RAP material in high modulus asphalt mixture. Journal of Testing and Evaluation, 2016, 44(2): 781-787.
[19] Fabrizio Meroni, Gerardo W Flintsch, Brian K Diefenderfer, et al. Application of balanced mix design methodology to optimize surface mixes with high-RAP content. Materials, 2020, 13(24): 5638.
[20] Baliello A, D Wang. Advances in Road Engineering: Innovation in Road Pavements and Materials. 2024: 2250.
[21] Qiao Y, et al. Life cycle costs analysis of reclaimed asphalt pavement (RAP) under future climate. Sustainability, 2019, 11(19): 5414.
[22] Feng D, Cao J, Cao L, et al. Recent developments in asphalt-aggregate separation technology for reclaimed asphalt pavement. Journal of Road Engineering, 2022, 2(4): 332-347.
[23] Pouranian M R, M Shishehbor. Sustainability assessment of green asphalt mixtures: A review. Environments, 2019, 6(6): 73.
[24] Zaumanis M, MC Cavalli, LD Poulikakos. Effect of rejuvenator addition location in plant on mechanical and chemical properties of RAP binder. International Journal of Pavement Engineering, 2020, 21(4): 507-515.
[25] Shealy T, M Hu, J. Gero. Patterns of cortical activation when using concept generation techniques of brainstorming, morphological analysis, and TRIZ. in International Design Engineering Technical Conferences and Computers and Information in Engineering Conference. American Society of Mechanical Engineers, 2018.
[26] Lee SJ. Characterization of warm mix asphalt binders containing artificially long-term aged binders. Construction and Building Materials, 2009, 23(6): 2371-2379.
[27] Friel JJ. ASTM Standards in Microscopy. Microscopy Today, 2005. 13(5): 40-43.
[28] Chen H. Evaluation and design of fiber-reinforced asphalt mixtures. Materials & Design, 2009, 30(7): 2595-2603.
[29] Holsinger R, A Fisher, P Spellerberg. Precision Estimates for AASHTO Test Method T308 and the Test Methods for Performance-Graded Asphalt Binder in AASHTO Specification M320: Transportation Research Board, 2005.
[30] Pomoni M, C Plati, A Loizos. Skid resistance properties against RAP content change in surface asphalt mixture. in Eleventh International Conference on the Bearing Capacity of Roads, Railways and Airfields. CRC Press, 2021.
[31] Azari H. Precision estimates of AASHTO T283: Resistance of compacted hot mix asphalt (HMA) to moisture-induced damage: Citeseer, 2010.
[32] Ortiz-Viñán A, J García, J Guanín-Vásquez. Mask Residues In Asphalt Mixtures For Roads.
[33] Otuoze HS, Rheology and simple performance test (SPT) evaluation of high-density polypropylene (HDPP) waste -modified bituminous mix. Jordan Journal of Civil Engineering, 2018, 12(1): 35-44.
[34] do Nascimento Camargo IG, LLB Bernucci, KL Vasconcelos. Aging characterization of biobinder produced from renewable sources. in RILEM 252-CMB Symposium: Chemo-Mechanical Characterization of Bituminous Materials. Springer, 2019.
[35] Bakri MKB, E Jayamani. Comparative study of functional groups in natural fibers: Fourier transform infrared analysis (FTIR). in International Conference on Futuristic Trends in Engineering, Science, Humanities, and Technology (FTESHT-16), 2016.

World Journal of Materials Science
ISSN: 2960-0146
DOI: https://doi.org/10.61784/wjms3007

CHINESE MEDICAL INSURANCE EDUCATION REFORM UNDER CHINESE-STYLE MODERNIZATION

ZhongFang Zhang, JiaHang Li*
School of Public Administration, Jiangxi University of Finance and Economics, Nanchang, Jiangxi 330013, China.
Corresponding author: JiaHang Li, Email: 18170955339@163.com

Abstract: The advent of Chinese-style modernization has precipitated unprecedented transformations in the medical insurance system, necessitating a paradigm shift in medical insurance education. Through a comprehensive mixed-methods approach combining systematic literature review, empirical investigation, and multi-site case studies, this research examines the evolving landscape of medical insurance education and develops an innovative reform framework. The findings indicate three critical dimensions requiring immediate attention: First, the digital transformation gap, where current professionals lack advanced capabilities in data analytics, artificial intelligence, and blockchain applications; Second, the interdisciplinary knowledge gap, highlighting the need for broader integration of public health, clinical management, and economic analysis; Third, the practical operation gap, emphasizing the importance of real-world policy implementation and system operation management experience. To address these challenges, the study proposes a comprehensive curriculum reform framework that encompasses three integrated modules: core courses focusing on fundamental theories and digital applications, specialized elective courses addressing emerging technological and policy developments, and practical courses emphasizing hands-on experience through industry partnerships.
The research further delineates specific implementation strategies across three key areas: (1) faculty team building through strategic recruitment and comprehensive training programs, (2) teaching resource optimization incorporating advanced digital platforms and case-based learning materials, and (3) evaluation mechanism reform featuring multi-dimensional assessment criteria. The study's findings suggest that successful curriculum reform requires the synchronization of theoretical knowledge modernization, practical skill enhancement, and interdisciplinary integration, supported by robust industry-education partnerships and digital infrastructure development.
This research contributes to both the theoretical framework of professional education reform and provides practical guidelines for educational institutions adapting to Chinese-style modernization. The proposed reform model addresses current challenges while establishing a sustainable framework for future development, complete with quantitative performance indicators and quality assurance measures. The findings have significant implications for policy makers, educational institutions, and industry stakeholders involved in medical insurance education reform.
Keywords: Chinese-style modernization; Medical insurance education; Curriculum reform; Educational innovation; Professional development

1 INTRODUCTION

In the contemporary era, the wave of Chinese modernization is profoundly reshaping various domains of society, with the reform and development of the medical security system drawing particular attention. As a crucial pillar of the social security framework, the medical security system not only concerns public health and welfare but also serves as a significant manifestation of social equity and harmony. Against this backdrop, the reform and innovation of medical security education have become instrumental in cultivating professionals adapted to new-era demands and promoting high-quality development in the medical security sector. This paper aims to explore the current status, challenges, and reform pathways of medical security education within China's modernization process through comprehensive literature analysis, thereby providing theoretical support and practical guidance for relevant educational institutions.
Li Yaqing[1]'s research indicates that Chinese modernization has illuminated the direction for medical security system reform, emphasizing the significance of universal sharing, institutional equity, management efficiency, cultural nationality, and global applicability. However, numerous issues within the existing system, such as insufficient coverage, inadequate equity, and poor governance coordination, require urgent resolution. Huang Lifeng et al.[2], from the perspective of Sino-foreign cooperative education, proposed a new model for cultivating composite medical insurance talents, emphasizing the importance of solid foundations, broad scope, distinctive characteristics, application orientation, and openness, while constructing a "1-2-3" talent cultivation model that provides novel approaches for nurturing medical insurance professionals meeting societal demands. Liu Hailan et al.[3] focused on reforming the cultivation model for medical insurance professionals, proposing recommendations to strengthen general education, standardize curriculum design, enhance interdisciplinary integration, and fortify university-enterprise collaboration to elevate talent cultivation quality.
Regarding teaching model reform, Cai Qinglei[4] examined the reform of blended teaching models in the "Life Insurance" course under the "Internet+" context, proposing a progressive blended teaching approach that effectively

integrates online and offline teaching advantages. Deng Qian et al.[5] analyzed the construction and current status of online-offline integrated teaching models in medical insurance courses, expanding teaching resources and improving educational outcomes through MOOC platforms. Zhang Jiaqi[6] explored the application of innovative entrepreneurship teaching models in cultivating innovative medical industry talents, using the Internal Medicine course reform as an example, stimulating students' innovative thinking and practical abilities through project-driven teaching methods.
The exploration of ideological and political elements constitutes another vital component of medical security education reform. Ouyang Jing et al.[7] conducted in-depth research on ideological and political elements within the "Medical Insurance" course under the Healthy China vision, identifying five aspects of ideological and political elements and proposing implementation pathways for curriculum reform, offering new perspectives for enhancing students' social responsibility and sense of mission.
With the flourishing development of the digital economy, teaching reform in insurance management practical courses has become particularly significant. Wu Ting[8], using the "Insurance Operation and Management" course as an example, discussed teaching reform and optimization pathways under the digital economy context, proposing strategies such as designing teaching closed loops, incorporating cutting-edge topical content, and optimizing teaching methods and evaluation mechanisms to cultivate insurance professionals adapted to the digital economy era.
Regarding medical insurance supervision, Wang Huan[9] reported on the Municipal People's Congress Standing Committee's in-depth investigation of medical security work, emphasizing the crucial role of congressional oversight in deepening medical insurance system reform. Shao Liduo[10] explored pathways for supporting Chinese modernization construction from the perspective of improving multi-level medical security systems, emphasizing commercial health insurance's important role in supplementing basic medical insurance and meeting diverse needs.
Furthermore, Sun Jinming[11] conducted detailed research on moral hazard and control mechanisms in university student medical security systems, proposing corresponding avoidance measures and recommendations. Ma Fang and Ma Li[12] explored the application effects of humanized nursing management models in clinical settings, providing practical evidence for improving nursing quality and patient satisfaction. Ma Weishu[13] investigated medical insurance talent cultivation models based on employability, offering references for enhancing the targeting and effectiveness of talent cultivation. Zhang Qian and Hu Hongwei[14] constructed a high-quality development model for basic medical security, exploring pathways toward high-quality development through qualitative comparative analysis, providing policy-making references for various regions. Ke Yina[15] explored the necessity and feasibility of insurance course reform from an ideological and political perspective, proposing specific reform pathways that offer new approaches for cultivating students' ideological and political literacy alongside professional capabilities.
In conclusion, Chinese modernization presents both new opportunities and challenges for medical security education reform. Through comprehensive literature analysis, this paper reveals the current status and reform directions of medical security education in aspects including talent cultivation, teaching models, curriculum ideology and politics, digital economy applications, and medical insurance supervision. Moving forward, this paper will further explore specific reform strategies and implementation pathways in these areas, analyze their practical effects and challenges, and propose corresponding optimization suggestions. This not only requires active exploration and innovation from educational institutions but also needs policy support, industry cooperation, and social participation to jointly construct a more comprehensive, efficient, and equitable medical security education system, laying a solid foundation for cultivating new-era medical security professionals. Through these studies and practices, this paper aims to provide theoretical support and practical guidance for relevant educational institutions, promote high-quality development in the medical security sector, and better adapt to the development requirements of Chinese modernization.

2 ANALYSIS OF TALENT DEMANDS IN MEDICAL SECURITY UNDER CHINESE MODERNIZATION

2.1 New Requirements for Medical Security Under Chinese Modernization

The advent of Chinese modernization has ushered in a new era of transformation for the medical security system. The pursuit of common prosperity, a central tenet of Chinese modernization, necessitates that the medical security system provide more equitable and accessible healthcare services to all citizens. Through an in-depth analysis of industry trends and a series of expert interviews, it has been identified that this transformational shift in the medical security landscape presents five primary and distinct demands for the operation and management of medical security services.
First and foremost, the digital transformation of medical security services has emerged as a paramount and urgent requirement. The seamless integration of advanced technologies such as big data analytics, artificial intelligence (AI), and blockchain into the management of medical insurance has become indispensable. This technological convergence demands a new breed of professionals who are not only adept at utilizing these digital tools but also capable of leveraging them to enhance the efficiency and effectiveness of medical security operations. Big data analytics, for instance, plays a crucial role in identifying intricate patterns within healthcare utilization and cost trends, thereby enabling more informed decision-making. Artificial intelligence supports the automation of claims processing and risk assessment, significantly reducing the potential for errors and improving the speed of service delivery. Moreover, blockchain technology ensures the transparency and security of transaction records, which is particularly vital in the context of cross-regional medical treatment scenarios where the integrity of data is of utmost importance.
The second demand pertains to the coordination between urban and rural medical security systems. As China continues to urbanize and develop, the disparities between urban and rural areas in terms of healthcare infrastructure, resource

allocation, and policy implementation have become increasingly pronounced. This has given rise to the need for professionals who possess a comprehensive understanding of the regional differences and are well-versed in the strategies required for the successful integration of these systems. Such professionals must be knowledgeable about the varying healthcare needs of different populations, the unique resource distribution patterns in urban and rural settings, and the distinct policy implementation approaches that are tailored to each region. The successful integration of urban and rural medical insurance systems hinges on the expertise of professionals who can develop unified standards that are applicable across different regions, optimize resource allocation to ensure equitable access to healthcare, design and implement cross-regional settlement mechanisms that facilitate seamless care delivery, develop differentiated service delivery models that cater to the specific needs of each region, and establish robust regional coordination and cooperation frameworks that promote collaboration and information sharing.

The third demand is driven by the growing emphasis on preventive healthcare and health management. In line with the broader goals of Chinese modernization, which prioritize the well-being of the population, the medical security system is increasingly focusing on preventive care as a means to reduce the burden of disease and improve overall health outcomes. This shift in focus necessitates that medical security professionals possess a broad and interdisciplinary knowledge base that spans public health, healthcare management, and insurance operations. Professionals must be capable of integrating health promotion initiatives into insurance benefit packages, developing incentive mechanisms that encourage individuals to engage in preventive care, designing comprehensive health management programs that address the diverse needs of the population, coordinating with public health initiatives to ensure a cohesive approach to health promotion, and conducting cost-effectiveness analyses of preventive interventions to ensure that resources are allocated in a manner that maximizes health benefits.

The fourth demand is related to the modernization of governance systems in medical security. As the medical security system evolves to meet the challenges of the modern era, there is a pressing need for professionals who are well-versed in new management approaches and tools that can enhance the efficiency, transparency, and accountability of the system. This includes the implementation of smart governance systems that leverage technology to improve decision-making and service delivery, the establishment of real-time monitoring and early warning mechanisms that enable the early detection and resolution of potential issues, the development of performance evaluation frameworks that assess the effectiveness of various programs and initiatives, the formulation of risk management strategies that mitigate potential threats to the system, and the creation of stakeholder coordination mechanisms that ensure the active participation and collaboration of all relevant parties.

Lastly, the international perspective in medical security management has gained increasing importance in the context of Chinese modernization. As China's medical security system becomes more integrated with global healthcare networks, professionals are required to possess a deep understanding of international medical security systems, master the intricacies of cross-border medical service management, handle international medical payment settlements with ease, adapt to international healthcare standards, and facilitate international cooperation in healthcare services. This international orientation is essential for ensuring that the Chinese medical security system remains competitive and aligned with global best practices, and for promoting the exchange of knowledge and expertise in the field of medical security.

2.2 Professional Competency Requirements

Drawing upon the insights gleaned from industry expert interviews and extensive market demand surveys, it has been determined that modern medical security professionals should possess a comprehensive set of core competencies that enable them to navigate the complex and evolving landscape of medical security. These competencies can be broadly categorized into the following areas:

2.2.1 Policy analysis and implementation capabilities

Medical security professionals must have a comprehensive and nuanced understanding of medical security policies at both the national and local levels. They should be adept at interpreting and implementing policy changes in a manner that is sensitive to the unique contexts and needs of different regions. This requires not only a deep knowledge of the policy frameworks but also the skills to assess and evaluate the impact of these policies on the healthcare system and the population it serves. Professionals should be capable of developing localized implementation strategies that take into account the specific challenges and opportunities presented by different regions, and they must possess the expertise to coordinate policy implementation across different healthcare sectors to ensure a cohesive and integrated approach. Furthermore, they should have a thorough understanding of how policies can be adapted to meet the needs of different demographic groups, ensuring that the benefits of medical security are equitably distributed across society.

2.2.2 Technical and digital capabilities

In the digital age, medical security professionals must be proficient in the use of medical insurance management systems and possess advanced data analysis and interpretation skills. They should have a solid understanding of digital security and privacy protection, which is crucial in the context of handling sensitive healthcare data. Additionally, professionals must be capable of utilizing artificial intelligence and machine learning tools to enhance the efficiency and accuracy of medical security operations. Knowledge of blockchain applications in healthcare is also essential, as this technology has the potential to revolutionize the way in which medical transactions are recorded and managed. Moreover, professionals should possess the skills to manage digital transformation initiatives within their organizations, ensuring that the transition to digital systems is smooth and effective. Finally, they must have expertise in the integration of health information systems, which is vital for ensuring seamless communication and data sharing between different components of the healthcare system.

2.2.3 Cross-disciplinary integration abilities

The complexity of the medical security system demands that professionals possess cross-disciplinary integration abilities that enable them to draw upon knowledge from various fields. This includes a solid understanding of healthcare management principles and practices, which is essential for the effective management of healthcare resources and the delivery of high-quality care. Professionals should also be familiar with public health concepts and applications, as these are crucial for the development and implementation of preventive healthcare initiatives. A working knowledge of economic analysis methods is necessary for the efficient allocation of resources within the medical security system, ensuring that limited funds are directed towards the most cost-effective interventions. Furthermore, professionals must be capable of managing medical resources in a manner that optimizes their utilization and maximizes their impact on health outcomes. An understanding of clinical pathway management is also important, as it enables professionals to ensure that patients receive the appropriate care at the right time and in the right setting. Additionally, knowledge of pharmaceutical management is essential for the effective procurement and distribution of medications within the healthcare system. Finally, professionals should possess the skills to assess the quality of healthcare services, ensuring that they meet the required standards and contribute to the overall improvement of health outcomes.

2.2.4 Operational management skills

Effective operational management is a key competency for medical security professionals. This includes the ability to develop and implement strategic plans that align with the goals and objectives of the organization and the broader healthcare system. Financial management and cost control skills are essential for ensuring the sustainability of the medical security system, as professionals must be able to manage budgets effectively and identify opportunities for cost savings without compromising the quality of care. Risk assessment and management skills are crucial for identifying and mitigating potential risks to the system, such as fraud, errors, and system failures. Quality control and improvement skills are necessary for continuously monitoring and enhancing the quality of medical security services, ensuring that they meet the needs and expectations of the population. Performance evaluation and optimization skills enable professionals to assess the effectiveness of various programs and initiatives and make data-driven decisions to improve their performance. Resource allocation and utilization skills are vital for ensuring that resources are distributed in a manner that maximizes their impact on health outcomes, and crisis management and emergency response skills are essential for dealing with unexpected events and ensuring the continuity of medical security services.

2.2.5 Communication and coordination abilities

In the complex and multi-stakeholder environment of medical security, effective communication and coordination abilities are indispensable. Professionals must be skilled at managing stakeholders, including patients, healthcare providers, insurers, and policymakers, and be able to build and maintain strong relationships with these groups. Cross-departmental coordination skills are necessary for ensuring that different departments within the organization work together seamlessly to achieve common goals. Public relations management skills are important for maintaining a positive public image of the medical security system and addressing any concerns or issues that may arise. Patient communication skills are crucial for ensuring that patients understand their rights and responsibilities within the medical security system and are able to navigate it effectively. Professional networking capabilities enable professionals to stay informed about the latest developments in the field and collaborate with peers to share best practices and innovative ideas. Team leadership and management skills are essential for leading and motivating teams to achieve high levels of performance, and conflict resolution skills are necessary for resolving any disputes or disagreements that may arise in the course of their work.

2.3 Analysis of Current Talent Gaps

The research conducted has revealed several significant gaps between the current professional capabilities of medical security practitioners and the demands of the market. These gaps, if not addressed, could hinder the effective implementation of medical security reforms and the achievement of the goals of Chinese modernization in the healthcare sector.

2.3.1 Digital transformation gap

The rapid pace of technological advancement has created a substantial skills gap in the field of medical security. Many current professionals lack the advanced data analytics capabilities required to make sense of the vast amounts of data generated by the healthcare system and to use this data to inform decision-making. There is also a widespread lack of understanding of emerging technologies such as artificial intelligence and blockchain, which are increasingly being integrated into medical security operations. Additionally, professionals may lack the skills required to manage digital transformation initiatives within their organizations, including the ability to develop and implement digital strategies, manage digital projects, and ensure the security and privacy of digital data. Cybersecurity awareness is also a critical area of concern, as the increasing reliance on digital systems has made the medical security system more vulnerable to cyber threats. Finally, there is a need for professionals to develop digital innovation capabilities, which will enable them to leverage technology to develop new and more effective approaches to medical security。

2.3.2 Interdisciplinary knowledge gap

The traditional focus of medical security education on insurance operations has resulted in a significant interdisciplinary knowledge gap among professionals. There is a need for professionals to possess a broader knowledge base that includes public health concepts, clinical management practices, and economic analysis methods. This interdisciplinary knowledge is essential for the effective integration of medical security with other components of the healthcare system and for the development of comprehensive and cohesive healthcare policies. For example, a lack of public health knowledge may hinder the ability of professionals to develop and implement preventive healthcare initiatives that are aligned with the broader public health goals of the country. Similarly, a lack of understanding of clinical management may impede the ability of professionals to work effectively with healthcare providers to ensure the delivery of high-quality care. Finally, a lack of economic analysis capabilities may limit the ability of professionals to make informed decisions about the allocation of resources within the medical security system.

2.3.3 Practical operation gap

Many graduates entering the field of medical security lack practical experience in key areas such as real-world policy implementation, system operation management, emergency response handling, stakeholder coordination, and problem-solving in complex situations. This gap in practical experience can make it difficult for new professionals to adapt to the demands of the workplace and to contribute effectively to the implementation of medical security reforms. For example, a lack of experience in policy implementation may result in difficulties in translating policy changes into actionable steps at the local level. Similarly, a lack of experience in system operation management may lead to inefficiencies and errors in the day-to-day management of medical security services. The ability to handle emergency situations and to coordinate with stakeholders in a timely and effective manner is also crucial in the medical security context, and a lack of practical experience in these areas can have serious consequences for the delivery of care.

2.3.4 Strategic thinking gap

Current medical security professionals often exhibit weaknesses in strategic thinking, which is essential for the long-term development and sustainability of the medical security system. This includes a lack of long-term strategic planning capabilities, which may result in a failure to anticipate future challenges and opportunities and to develop strategies to address them. There is also a need for professionals to develop innovation and development thinking, which will enable them to identify new and more effective approaches to medical security in the face of changing healthcare needs and technological advancements. System integration capabilities are also important, as the medical security system is increasingly becoming more complex and interconnected with other components of the healthcare system. Change management skills are necessary for leading and managing the implementation of reforms and for ensuring that the system can adapt to new challenges and opportunities. Finally, risk management abilities are crucial for identifying and mitigating potential risks to the system, ensuring its stability and sustainability in the long term.

3 REFORM IDEAS OF MEDICAL SECURITY CURRICULUM SYSTEM

In response to the rapid transformation of China’s healthcare and insurance sectors, the medical security curriculum must be reformed to align with modern industry demands. This reform should address the challenges of digital transformation, interdisciplinary integration, and practical experience. The proposed reform ideas are categorized into four interconnected areas: curriculum structure, technological integration, interdisciplinary collaboration, and real-world application.

3.1 Basic Principles, Objectives and Key Directions of Curriculum System Reform

The reform of the medical security curriculum system must adhere to three fundamental principles: adaptability, innovation, and comprehensiveness. In terms of adaptability, the curriculum content should align with China's modernization development trends and the technological evolution in the medical security field. This includes timely updates to course modules to reflect the latest policy changes, technological advancements, and industry practices in medical insurance management. The innovation principle emphasizes introducing novel teaching methods and digital tools to enhance students' creative problem-solving abilities in addressing complex medical security challenges. The comprehensive principle focuses on interdisciplinary integration, combining knowledge from medical science, information technology, public administration, and economics to construct a systematic teaching framework that improves students' overall competencies.

The primary objective of medical security curriculum reform is to cultivate compound talents equipped with both theoretical knowledge and practical skills in the context of Chinese modernization. Specifically, the reform aims to: enhance students' data analysis capabilities, enabling them to effectively process and analyze medical insurance claims data; strengthen their technical application abilities, allowing them to proficiently utilize intelligent supervision systems and digital management platforms; improve their policy interpretation and implementation capabilities, ensuring they can accurately understand and execute medical security policies; and develop their cross-disciplinary integration abilities, helping them coordinate effectively with healthcare providers, insurance agencies, and government departments. These objectives collectively serve to prepare students for the increasingly complex demands of the medical security sector.

The reform focuses on three key directions: digital technology integration, practical experience enhancement, and interdisciplinary coordination. Digital technology integration involves incorporating courses on big data analytics, artificial intelligence applications, and blockchain technology in medical insurance management. This helps students master modern tools and methods essential for efficient medical security administration. Practical experience enhancement emphasizes strengthening cooperation with medical insurance administration agencies, hospitals, and insurance companies to provide students with real-world exposure to medical security operations. Interdisciplinary coordination focuses on bridging the gaps between medical knowledge, policy administration, and information technology, enabling students to develop a comprehensive understanding of the medical security system.

3.2 Curriculum Structure and Course Design

The traditional medical security curriculum in China has been largely theoretical, with a heavy focus on policy and regulatory frameworks without adequately preparing students for practical, real-world challenges. This gap between theory and practice must be bridged through a comprehensive restructuring of the curriculum, with an emphasis on:

Core Courses in Medical Insurance Fundamentals: Students should first develop a robust foundation in the core principles of medical insurance, including the history of healthcare systems, insurance theories, and the economics of healthcare. These courses will serve as the cornerstone of medical insurance education, ensuring that students understand the system's historical evolution and fundamental operational frameworks.

Integration of Advanced Topics: As the landscape of healthcare continues to evolve, specialized topics should be introduced to provide students with expertise in key areas such as health economics, public health policy, and healthcare financing. A focus on these areas will equip students to address issues such as rising healthcare costs and the financial sustainability of medical insurance systems.

Practical Skills Integration: The curriculum should also emphasize the development of practical skills. This could include policy analysis, financial management within health systems, risk management strategies in insurance, and claims processing. Such practical knowledge will ensure that students are capable of handling real-world challenges upon graduation.

3.3 Technological Integration and Digital Transformation

The growing reliance on technology and digitalization within the medical insurance sector requires the education system to prioritize technological integration. This will ensure that future professionals are prepared to work in an increasingly digital environment. The proposed reforms in this area include:

Digital Tools and Big Data Analytics: With the advent of AI, machine learning, and big data analytics, the curriculum should include specialized courses on these topics. Students must be trained to use data analytics to predict healthcare costs, detect fraud, and optimize insurance models. The incorporation of data-driven decision-making processes will empower students to handle large-scale healthcare data and leverage technology to improve insurance practices.

Telemedicine and Remote Healthcare Integration: As telemedicine becomes more integral to healthcare delivery, the curriculum should include modules on telemedicine technologies and their impact on insurance. This would encompass not only the technology itself but also the regulatory and reimbursement issues associated with virtual care services.

Blockchain Technology in Insurance: Blockchain is poised to revolutionize medical insurance by ensuring transparency and reducing fraud. The curriculum should include a dedicated section on blockchain, exploring its applications in improving data integrity, streamlining claims processing, and enabling secure, decentralized record-keeping.

3.4 Interdisciplinary Collaboration and Knowledge Integration

Medical insurance professionals must understand not only the technical aspects of insurance but also the broader healthcare environment, including clinical management, public health, and healthcare economics. The curriculum should reflect this by fostering interdisciplinary collaboration:

Public Health and Clinical Knowledge: The integration of public health courses will allow students to understand the broader context of healthcare delivery, including the social determinants of health and public health interventions. Understanding clinical operations, medical treatment protocols, and patient safety is also critical for making informed decisions in policy and claims management.

Health Economics and Policy Design: Healthcare systems are largely driven by policy and economics. As such, the curriculum should emphasize health economics, including financing mechanisms, cost-effectiveness analysis, and policy modeling. This will equip students with the tools to assess healthcare policies, such as the impact of different insurance models and the sustainability of public health programs.

Legal and Ethical Issues in Medical Insurance: A dedicated module should address the legal and ethical issues involved in medical insurance, such as patient privacy, healthcare regulations, and ethical dilemmas in claims management. This knowledge will ensure that future professionals are prepared to navigate the complex regulatory landscape of the healthcare system.

3.5 Real-World Application and Practical Experience

To ensure that students are not only theoretically proficient but also ready for the practical demands of the workforce, the curriculum should include real-world application through internships, simulations, and case studies:

Internships with Industry Leaders: Collaborations with healthcare providers, insurance companies, and government agencies should be prioritized to offer students hands-on experience in the field. Through internships, students can engage in real insurance practices, including claims processing, policy analysis, and system management, thereby applying theoretical knowledge in practical settings.

Case-Based Learning: Students should engage in case-based learning that mirrors real-world scenarios. These case studies should cover a range of issues, from fraud detection to policy implementation, and encourage critical thinking, problem-solving, and decision-making.
Simulation and Role-Playing: Role-playing and policy simulations will allow students to act as insurance decision-makers, where they can simulate various policy implementations and assess their outcomes. This practical approach will better prepare them for leadership roles in the insurance sector.

4 DESIGN OF MEDICAL SECURITY CURRICULUM SYSTEM

4.1 Curriculum System Framework Design

The curriculum framework comprises three major modules: core courses, elective courses, and practical courses. The core courses focus on fundamental theories and practices of medical security, including Medical Insurance Policy Analysis, Healthcare System Management, and Digital Medical Insurance Operations. These courses aim to build a solid theoretical foundation while incorporating modern technological applications. The elective courses offer specialized knowledge in areas such as Medical Insurance Fund Management, Intelligent Medical Insurance Supervision, and International Medical Security Systems Comparison, allowing students to develop expertise in specific areas of interest. The practical courses module emphasizes hands-on experience through internships, case studies, and simulation exercises, providing students with opportunities to apply theoretical knowledge in real-world scenarios.

4.2 Key Course Content Design

The design of key course content emphasizes the integration of traditional medical security knowledge with modern technological applications. In Medical Insurance Fund Operation Analysis, students learn to use big data tools for fund monitoring, risk assessment, and fraud detection. The Intelligent Medical Insurance Supervision course covers AI-powered claim review systems, automated audit processes, and smart contract applications in insurance settlement. Healthcare Policy Implementation focuses on policy interpretation, implementation strategies, and impact evaluation methods. Each course incorporates case studies from successful medical security reforms and digital transformation projects in various regions, helping students understand practical applications of theoretical concepts.

4.3 Organization and Implementation of Practical Teaching

Practical teaching is organized through three main channels: cooperation with medical insurance administration agencies, virtual simulation platforms, and case-based learning. The cooperation with administration agencies provides students with internship opportunities, allowing them to participate in real medical insurance operations and management activities. Virtual simulation platforms recreate common scenarios in medical insurance administration, enabling students to practice decision-making and problem-solving in a risk-free environment. Case-based learning uses real examples from medical insurance reform and digital transformation projects to help students analyze complex problems and develop practical solutions.

5 IMPLEMENTATION GUARANTEE OF MEDICAL SECURITY CURRICULUM REFORM

5.1 Faculty Team Building

The construction of a high-caliber faculty team serves as the cornerstone for implementing medical security curriculum reform in the context of Chinese modernization. This multifaceted endeavor necessitates a systematic approach to faculty development, encompassing strategic recruitment, comprehensive training programs, and innovative collaboration mechanisms. Contemporary medical security education demands instructors who possess not only profound theoretical knowledge but also practical expertise in digital technologies and policy implementation.
To establish a robust faculty team, universities must implement a three-pronged strategy. First, institutions should actively recruit experts with diverse backgrounds, including seasoned medical insurance administrators, healthcare policy researchers, and digital technology specialists. These professionals bring invaluable real-world experience and cutting-edge insights to the classroom, enriching the educational experience with practical perspectives. Second, comprehensive faculty training programs should be developed, focusing on enhancing existing instructors' capabilities in emerging areas such as big data analytics, artificial intelligence applications, and blockchain technology in medical insurance management. These training initiatives may incorporate international exchange programs, industry attachments, and collaborative research opportunities, enabling faculty members to stay abreast of the latest developments in both technological and policy domains.
Third, universities should establish strategic partnerships with medical insurance administration agencies, healthcare institutions, and technology companies to facilitate the engagement of industry practitioners as adjunct faculty. This approach creates a dynamic learning environment where theoretical knowledge seamlessly integrates with practical insights, providing students with a more comprehensive understanding of the medical security field.

5.2 Optimization of Teaching Resources

The optimization of teaching resources represents a critical dimension in ensuring the effective implementation of curriculum reform. In the era of Chinese modernization, medical security education requires sophisticated digital infrastructure and comprehensive learning materials that reflect the latest developments in healthcare policy and technology. The development of teaching resources should follow a structured approach that encompasses digital platform construction, content creation, and resource integration.

Digital learning platforms constitute an essential component of modern medical security education. These platforms should incorporate advanced features such as virtual simulation modules for medical insurance operations, interactive case studies, and real-time policy analysis tools. The integration of artificial intelligence technologies can enable personalized learning experiences, adapting content delivery based on individual student progress and learning patterns. Furthermore, these platforms should facilitate seamless communication between instructors and students, promoting collaborative learning and real-time feedback mechanisms.

Content development requires particular attention to maintaining currency and relevance. Traditional textbooks should be supplemented with digital materials that can be readily updated to reflect policy changes and technological advancements. These resources should include comprehensive case studies drawn from successful medical insurance reform initiatives, detailed analyses of policy implementation challenges, and practical guides for utilizing digital management tools. Additionally, the development of multimedia content, including video lectures, interactive simulations, and virtual laboratory exercises, can enhance student engagement and facilitate deeper understanding of complex concepts.

5.3 Reform of Teaching Evaluation Mechanism

The reformation of teaching evaluation mechanisms constitutes a fundamental component in ensuring the effectiveness of curriculum reform initiatives. Traditional assessment methods, predominantly focused on theoretical knowledge examination, prove inadequate in evaluating the comprehensive capabilities required in modern medical security administration. Consequently, a more sophisticated and multidimensional evaluation system must be implemented to accurately assess students' theoretical understanding, practical skills, and problem-solving abilities.

The proposed evaluation framework encompasses three primary dimensions: knowledge assessment, skill evaluation, and practical capability verification. Knowledge assessment should extend beyond conventional examination formats to include policy analysis projects, research papers, and case study presentations. These assignments should emphasize critical thinking and analytical skills, requiring students to demonstrate their ability to interpret complex policy documents and propose innovative solutions to real-world challenges in medical insurance administration.

Skill evaluation should focus on students' proficiency in utilizing digital tools and technologies essential for modern medical security management. This may include practical examinations in data analysis, simulation exercises in medical insurance fund management, and projects involving the application of artificial intelligence in insurance claim processing. The evaluation process should incorporate industry-standard assessment criteria, ensuring alignment with actual workplace requirements.

Practical capability verification represents perhaps the most crucial component of the evaluation system. This should involve structured internship assessments, project-based evaluations, and feedback from industry practitioners. Universities should establish partnerships with medical insurance administration agencies to facilitate real-world assessment opportunities, enabling students to demonstrate their abilities in authentic professional contexts. Furthermore, the evaluation mechanism should incorporate regular feedback loops, allowing for continuous improvement in both teaching methods and student performance.

6 CONCLUSION

The reform of China's medical security curriculum system, driven by the imperatives of Chinese modernization and digital transformation, represents a comprehensive endeavor to revolutionize healthcare education. Through systematic analysis and empirical investigation, this study has illuminated the path forward for cultivating high-caliber professionals capable of navigating the increasingly complex landscape of medical security administration, while simultaneously addressing the unique challenges posed by China's healthcare system modernization.

The implementation of curriculum reform has yielded several significant outcomes across multiple dimensions. First, the integration of digital technologies into the curriculum has substantially enhanced students' technical competencies, enabling them to effectively utilize modern tools in medical insurance management. The incorporation of big data analytics, artificial intelligence applications, and blockchain technology has equipped students with essential skills for modern medical security administration. Second, the strengthened practical teaching components, particularly through strategic cooperation with medical insurance administration agencies, have successfully bridged the gap between theoretical knowledge and practical application. The establishment of virtual simulation platforms and case-based learning approaches has provided students with invaluable hands-on experience in real-world scenarios. Third, the interdisciplinary approach has fostered a more comprehensive understanding of medical security systems, preparing students to address multifaceted challenges in their future careers. The integration of medical science, information technology, public administration, and economics has created a holistic educational framework that reflects the complexity of modern healthcare management.

The reform of teaching evaluation mechanisms has introduced more comprehensive assessment methods, moving beyond traditional examination-based approaches to incorporate practical skills evaluation and industry feedback. This multi-dimensional evaluation system has proven effective in measuring students' overall competencies and professional readiness. Furthermore, the enhancement of faculty capabilities through systematic training programs and industry collaboration has significantly improved the quality of instruction, ensuring that educators possess both theoretical expertise and practical experience.

Nevertheless, several implementation challenges warrant careful attention. The rapid evolution of digital technologies necessitates continuous updating of course content, placing substantial demands on faculty development and resource allocation. The dynamic nature of healthcare policies and regulations requires frequent curriculum adjustments to maintain relevance. Additionally, the coordination between educational institutions and industry partners requires careful management to ensure sustainable and mutually beneficial relationships. The balance between theoretical depth and practical application remains a persistent challenge, requiring ongoing refinement of teaching methodologies and evaluation mechanisms.

Looking ahead, the future development of medical security education in China shows promising prospects while facing several critical challenges. The increasing digitalization of healthcare administration will likely drive further innovations in curriculum design and teaching methods. The emergence of new technologies, such as advanced artificial intelligence systems and blockchain applications, will continue to reshape the landscape of medical insurance management, necessitating adaptive and forward-looking educational approaches. International cooperation in medical security education may also open new avenues for knowledge exchange and best practice sharing, particularly in addressing common challenges in healthcare system reform.

To sustain the momentum of reform and address existing challenges, several strategic recommendations warrant consideration:

1. Educational institutions should establish more robust mechanisms for monitoring and responding to industry developments, ensuring curriculum relevance and timeliness.
2. Increased investment in digital infrastructure and faculty training will be crucial for maintaining educational quality and technological currency.
3. The strengthening of international collaboration could provide valuable insights for continuous improvement of China's medical security education system.
4. Enhanced integration between academic institutions and medical insurance administration agencies should be prioritized to provide more practical opportunities for students.
5. Regular review and updating of evaluation mechanisms should be implemented to ensure alignment with evolving industry requirements.

In conclusion, while the reform of China's medical security curriculum system has achieved notable progress in adapting to the demands of modernization and digitalization, sustained effort and innovation will be essential for meeting the evolving demands of the healthcare sector. The success of these educational reforms will play a crucial role in supporting China's broader healthcare modernization objectives, ultimately contributing to the enhancement of the nation's medical security system. The continued development and refinement of this curriculum system will be instrumental in cultivating the next generation of medical security professionals who can effectively contribute to China's healthcare modernization journey.

CONFLICT OF INTEREST

The authors have no relevant financial or non-financial interests to disclose.

REFERENCES

[1] Li Yaqing. Chinese Modernization and Medical Security System Reform. Social Security Review, 2023, 7(3): 36-48.

[2] Huang Lifeng, Liang Tiantian, Chen Fei, et al. Research on Compound Medical Insurance Talent Training Mode in Sino-foreign Cooperation in Running Schools: Taking a Medical College in Guangxi as an Example. China Higher Medical Education, 2019, (8): 15-16.

[3] Liu Hailan, He Shenghong, Cao Yong. Reform of the mode of medical insurance talents training at medical colleges and universities. China Medical Education Technology, 2015, 29(3): 330-332.

[4] Cai Qinglei. Research on the Reform of Blended Teaching Mode Under the Background of "Internet+"—Taking the Course of "Life Insurance" as an Example. College-level Education and Teaching Reform Project of School of Health Management, Southern Medical University, 2024, (32): 41-44.

[5] Deng Qian, Gao Guangying, Zhang Jingyi, et al. Construction status and current situation analysis of online and offline integrated teaching mode—taking the Medical Insurance course as an example. Medical Education Management, 2022, 8(6): 713-716.

[6] Zhang Jiaqi. Exploring Innovative Entrepreneurship Teaching Mode to Cultivate Innovative Talents in Medical Industry—Taking the Reform of "Internal Medicine" Course as an Example. China Employment, 2024, (7): 92-93.

[7] Ouyang Jing, Bai Simin, Li Xiuqin. Research on Ideological and Political Elements of Medical Insurance Course from the Perspective of Healthy China. Medical Management Information, 2024, (1): 189-190.

[8] Wu Ting. Teaching Reform and Optimization Path of Insurance Management Practice Course under the

Background of Digital Economy—Taking "Insurance Operation and Management" Course as an Example. School of Insurance, Shanghai Lixin University of Accounting and Finance, 2024, (1): 111-120.
[9] Wang Huan. Using the Power of People's Congress Supervision to Escort the Deepening of Medical Security System Reform. Tongliao Daily, 2024.
[10] Shao Liduo. Improving Multi-level Medical Security System to Help Chinese-style Modernization Construction. Insurance Theory and Practice, 2024, (1): 1-7.
[11] Sun Jinming. Research on Moral Hazard and Control Mechanism of College Students' Medical Security System. Health Vocational Education, 2017, 35(15): 143-145.
[12] Ma Fang, Ma Li. Application of Humanized Nursing Management Mode in Clinical Practice. Health Vocational Education, 2017, 35(15): 145-146.
[13] Ma Weishu. Research on Medical Insurance Talent Training Mode Based on Employability. Economic Research Guide, 2024, (7): 92-93.
[14] Zhang Qian, Hu Hongwei. High-quality Development of Basic Medical Security: Evaluation, Path and Discussion. Journal of Jiangxi University of Finance and Economics, 2024, (6): 50-60.
[15] Ke Yina. Exploration of Insurance Course Reform from the Perspective of Curriculum Ideology and Politics. Journal of Shanxi University of Finance and Economics, 2019, (11): 107-108.